

AFML-TR-74-197

12

FG

ADA 026408

# RELIABILITY PREDICTION FOR COMPOSITE JOINTS - BONDED AND BOLTED

*GENERAL DYNAMICS  
FORT WORTH DIVISION  
FORT WORTH, TEXAS*

MARCH 1976

TECHNICAL REPORT AFML-TR-74-197  
FINAL REPORT FOR PERIOD MAY - MAY 1974

Approved for public release; distribution unlimited

DDC  
RECEIVED  
JUN 6 1976  
A

AIR FORCE MATERIALS LABORATORY  
AIR FORCE WRIGHT AERONAUTICAL LABORATORIES  
Air Force Systems Command  
Wright-Patterson Air Force Base, Ohio 45433

NOTICE

When Government drawings, specifications, or other data are used for any purpose other than in connection with a definitely related Government procurement operation, the United States Government thereby incurs no responsibility nor any obligation whatsoever; and the fact that the Government may have formulated, furnished, or in any way supplied the said drawings, specifications, or other data, is not to be regarded by implication or otherwise as in any manner licensing the holder or any other person or corporation, or conveying any rights or permission to manufacture, use, or sell any patented invention that may be related thereto in any way.

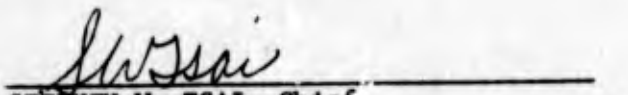
This final report was submitted by The Fort Worth Division of General Dynamics, Fort Worth, Texas, under Contract No. F33615-73-C-5061, with the Mechanics and Surface Interactions Branch, Nonmetallic Materials Division, Air Force Materials Laboratory, Wright-Patterson Air Force Base, Ohio. Dr. James M. Whitney was the Project Monitor.

R. V. Wolff and G. H. Lemon were the principal investigators.

This technical report has been reviewed and is approved for publication.

  
JAMES M. WHITNEY  
Project Monitor

FOR THE DIRECTOR

  
STEPHEN W. TSAI, Chief  
Mechanics & Surface Interactions Branch  
Nonmetallic Materials Division

Copies of this report should not be returned unless return is required by security considerations, contractual obligations, or notice on a specific document.

UNCLASSIFIED

SECURITY CLASSIFICATION OF THIS PAGE (When Data Entered)

REPORT DOCUMENTATION PAGE		READ INSTRUCTIONS BEFORE COMPLETING FORM	
1. REPORT NUMBER AFML-TR-74-197	2. GOVT ACCESSION NO.	3. RECIPIENT'S CATALOG NUMBER 9	
4. TITLE (and Subtitle) RELIABILITY PREDICTION FOR COMPOSITE JOINTS - BONDED AND BOLTED.		5. TYPE OF REPORT & PERIOD COVERED Final Report • 1 May 73 - 31 Mar 74 15 May 1973 - 31 May 1974	
7. AUTHOR(s) R. V. Wolff C. H. Lemon		8. CONTRACT OR GRANT NUMBER(s) F33615-73-C-5061 NEW	
9. PERFORMING ORGANIZATION NAME AND ADDRESS General Dynamics Fort Worth Division Fort Worth, Texas		10. PROGRAM ELEMENT, PROJECT, TASK AREA & WORK UNIT NUMBERS 73400212	
11. CONTROLLING OFFICE NAME AND ADDRESS Air Force Materials Laboratory (AFML/MBM) Air Force Wright Aeronautical Laboratories Wright-Patterson AFB, Ohio 45433		12. REPORT DATE March 1976	
14. MONITORING AGENCY NAME & ADDRESS (if different from Controlling Office) Same		13. NUMBER OF PAGES 107	
16. DISTRIBUTION STATEMENT (of this Report) Approved for public release; distribution unlimited.		15. SECURITY CLASS. (of this report) Unclassified	
17. DISTRIBUTION STATEMENT (of the abstract entered in Block 20, if different from Report) Same		15a. DECLASSIFICATION/DOWNGRADING SCHEDULE	
18. SUPPLEMENTARY NOTES			
19. KEY WORDS (Continue on reverse side if necessary and identify by block number) Composite Structures Fatigue Random Spectrum Bolted Joints Adhesively Bonded Composite-to-Metal Splice Wear-out Model Statistical Pooling Estimators			
20. ABSTRACT (Continue on reverse side if necessary and identify by block number) An experimental program was conducted on coupon-sized graphite-epoxy laminate-to-metal joints. Both adhesively bonded and mechanically fastened joints were tested in fatigue to the same random (flight-by-flight) spectrum to provide lifetime and residual strength data.  The empirical data developed for both types of joints was analyzed using structural reliability techniques that included the use of a probabilistic fatigue model previously introduced by Dr. J. C. Halpin of AFML and M. E.			

402 709

UNCLASSIFIED

SECURITY CLASSIFICATION OF THIS PAGE(When Data Entered)

20. Abstract - Continued

Waddoups of the Fort Worth Division of General Dynamics.

The program also included the development of methods for pooling dispersion data to estimate the Weibull shape parameter. Three methods were developed and directly compared: parameter averaging, normalization, and maximum likelihood.

The program was a follow-on to the program reported in AFML-TR-72-121, dated March 1972.

ACCESSION SET	
NTIS	Write Station <input checked="" type="checkbox"/>
ERIC	Full Text <input type="checkbox"/>
	<input type="checkbox"/>
A	

UNCLASSIFIED

SECURITY CLASSIFICATION OF THIS PAGE(When Data Entered)

## F O R E W O R D

The research and development work reported herein was conducted under Air Force Contract F33615-73-C-5061 by the Fort Worth Division of General Dynamics. The work was initiated under Project 7340, Task No. 734003. The Air Force Project Monitor directing the program was Dr. J. M. Whitney (AFML/MBM) of the Mechanics and Surface Interactions Branch, Nonmetallic Materials Division, Air Force Materials Laboratory at Wright-Patterson Air Force Base, Ohio. Mr. R. V. Wolff served as program manager and Dr. G. H. Lemon conducted the reliability analysis. This work is a follow-on to report AFML-TR-72-121.

Other key technical personnel participating in the program included

- o Testing - Mr. Fred Vercruysse and Mr. Bill Brubaker
- o Manufacturing Engineering - Mr. Bedford Beaty
- o Reporting - Mr. Marvin Howeth

The report covers work conducted from 1 May 1973 through 31 March 1974. This technical report has been reviewed and is approved for public release.

# T A B L E O F C O N T E N T S

<u>Section</u>		<u>Page</u>
I	INTRODUCTION	1
II	FATIGUE AND RELIABILITY METHODOLOGY-BACK-GROUND	2
	2.1 Bonded Joint Fatigue Programs	2
	2.2 Bolted Joint Fatigue Programs	3
III	DATA DEVELOPMENT	4
	3.1 Specimen Preparation	4
	3.1.1 Graphite-Epoxy Laminates	4
	3.1.2 Metal Adherend	8
	3.1.3 Adhesive	8
	3.2 Fatigue Spectrum	8
	3.3 Test Facility	11
	3.3.1 Bonded Joint Fixtures	11
	3.3.2 Bolted Joint Fixtures	11
	3.4 Bonded Joint Testing	11
	3.4.1 Bonded Joints - Comparison with Previous Program	16
	3.4.2 Test Results	18
	3.4.3 Failure Modes	23
	3.5 Bolted Joint Testing	28
	3.5.1 Test Results - Specimens Retorqued During Fatigue Loading	30
	3.5.2 Test Results - Specimens Torqued Only at Time = 0	32
	3.5.3 Failure Modes	38
IV	DATA ANALYSIS	44
	4.1 Wear-Out Model	44
	4.2 Application To Bonded Joints	47
	4.2.1 Evaluation of Bonded Joint Data	48
	4.2.2 Recalculation of Parameters from Previous Program	50
	4.2.3 Comparison of Wear-Out Model	54
	4.3 Application To Bolted Joints	57
	4.4 Comparison of Joint Types	60

## TABLE OF CONTENTS (Continued)

<u>Section</u>	<u>Page</u>
V	<p>STATISTICAL POOLING STUDY <span style="float: right;">65</span></p> <p>5.1 Normalization of Data Base <span style="float: right;">65</span></p> <p>5.2 Parametric Averaging <span style="float: right;">66</span></p> <p>5.3 Maximum Likelihood Pooled Estimation of the Weibull Shape Parametric <span style="float: right;">66</span></p> <p>    5.3.1 Single Censoring From the Right <span style="float: right;">67</span></p> <p>    5.3.2 Progressive Censoring From the Right <span style="float: right;">67</span></p> <p>5.4 Numerical Example <span style="float: right;">69</span></p>
VI	<p>CONCLUSIONS AND RECOMMENDATIONS <span style="float: right;">75</span></p> <p>6.1 Conclusions <span style="float: right;">75</span></p> <p>6.2 Recommendations <span style="float: right;">76</span></p> <p>APPENDIX I - RESULTS OF BONDED JOINT TESTS <span style="float: right;">78</span></p> <p>APPENDIX II - RESULTS OF BOLTED JOINT TESTS <span style="float: right;">82</span></p> <p>APPENDIX III - TRUNCATION LEVEL AND RMS LEVEL IN RANDOM FATIGUE TESTING <span style="float: right;">93</span></p> <p>REFERENCES <span style="float: right;">97</span></p>

## L I S T   O F   I L L U S T R A T I O N S

<u>Figure</u>		<u>Page</u>
1	Fabrication of Bonded Joint Specimens	5
2	Fabrication of Bolted Joint Specimens	6
3	Double Overlap Shear Specimen	7
4	Typical Mission Profile	10
5	Laboratory Load Control System	12
6	Bonded Joint Test Fixtures	13
7	Lateral Support System - Bonded Joints	14
8	Single Shear Test Fixture - Bolted Joint Specimen	15
9	Bonded Joint - Truncation Load Vs Lifetimes	19
10	Bonded Joint - Residual Strength Vs Lifetime	21
11	Empirical Wear-Out Model Data From References	22
12	Probability of Survival Percentiles of Bonded Joints Predicted by Model	24
13	Static Bonded Joint Failure Modes	25
14	Bonded Joint Residual Strength Failures	26
15	Bonded Joint Residual Strength Specimen No. 3-7	27
16	Bolted Joints - Truncation Load Vs Lifetime	31
17	Residual Strength at Several Truncation Levels - Bolted Joints	34
18	Residual Strength Experiment - Bolted Joints	35
19	Bolted Joints - Truncation Load Vs Lifetime (Not Retorqued)	37

## LIST OF ILLUSTRATIONS (Continued)

<u>Figure</u>		<u>Page</u>
20	Static Bolted Joint Laminate Failures	39
21	Shear-Out Fatigue Failures	40
22	Elongated Hole Fatigue "Failures"	41
23	Residual Strength - Lifetime Model for Bonded Joints	49
24	Residual Strength - Lifetime Model for Data of Prior Program	51
25	Comparison of Original and Revised Model Fits to 4 Lifetime Data of Reference 6	53
26	Wear-Out Model of Figure 23 Shifted to 3000 Pounds Truncation	55
27	Wear-Out Model of Figure 24 Shifted to 2850 Pounds Truncation	56
28	Residual Strength - Lifetime Model Bolted Joints (Retorqued)	58
29	Residual Strength - Lifetime Model Bolted Joints (Non-Retorqued)	59
30	Wear-Out Model of Figure 28 Shifted to 3875 Pounds Truncation	61
31	Wear-Out Model of Figure 28 Shifted to 3500 Pounds Truncation	62
32	Comparison of Pooling Methods for Estimating Weibull Shape Parameters	73
33	Cumulative Frequency Diagram	94
34	Effects of Changing $P_T$ and $P_H$	94
35	Relationship of $P_H$ to Strength Distribution	94

## L I S T   O F   T A B L E S

<u>Table</u>		<u>Page</u>
I	Frequency of Occurrence for Spectrum Load Levels	9
II	Bonded Joint Test Conditions and Parameter Estimates	17
III	Bolted Joint Test Conditions and Parameter Estimates	29
IV	Laminate Resin Content	30
V	Bolt Bearing Results - Selection of Truncation Load	33
VI	Comparison of Torque Effects in Fatigue Loading	36
VII	Bolted Joint Failure Mode Summary	42
VIII	Comparison of Wear-Out Models - Bonded Joints	54
IX	Comparison of Bonded and Bolted Joints	63
X	Weibull Distribution Data With Common Shape Parameter $\alpha = 10$	70
XI	Estimated MLE Weibull Parameters for Table X Data	71
XII	Pooled Estimated Results for Weibull Shape Parameter	72
XIII	Static Ultimate Strength of Graphite-to-Ti Bonded Joint Specimens	79
XIV	Bonded Joint Fatigue Test Results	80
XV	Bonded Joint Residual Strength/Fatigue Test Results Truncation Load 3550 Pounds	81
XVI	Static Bolted Joint Test Results - Single Shear	83

LIST OF TABLES (Continued)

<u>Table</u>		<u>Page</u>
XVII	Bolted Joint Single Shear Fatigue Test Results	84
XVIII	Correlation of Residual Strength - Lifetime Data	89
XIX	Bolted Joint Residual Strength/Fatigue Test Results	90
XX	Bolted Joint Fatigue Test Results - Specimens Not Retorqued	91
XXI	Bolted Joint Residual Strength (Fatigue Test Results)	92

## S E C T I O N I

### I N T R O D U C T I O N

The main objective of this program was to further examine the rms stress versus life relationship of a previously developed analytical model with respect to adhesively bonded joints and to determine the applicability of the model to bolted joints. In addition, the two joint types were compared through safe-life predictions using reliability methodology. The model and methodology applicable to this program are given in AFML-TR-72-121.

This report is divided into the following main parts.

- o Fatigue and Reliability Methodology - Background
- o Data Development
- o Analysis
- o Pooling Study
- o Conclusions and Recommendations

## S E C T I O N   I I

### F A T I G U E   A N D   R E L I A B I L I T Y

#### M E T H O D O L O G Y   -   B A C K G R O U N D

Reliability procedures were developed by Whittaker and Besuner (Reference 1) to provide a statistical approach to certifying the life of metallic airframe structure rather than through use of arbitrary scatter factors. These procedures have also been related directly to composite materials by Halpin, Kopf, and Goldberg (Reference 2). Later, probabilistic mathematical models were introduced by Halpin and Waddoups at the National Symposium on Computerized Structural Analysis and Design, George Washington University, Washington, D. C. 27-29 March 1972 and these models are discussed and reported in References 3 and 4.

Experimental programs that were designed to develop the data required for reliability analysis as related to composite structure have since been sponsored by the Air Force. Initially, these programs concentrated on adhesively bonded joints (References 5, 6, and 7). In these programs the approach has been to evaluate fatigue in the laboratory using flight-by-flight random spectra that simulate service conditions. Each program in turn has advanced the degree to which the laboratory conditions simulate the service conditions.

#### 2.1 BONDED JOINT FATIGUE PROGRAMS

In the first program, only positive loads were used to develop the loading spectrum, which had a narrow-band frequency content (Reference 5). The spectrum derived was stored on a magnetic tape. The digital data of the magnetic tape were converted by a laboratory mini-computer to analog signals used as "commands" in a closed-loop electrohydraulic test system. Boron-epoxy to titanium double scarf joints that were 1/5- and 1/2-scale versions of a full-scale wing root splice joint were studied.

In the second program (Reference 6), the test spectrum included negative loads and ground-air-ground (GAG) cycles. The existing closed-loop test facility was used again. Enough small, double-overlap graphite-epoxy to titanium bonded joints were tested to develop statistical data for the fatigue model derived in References 3 and 4.

The realism of both the spectrum and the test facility were improved in the third program, (Reference 7). A broad band spectrum that included mission profile service temperatures was generated. Two versions of this spectrum were used in testing. In the first version, mission temperatures were not included and the spectrum was accelerated to compress a service life (4000 flight hours) into 24 test hours. In the second version, the mission temperature profiles were included. The spectrum was accelerated only at temperatures below 75°F and was real time for temperatures above 75°F. The inclusion of real-time segments lengthened a simulated service life to 420 test hours. Mission temperature extremes were -60 to +300°F, and these were applied and controlled (through the same mini-computer) similar to the control used for loads. Full-scale, double-step-lap boron-epoxy to titanium bonded joints based on the lower wing skin splice of an air-superiority fighter were tested in this program to demonstrate the feasibility of this type of testing on large-scale components.

## 2.2 BOLTED JOINT FATIGUE PROGRAMS

A current program (Reference 8) will continue upgrading testing realism by combining mission temperature profiles, two degrees of freedom in loading, and humidity exposures. The major test article will be a two-spar graphite-epoxy box beam component that simulates a full-scale wing section selected from a conceptual composite design (Reference 9). Large quantities of smaller scale specimens that represent the fatigue critical elements of the beam will also be tested. The critical elements of the component are the joints, all of which are mechanically fastened. As in the bonded joint programs, reliability procedures will be used in evaluation.

## 2.3 SUBJECT FATIGUE PROGRAM

The subject program is a follow-on to the Reference 6 program. Therefore, the spectrum used in the earlier program was used in the subject program. Bonded joints have been included to examine additional details of the rms stress-life fatigue model, and bolted joints have been included to test the general applicability of the model.

## S E C T I O N   I I I

### D A T A   D E V E L O P M E N T

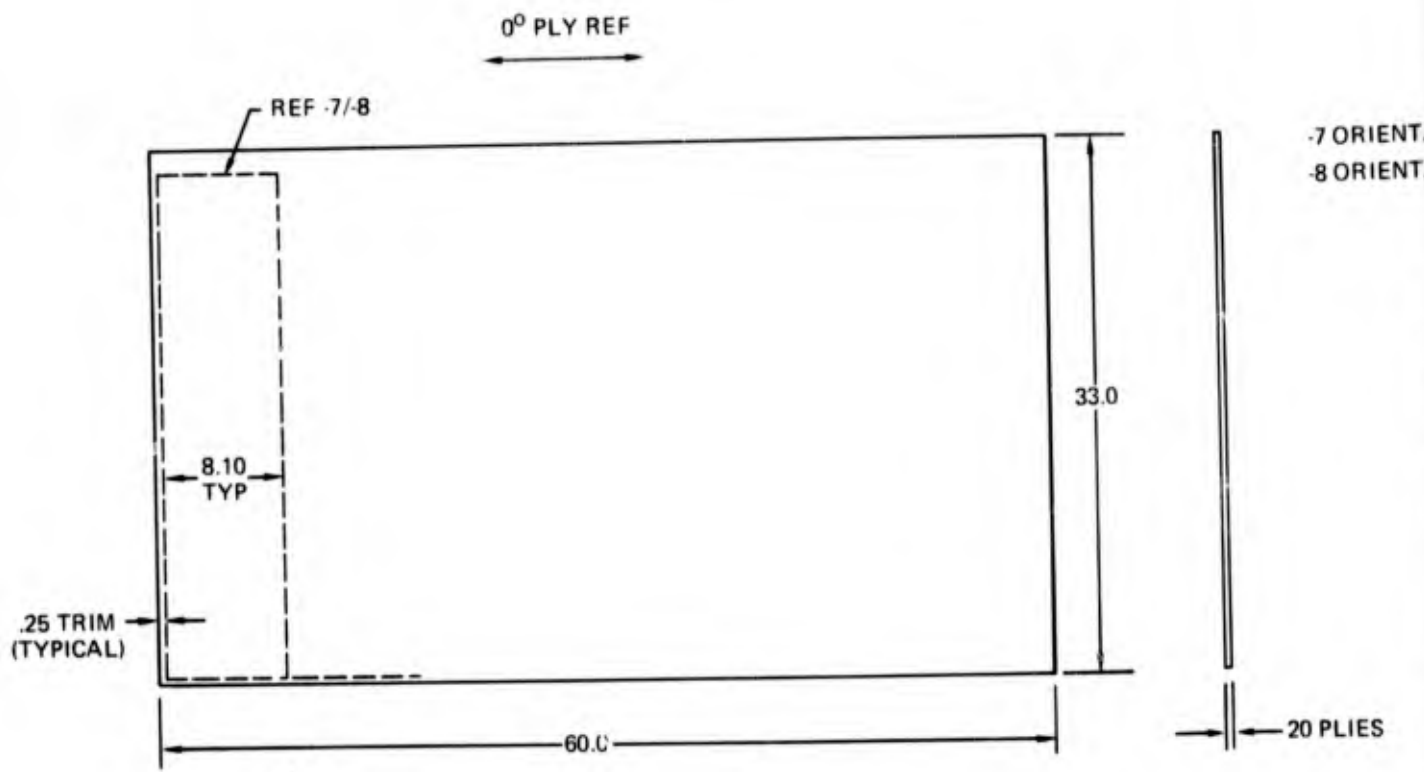
The original plan for studying mechanical joints required connecting a graphite-epoxy laminate to metal plates with a tight fitting pin to allow fatigue loading in double shear. The test method proved inadequate for a spectrum that included negative loads. The specimen was changed to a bolted joint and the bolt was torqued to a level consistent with aircraft standards. The forced modifications to the four test fixtures (initially designed for pin-loading) were suspected to have introduced an undesirable lifetime-fixture interaction effect; hence, new fixtures were designed and specimen loading was revised to single shear. In all, 28 pinned joints, 59 double shear bolted joints, and 263 single shear bolted joints were tested. The bonded joint design used was similar to that used in the Reference 6 program. A total of 152 coupons were tested.

Fatigue tests were conducted using the spectrum used in the Reference 6 program. The details of the data development are given in the following paragraphs.

#### 3.1 SPECIMEN PREPARATION

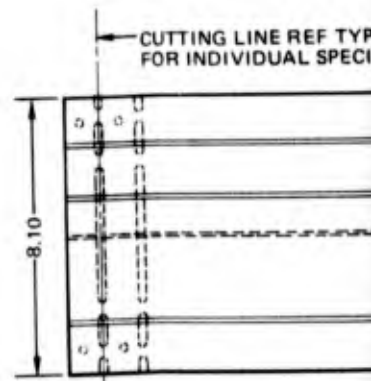
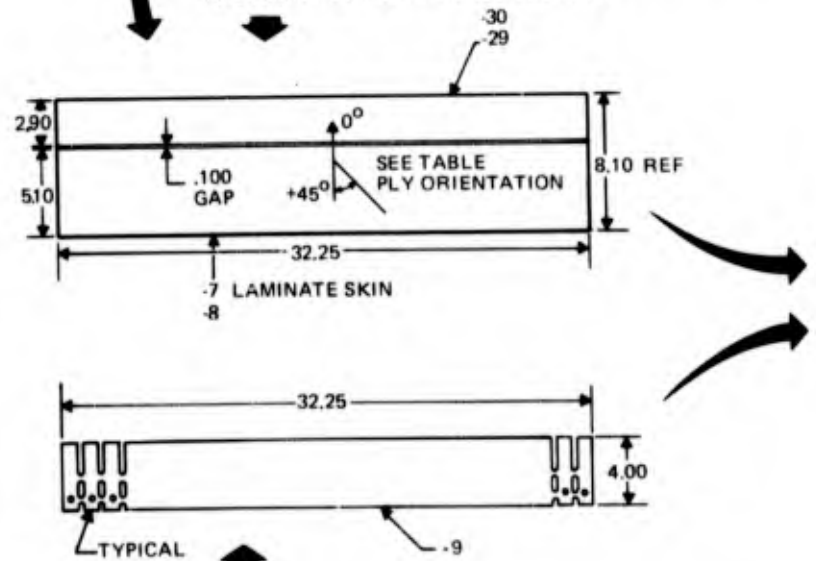
##### 3.1.1 Graphite-Epoxy Laminates

Thornel 300/5208 graphite-epoxy material (a product of Narmco Materials of Costa Mesa, California) purchased in accordance with General Dynamics specification FMS-2023 Type III, Form C was used to fabricate laminates used in bonded and bolted specimens. Fabrication costs were minimized by precuring large laminates and cutting them into details for use in both bonded and bolted specimens. The detailed steps of laminate fabrication are shown in Figures 1 and 2. In the case of the bonded specimens, precured laminates were secondarily bonded to titanium sheet material, Figure 3. A "nylon" peel ply was included on each laminate to provide a bonding surface. The "nylon" peel ply had been used successfully for bonding graphite-epoxy laminates for eight years, but in the case of this particular laminate material, Thornel 300/5208, the bonded specimens were found to have poor static ultimate shear strength. Two companies currently conducting programs in which graphite-epoxy laminates were used



**STEP 1**  
TWO LAMINATES FABRICATED AS SHOWN ABOVE  
EACH LAMINATE CUT INTO SEVEN ASSEMBLY DETAILS

**STEP 2**  
LAMINATE DETAILS FROM STEP 1 CUT INTO  
TWO DETAILS FOR FINAL ASSEMBLY



**STEP 3**  
TITANIUM DETAILS PUNCHED AND CLEANED

-7 ORIENTATION [0, +45, 0, -45, 0<sub>2</sub>, -45, 0, +45, 0]<sub>S</sub>  
 -8 ORIENTATION [0, -45, 0, +45, 0<sub>2</sub>, +45, 0, -45, 0]<sub>S</sub>

20 PLIES

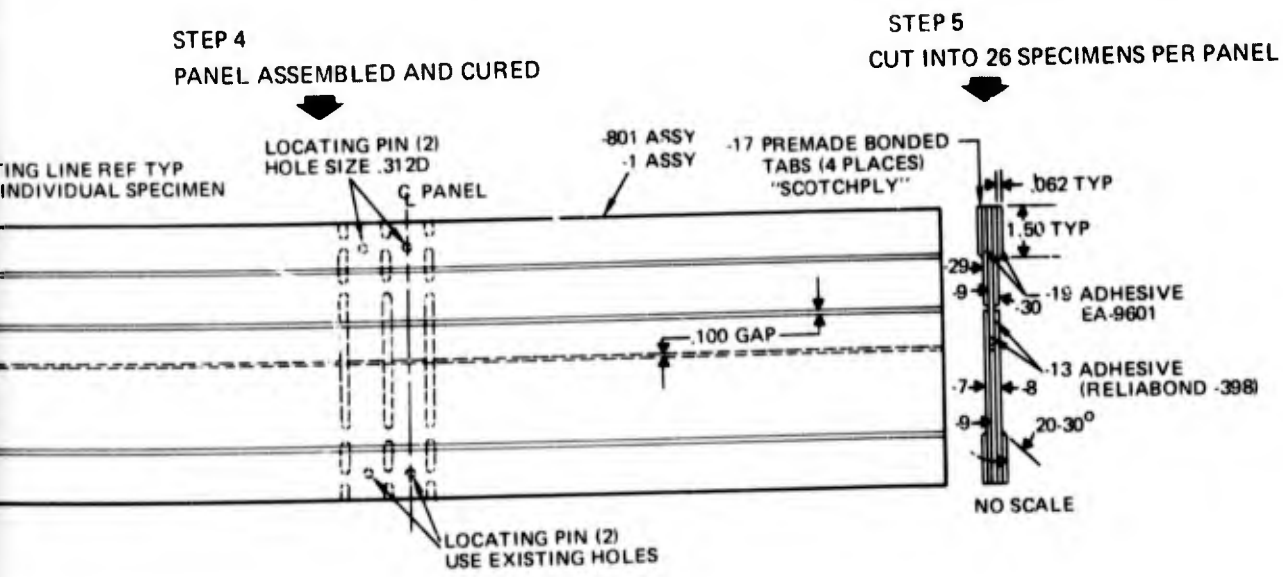
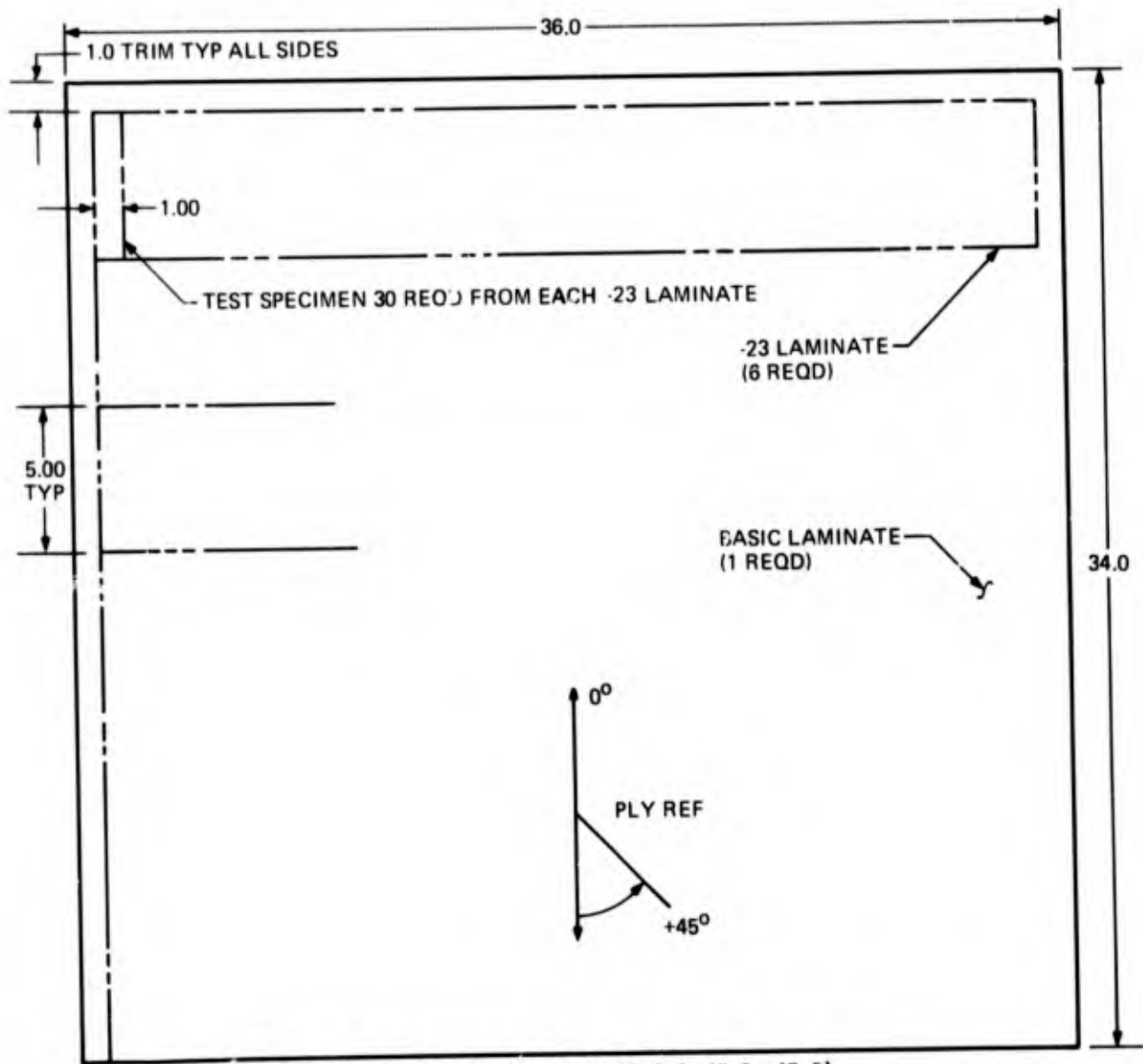


Figure 1 Fabrication of Bonded Joint Specimens



LAYUP, 20 PLYS TOTAL,  $[0, +45, 0, -45, 0, 0, -45, 0, +45, 0]_S$   
 LAMINATE FOR BOLTED JOINT SPECIMENS

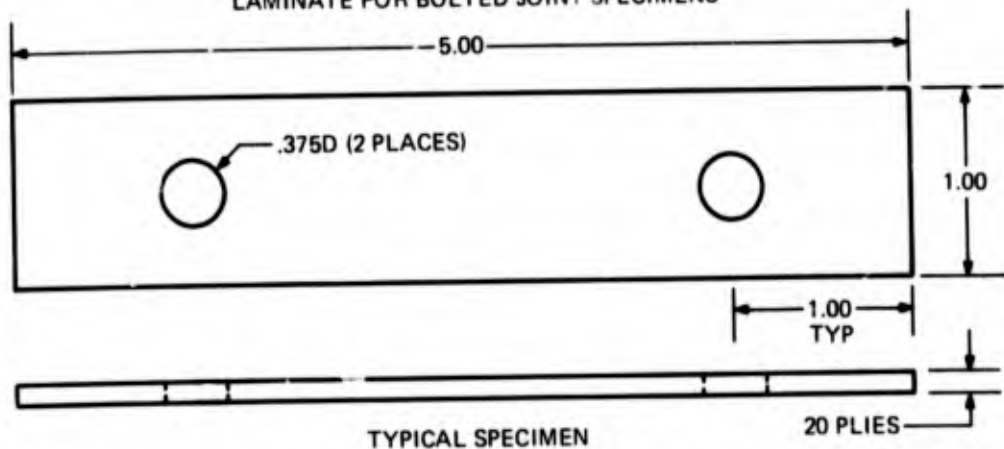


Figure 2 Fabrication of Bolted Joint Specimens

LAMINATE ORIENTATION  $[(0, +45, 0, -45, 0)_S]_2$

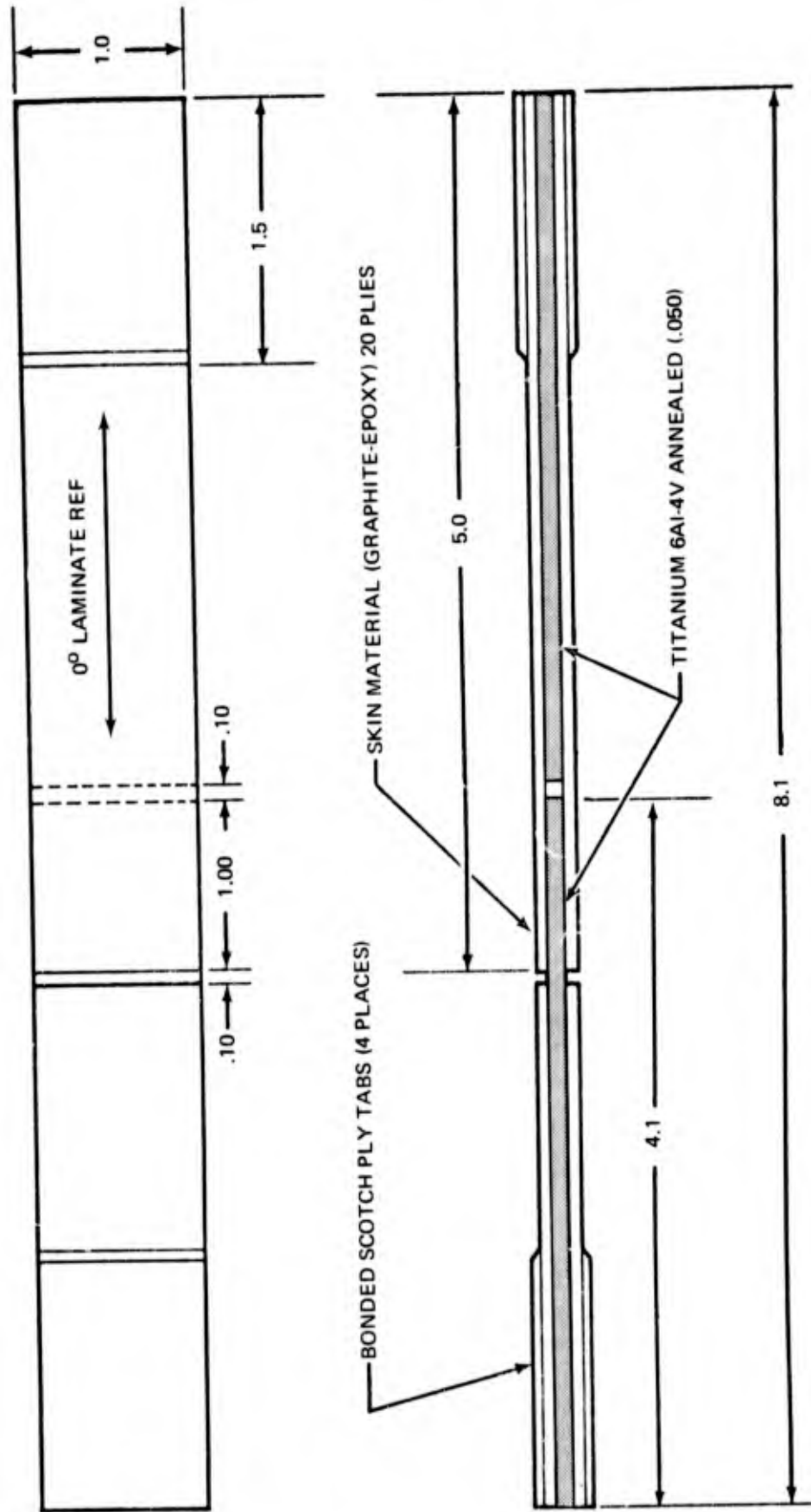


Figure 3 Double Overlap Shear Specimen

in bonded joints have also reported problems with nylon peel ply materials, see References 10 and 11. An investigation was conducted to determine the most expedient process to use in fabricating higher strength specimens. For program purposes, the replacement specimens were fabricated by thoroughly sanding the laminate bond surfaces. Specimens used in bolted joint tests are shown in Figure 2.

### 3.1.2 Metal Adherend

Titanium alloy 6Al-4V, per MIL-T-9046, Type III, Composition C, annealed was used in the bonded specimens. The titanium details were cleaned by solvent wiping, followed by grit blasting, solvent wiping again, vapor degreasing, and finally acid cleaning by immersion in Pasa Jell 107M, which is a product of Semco Sales and Service of Los Angeles, California. Parts were rinsed in distilled water and oven dried. After cleaning, the details were primed using EC-2333, which is a product of the 3M Company of St. Paul, Minnesota.

### 3.1.3 Adhesive

The adhesive used was "Reliabond 398," a product of the Reliable Manufacturing Company of Costa Mesa, California. Reliabond 398 is a supported, epoxy-novalac film material and was purchased in accordance with General Dynamics specification FMS-1013 Form 1A. Bonded panels were assembled using one adhesive layer between each faying surface and were cured at 350°F. This same adhesive product was used in the Reference 6 program.

## 3.2 FATIGUE SPECTRUM

The random spectrum used was identical to that of the Reference 6 program to allow a comparison of data developed. Characteristics of the spectrum are summarized as follows:

1. Asymmetric about +lg load level
2. Irregularity parameter of unity (Rayleigh distribution)
3. 738,742 random loads in one lifetime
4. Maximum truncation is 81.7 percent of limit bending moment

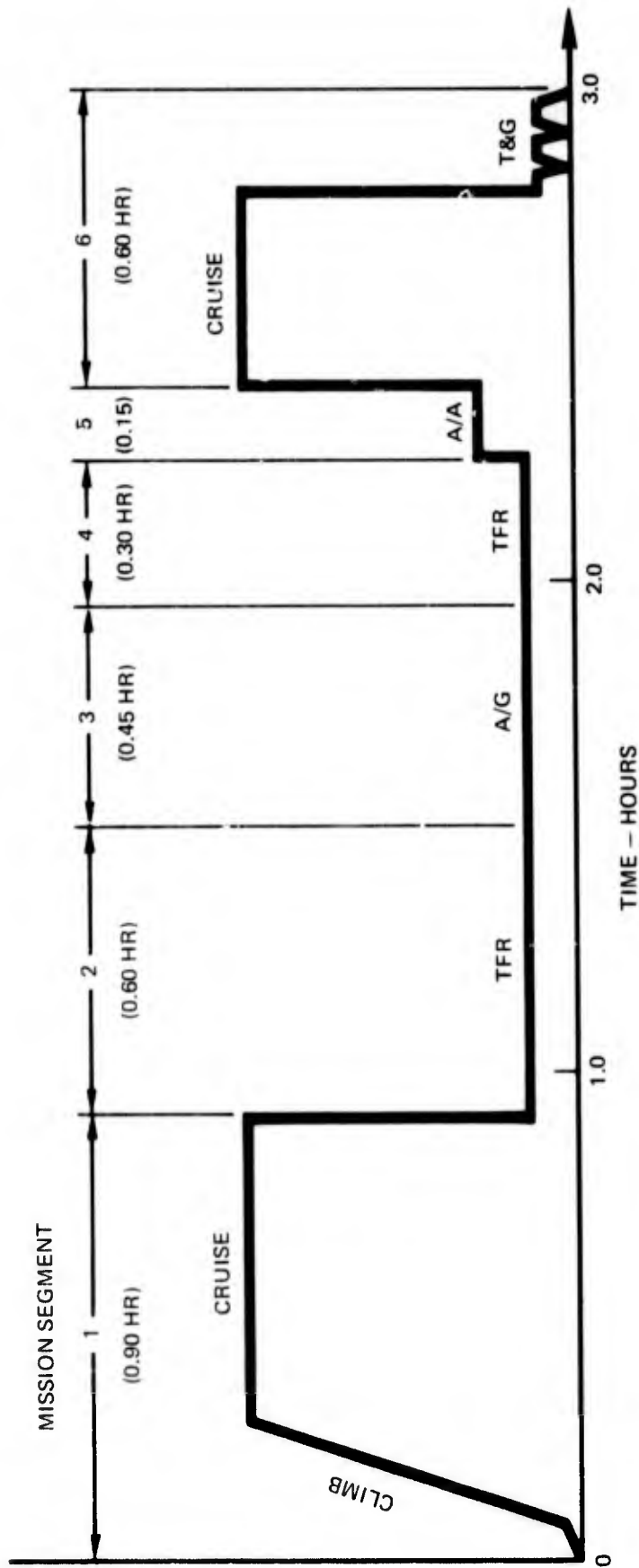
5. Minimum truncation is -66.3 percent of limit bending moment
6. Accelerated time base (10 load changes per second), narrow band PSD shape.

A typical mission profile, Figure 4, was developed for use in generating the spectrum. Mission length was defined as 3 hours and a service lifetime as 4000 hours (real time), i.e., 1334 missions per lifetime. The spectrum was stored on a magnetic tape using a simulation procedure developed during the Reference 5 program. The load signals on the magnetic tape were normalized to permit load magnification to be varied in the laboratory. For test specimens that required multiple lifetimes, the magnetic tape was simply restarted and used again. As stated above, the test spectrum is truncated at 81.7 percent and -66.3 percent of limit bending moment; therefore, a fatigue specimen reaches the peak (truncation) load level many times in a lifetime. The total occurrences per mission are shown in Reference 6. The frequency at which several discrete load levels occur in a lifetime is illustrated in Table I. Since the sequence of loads was selected at random for the magnetic tape, the number of loads of a specific magnitude for fractions of a lifetime can be approximated by that fraction times the total per lifetime. The randomness of the spectrum also permits initiating a fatigue specimen at any time in the test sequence; therefore, test time is not lost in waiting on the magnetic tape to finish a complete life before starting new specimens.

Table I FREQUENCY OF OCCURRENCE FOR SPECTRUM LOAD LEVELS

Spectrum Load Level (2), (3)	Frequency/Lifetime (1)
+81.7%	293
+76	680
+70	974
+67.5	1334
+64.5	1961
...	...
-66.3	1334

- NOTES: (1) Lifetime 738,742 Random Loads  
 (2) Upper Truncation +81.7%  
 (3) Lower Truncation -66.3%



- NOTES:
- 1 TFR IS TERRAIN FOLLOWING RADAR
  - 2 A/G IS AIR-GROUND
  - 3 A/A IS AIR-AIR
  - 4 T&G IS TOUCH & GO

Figure 4 Typical Mission Profile

### 3.3 TEST FACILITY

The test facility load control system is shown schematically in Figure 5. The facility is capable of operating 24 channels (i.e. fatigue fixtures) simultaneously. The subject program required only 8 load channels; however, two concurrent programs resulted in 22 channels being used simultaneously for a period of time. The magnetic tape can store a maximum of five random spectra if the time bases ("frequency") of the spectra are compatible. Separate magnetic tapes are required for cases in which the random spectra have dissimilar time bases. The facility also has closed-loop temperature control capability; however, it was not necessary for the subject program.

#### 3.3.1 Bonded Joint Fixtures

The four fixtures (Figure 6) used in the Reference 6 program were used to load bonded joints in this program. Three simultaneous tests per fixture are possible through use of a clamping arrangement on the specimen ends and stabilizing guideblocks. Each fixture is controlled separately; hence, load magnitude may be varied for each. Specimens were stabilized during loading by a lateral support system (Figure 7) also used on the earlier program.

#### 3.3.2 Bolted Joint Fixtures

The final load fixture design for bolted joint specimens in single shear is shown in Figure 8. Four duplicate fixtures were used. The ends of the fixtures were tap drilled to connect them directly to a hydraulic loading ram on one end and a load cell on the opposite end. Then, the load cell was connected to a rigid, fixed frame. The bolted specimens did not require lateral support plates.

### 3.4 BONDED JOINT TESTING

In this program, the approach was to evaluate fatigue in the laboratory under simulated service load conditions. The empirical data developed to allow determination of fatigue

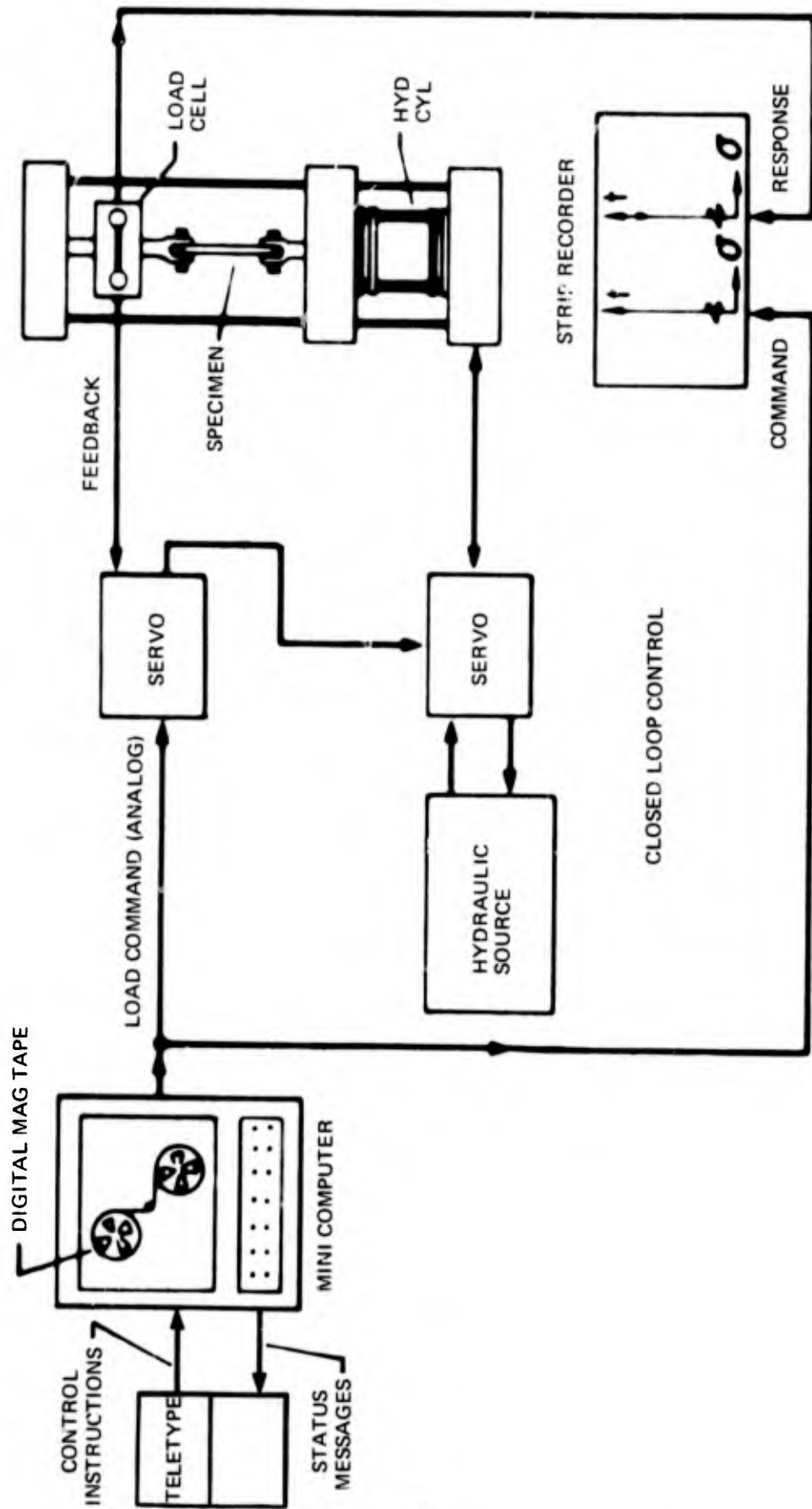


Figure 5 Laboratory Load Control System

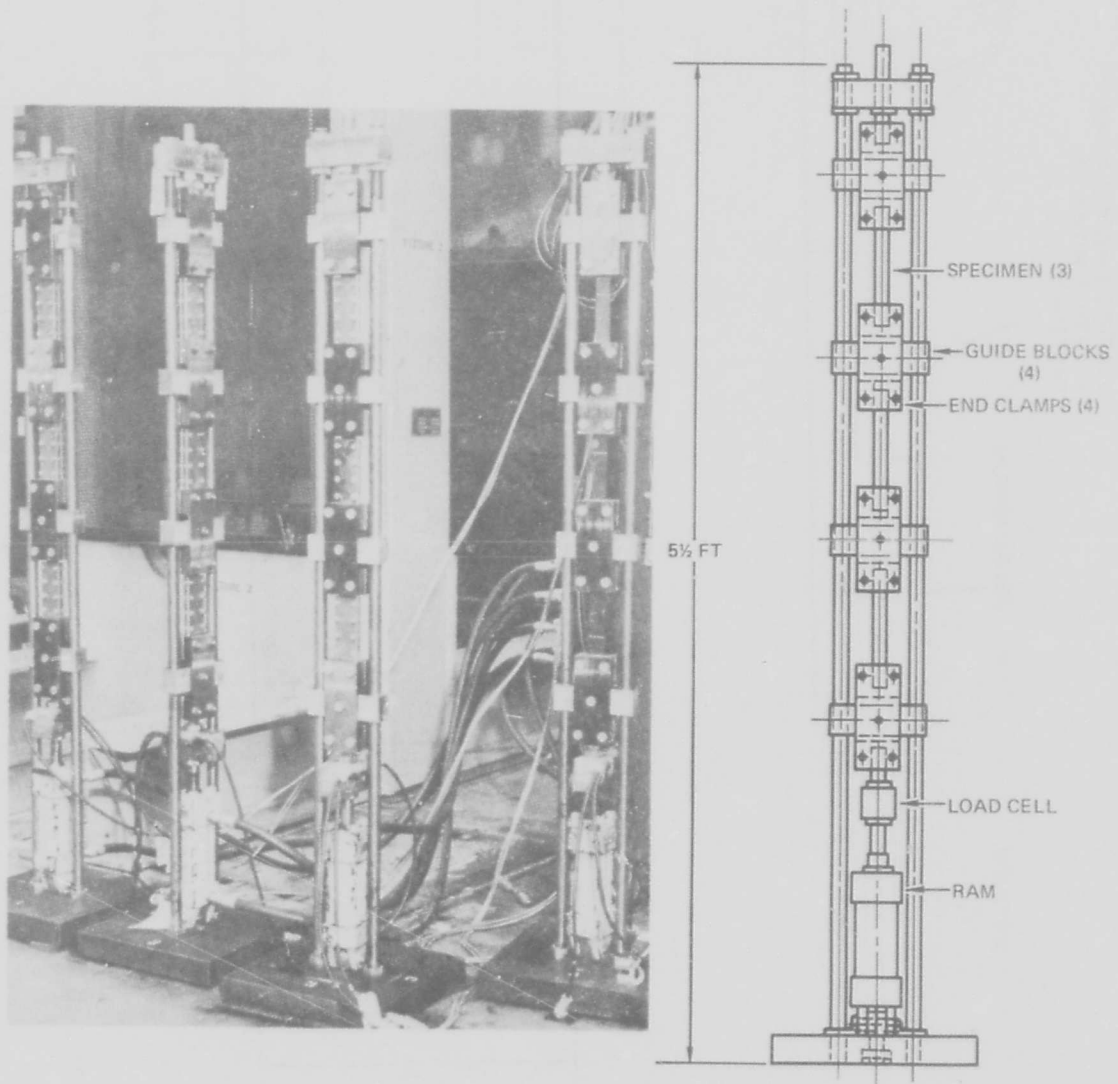
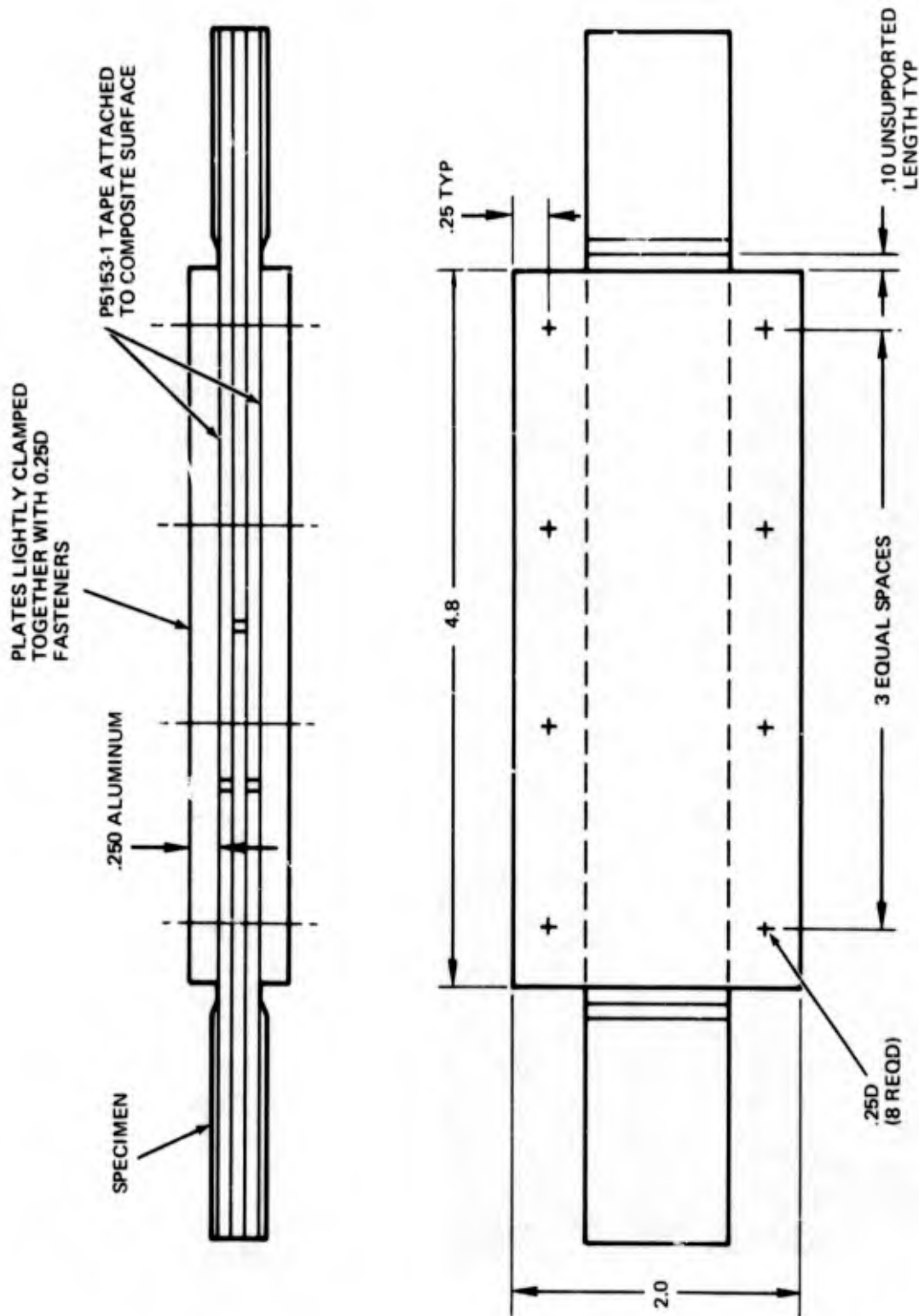


Figure 6 Bonded Joint Test Fixtures



NOTE: (1) P5153-1 IS "TEFLON" TAPE .005-INCH THICK ADHESIVE APPLIED ON ONE SIDE

Figure 7 Lateral Support System - Bonded Joints

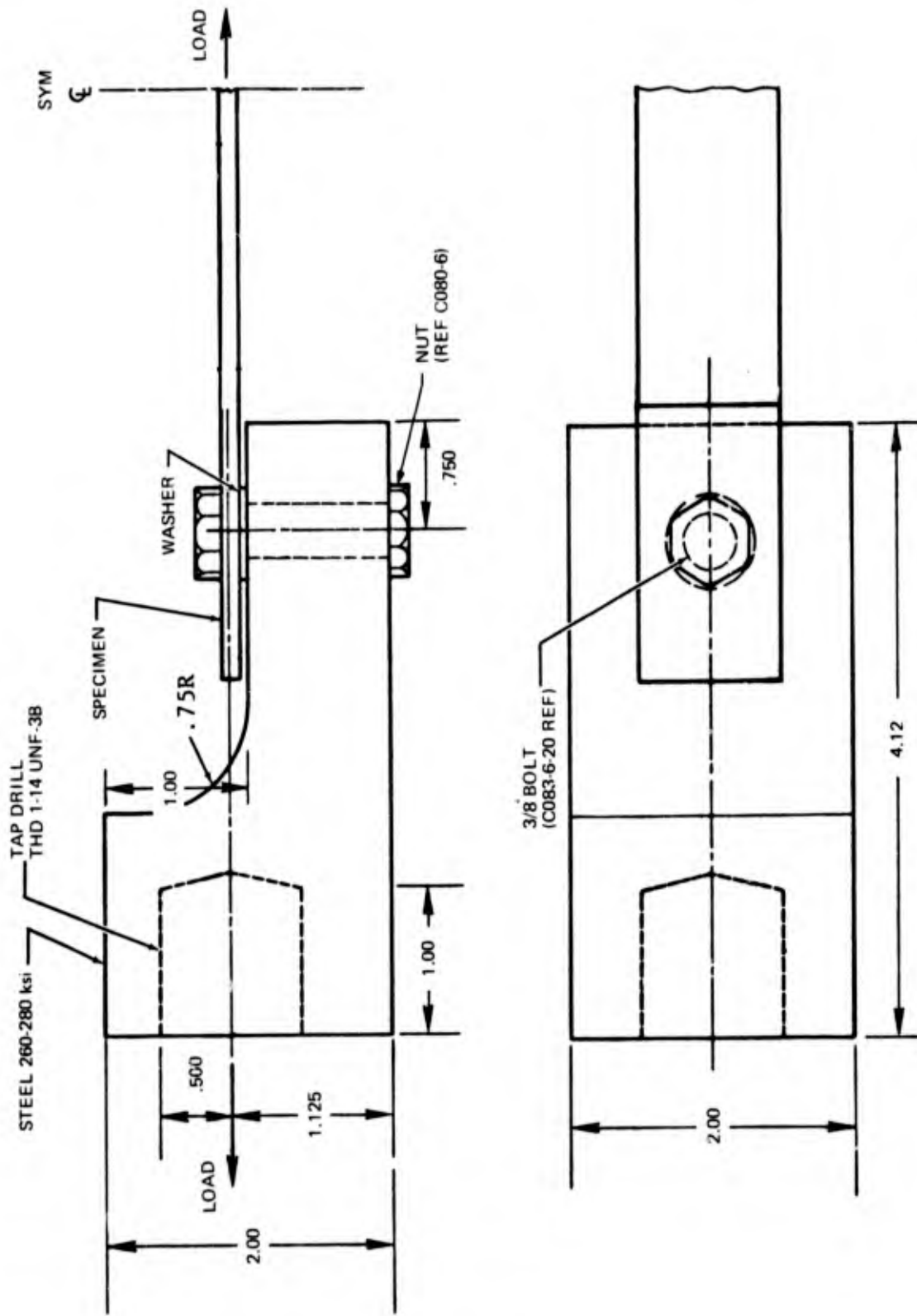


Figure 8 Single Shear Test Fixture - Bolted Joint Specimen

model parameters included residual strength versus lifetime, maximum stress (or truncation load) versus lifetime, and static strength. These three conditions and the Weibull distribution parameter estimates for each are shown in Table II.

### 3.4.1 Bonded Joints - Comparison With Previous Program

A comparison of the joints tested on this program and Reference 6 are summarized below.

<u>Item</u>	<u>Current Program</u>	<u>Prior Program</u>
Laminating material	Narmco 5208/Thornel 300	Fothergill & Harvey ERLA4617/HTS
Adhesive material	Reliabond 398	Reliabond 398
Titanium 6Al-4V gage	0.050 inch	.040 inch
Laminate thickness, average	20 plies; .120 in.	10 plies, .090-inch
Laminate orientation	$\left[ (0, +45, 0, -45, 0)_s \right]_2$	$(0, +45, 0, -45, 0)_s$
Joint parameter, L/t	20	25
(Thick.laminate/ Thick.Ti)	2.40	2.25
Joint strength, average	5245 lb.	5950 lb.
Stress in Ti at joint ult	105 ksi	149 ksi

The highest load level used in fatigue on the prior program was 3130 pounds. The stress level in the metal tongue of the specimen at 3130 pounds was 78 ksi. The 3850 load level of the subject program gave a stress in the Ti of 77 ksi. The mean life of 5 specimens at 3130 pounds was 1.13. The mean life of 20 specimens at 3850 pounds was 1.42. The endurance capability of the joints tested on either program appears to be similar at equal stress levels in the titanium adherend.

The static capacity of the joints in the two programs was dissimilar. The adherend stress level, at the average joint strength, was well above titanium yield strength (approximately 126 ksi) on the earlier program, but it was below yield on the subject program. The difference in being above or below yield strength is reflected in the static test results. In the earlier program, 24 static test specimens failed at an average strength

Table II BONDED JOINT TEST CONDITIONS AND PARAMETER ESTIMATES

Condition	Spectrum Truncation (lb.)	Runout Limit (lifetimes)	Number of Tests	Weibull Estimates (1)			Static P(s) % (3)
				Scale Parameter (lifetimes)	Shape Parameter	Scale Parameter (lb.)	
Static	---		12	---	14.0	5350	---
Fatigue (lifetime)	5000	Failure	9	0.195	2.0		75
	4700	Failure	20	0.404	1.4		90
	4500	Failure	5	1.03	1.1		95
	4100	Failure	20	0.90	1.5		99
	3850	Failure	20	1.69	2.1		>99
	3500	Failure	9	6.82	2.2		>99
Residual Strength (2)	3550	0.1	13		15.0	5800	
		1.0	19		8.8	5592	
		3.25	25	3.11	2.4		

NOTES:

- (1) Maximum Likelihood Estimates (MLE)
- (2) Includes specimens failing in fatigue prior to specified runout condition.
- (3) P(s) = Probability of survival for truncation load shown.

of 5950 pounds, and with a Weibull shape parameter estimate of 47.34 (coefficient of variation of 2.7 percent). In this program, 12 static test specimens failed at an average strength of 5245 pounds, and with a Weibull shape parameter estimate of 14 (coefficient of variation of 8.7 percent). In other words, bonded joints that fail statically through induced cracking, as a result of yielding of the metal adherend, have significantly less scatter than specimens that fail due to interface weaknesses that propagate into flaw growth randomly at stress levels below metal yield strength. However, in either case, fatigue loading apparently activates the inherent "flaws" to propagate in an almost identical rate and manner so that for comparable stress levels the two specimen types have similar lifetime characteristics.

NOTE: The "flaws" in the material are not quality discrepancies. The Reference 6 program included ultrasonic NDT evaluation of every specimen tested. All specimens were void-free within the resolution of the NDT equipment. In this case, "flaw" indicates the latent material flaw.

### 3.4.2 Test Results

The total listing of individual bonded joint test results is given in Appendix I, and the results are discussed in this section. Reliability analyses are given in Section IV. Failure modes are discussed in subsection 3.4.3. The average static strength (and the Weibull mean) of bonded joints was 5150 pounds. Based on the MLE estimates of Table II, the static probability of survival was calculated (also in Table II) to aid in setting truncation load levels for fatigue testing.

The highest truncation load selected, 5 kips, was introduced after the results at 4.7 kips were known. The 5 kips truncation was expected to give failures in a shorter lifetime than was observed (scale parameter was 0.195 lifetime) so that the truncation load-endurance relationship might include three decades of life. Raising the truncation level above 5 kips was not risked due to the high probability of static failure. The results are presented in Figure 9.

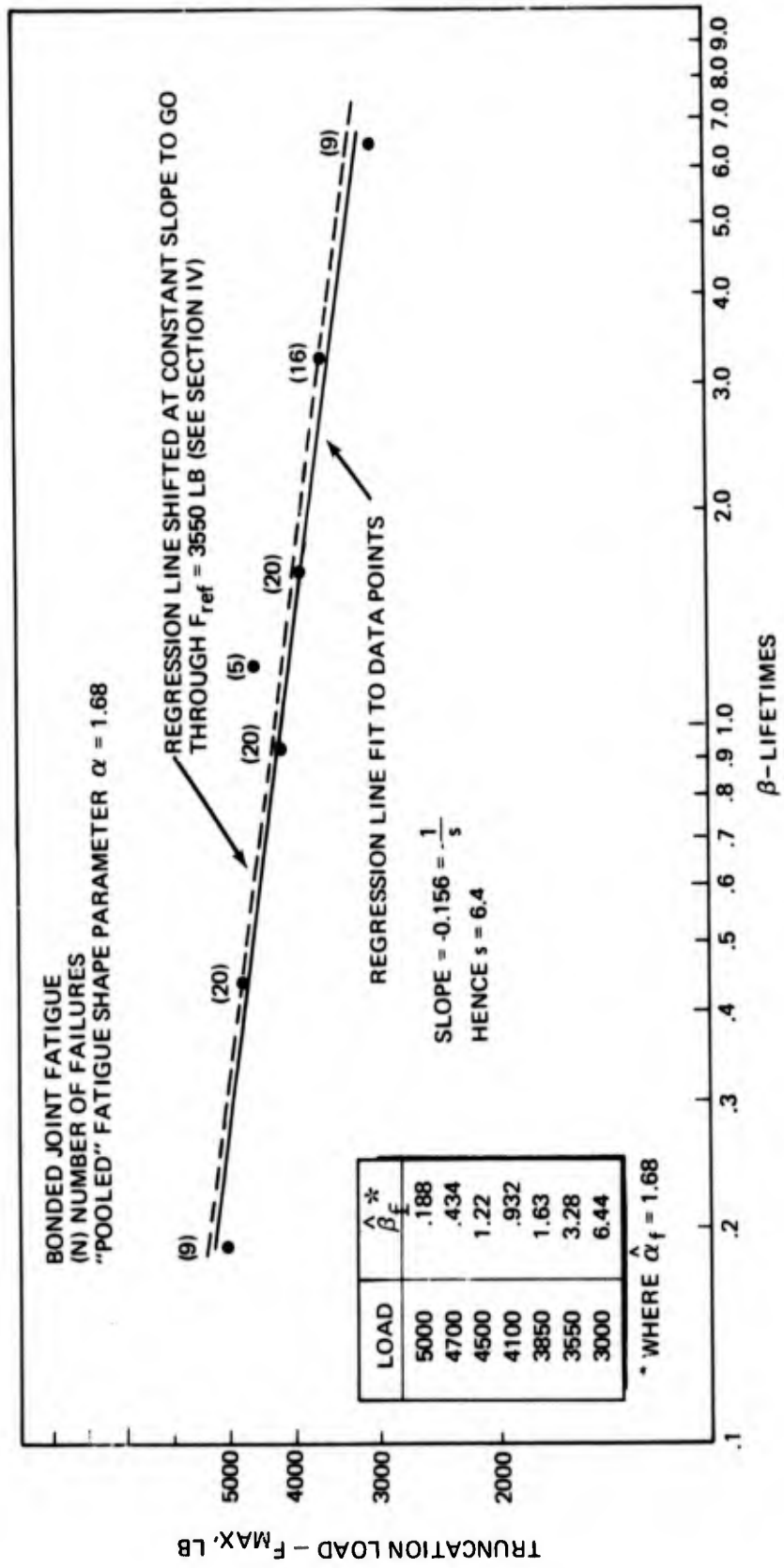


Figure 9 Bonded Joint - Truncation Load Vs Lifetimes

The model assumption that the relationship between truncation load and lifetime is linear when plotted on logarithmic paper is substantiated by this data set. The relationship is given as

$$\left( \frac{A_1}{A_2} \right)^{-s} = \frac{\beta_1}{\beta_2}$$

where  $A_1$  and  $A_2$  are spectrum magnification parameters ( $F_1(t) = A_1 F_{ref}(t)$ )

$\beta_1$  and  $\beta_2$  are the corresponding characteristic lifetimes

and  $s$  is related to  $r$ , the model flaw growth rate exponent (Section IV).

A linear regression of the data points of Figure 9 gives a slope of  $-6.4 = -s$ . This value is used in the analysis presented in Section IV.

The data of Figure 9 was studied to determine a truncation load level to conduct residual strength tests. (Note the data point for truncation load of 3550 was not known when residual strength load level was selected.) A load level of 3550 pounds was chosen. Lifetime "cut off points" of 0.1, 1.0, and 3.25 were selected as residual strength conditions. The latter condition was actually set empirically. It was decided that the longest lifetime condition should have approximately 2/3 fatigue failures, and the endurance data indicated that this should occur between 2 and 3.5 lifetimes at 3350 pounds. Six specimens were loaded to check the selection of load level. Three specimens failed at 2.11, 2.50, and 1.52 lifetimes, respectively, and the survivors were stopped at 3.25 lifetimes. Then, the remaining specimens were committed for test under the same conditions. The results, 16 fatigue failures in 25 tests, satisfied the load level selection criteria almost exactly.

The residual strength-lifetime results are presented in Figure 10. Comparative data from Reference 6 are presented in Figure 11. The initial Weibull parameter estimates of  $\alpha_0$  are dissimilar in the two programs (Paragraph 3.4.1); however, the characteristics of the strength-lifetime relationship are similar, i.e., mean residual strength degrades gradually and variability broadens rapidly as life increases.

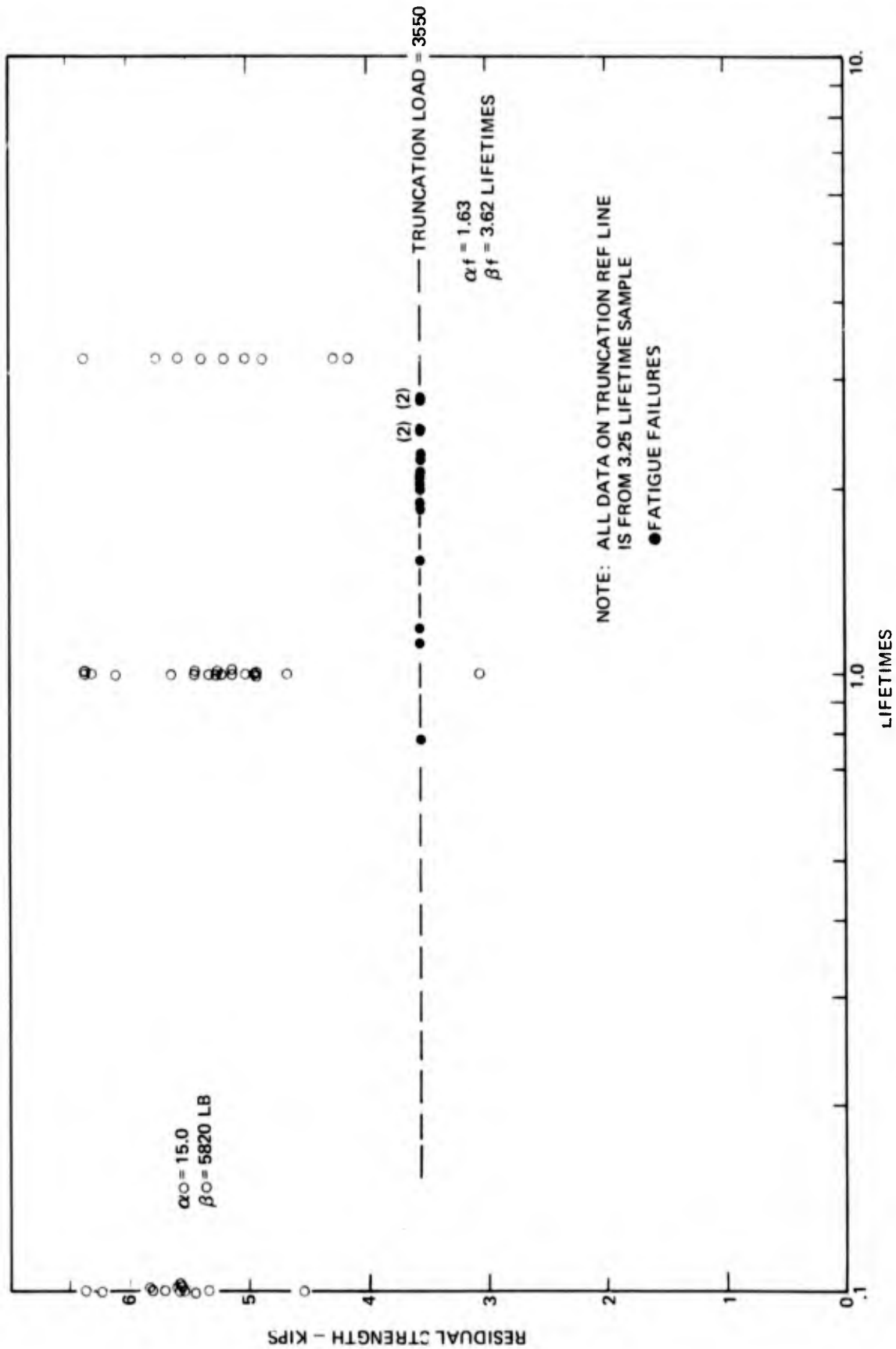


Figure 10 Bonded Joint - Residual Strength Vs Lifetime

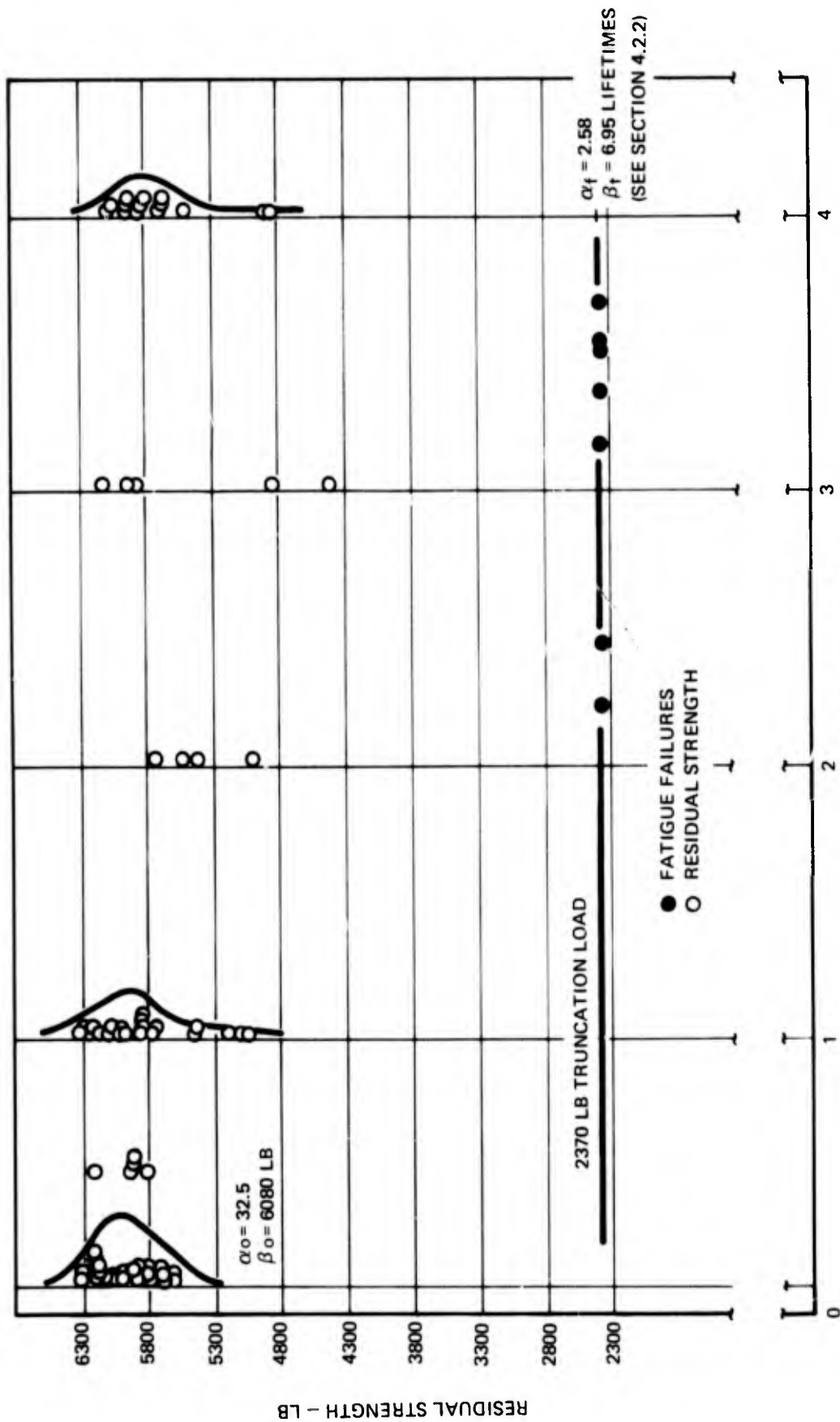


Figure 11 Empirical Wear-Out Model Data From Reference 6

The anomaly of static strength  $\beta$  estimates being less than  $\beta$  estimates after 0.1 lifetime is believed to be due to initial specimen relaxation.

A second, apparent anomaly is the residual strength result at the 1 lifetime condition, which is less than the truncation load. Obviously, the fatigue loads did not exceed the final specimen residual strength of 3050 pounds before the 1 lifetime run-out. The load of 3050 is a 70 percent load for a spectrum with a 3550-pound truncation load. Since loads of 70 percent and higher occur frequently in a spectrum (Table I), the residual strength of the subject specimen degraded slowly in time until just before it reached 1-lifetime runout when the strength loss rate must have accelerated rapidly. The characteristic residual strength-lifetime behavior described above for this particular specimen (or any specimen) is predicted by the fatigue model as illustrated in Figure 12 (adapted from Reference 6). The probability of a specimen surviving fatigue loading during this accelerated strength loss phase is very low; the subject specimen is the only such survivor in a total of 155 tested on this and the Reference 6 program.

### 3.4.3 Failure Modes

The bonded joint static ultimate specimen failed interlaminarily, possibly due to the high tension (peel) forces that occur at the edges of the joint overlap. Typical failures are illustrated in Figure 13.

Residual strength failures are illustrated in Figure 14. Each failure surface of the three specimens selected for documentation is shown. The right-hand failure surfaces illustrate the progression of the fatigue crack across the bond area as characterized by a roughly parabolic line (approximately at the center of the surface). The left-hand failure is interlaminar and is believed to be secondary, i.e., a peel failure induced after the initial shear failure on the opposite bond surface.

An unusual residual strength failure mode is illustrated in Figure 15. This is the specimen (Figure 10) that survived fatigue loading, but it had residual strength less than the spectrum truncation load. This specimen is the only one that had an angle ply (45-degree lamina) separate during loading.

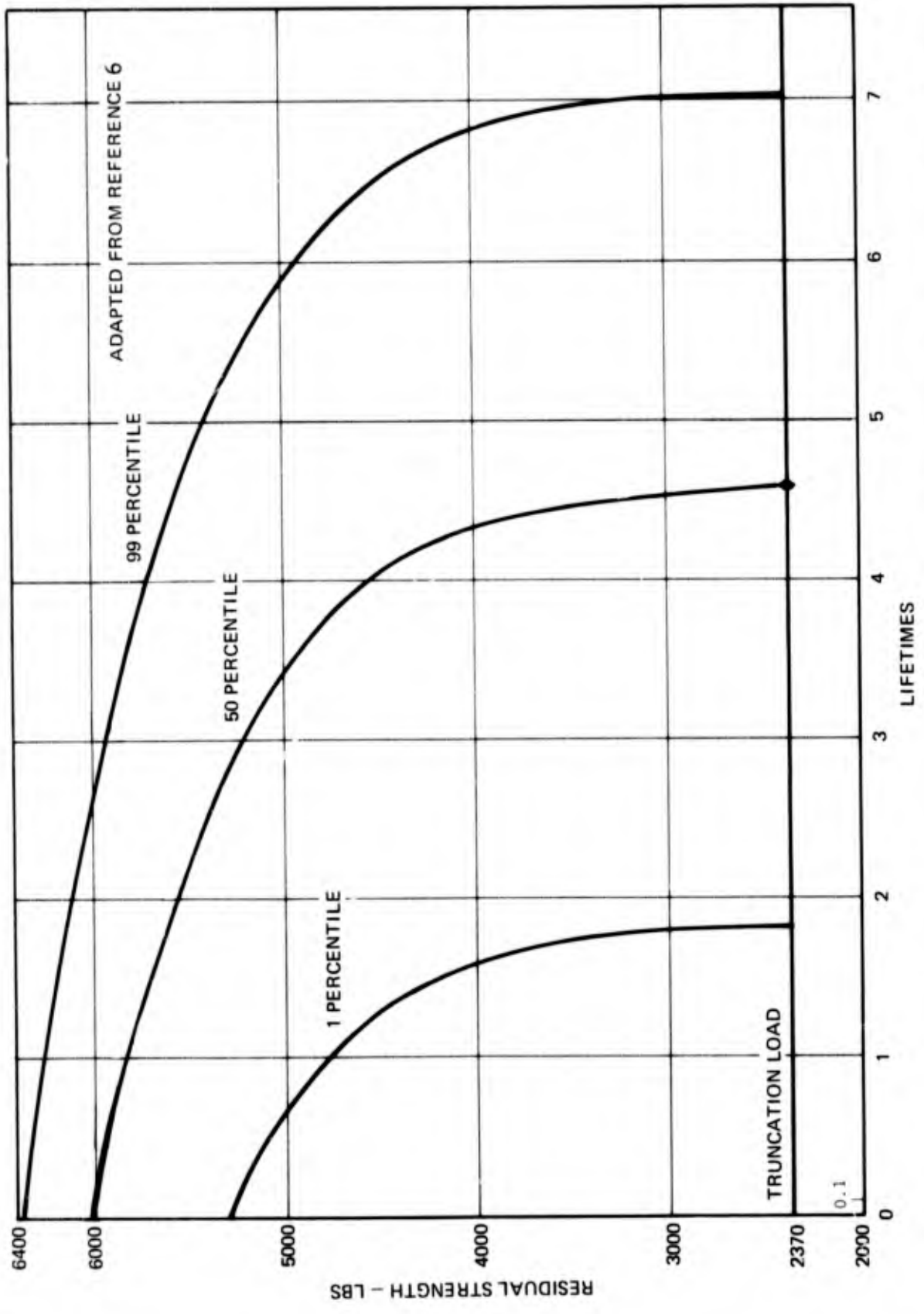


Figure 12 Probability of Survival Percentiles of Bonded Joints Predicted by Model

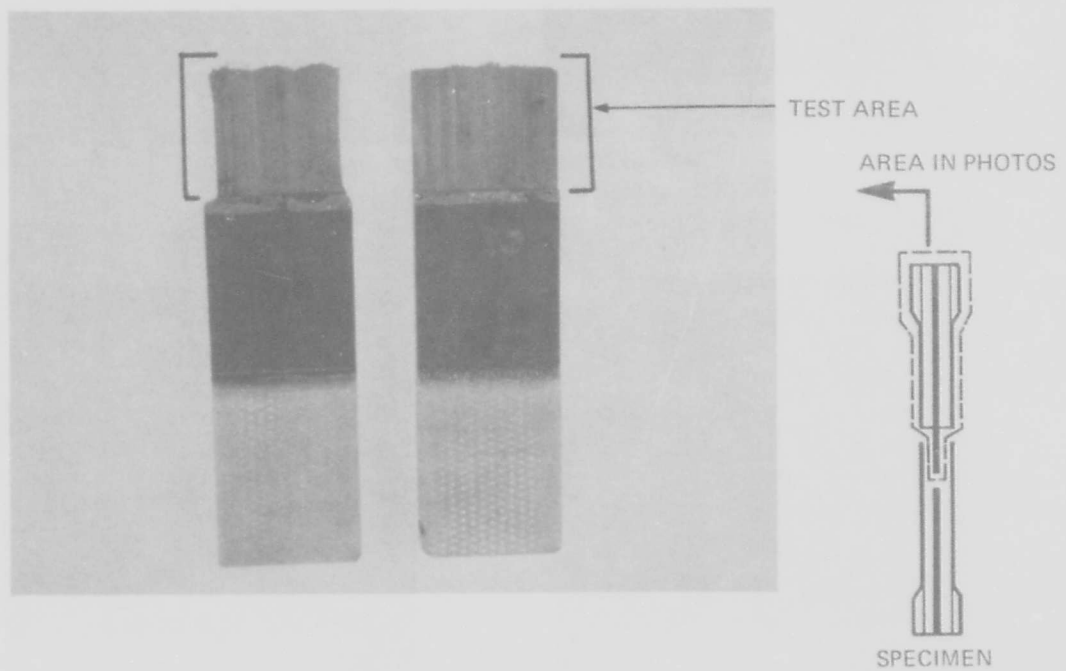
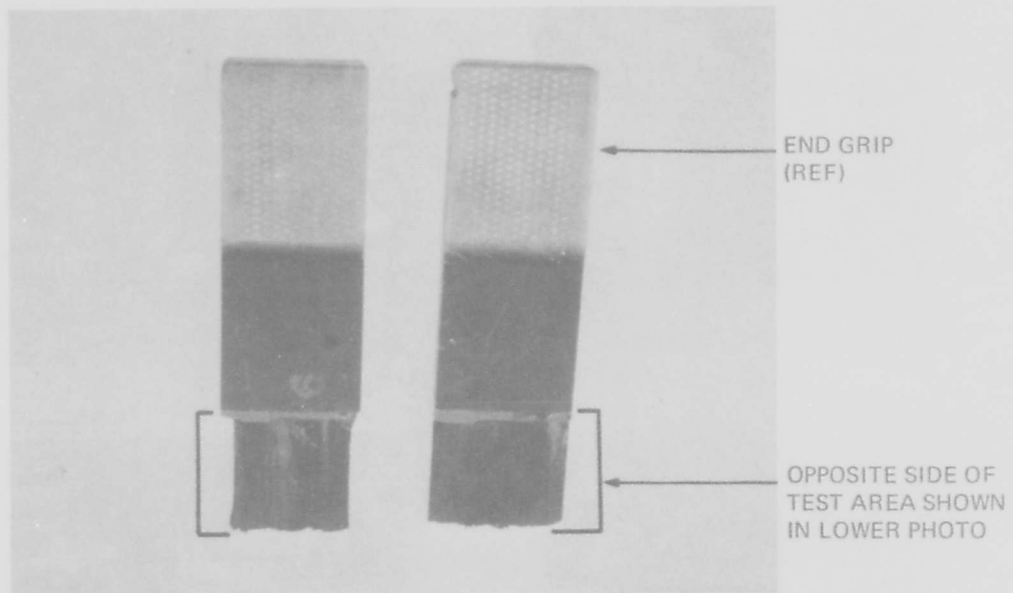
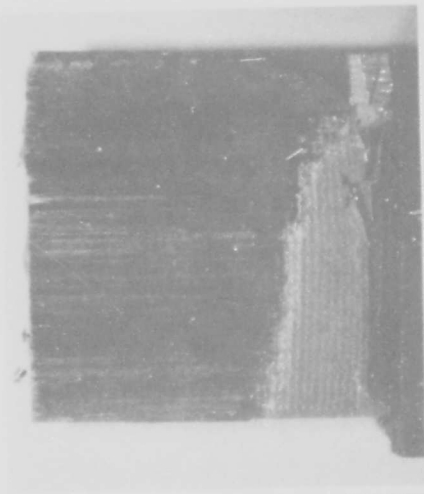
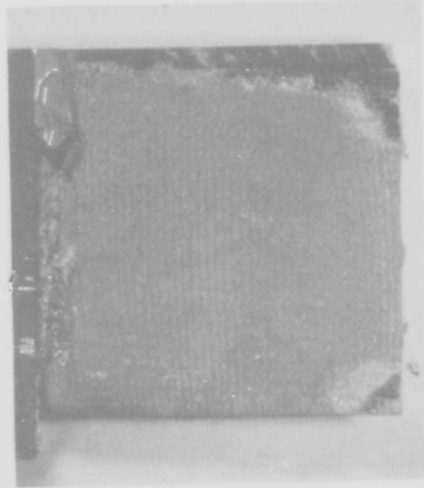


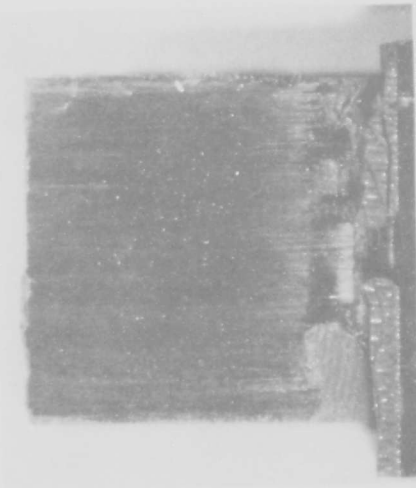
Figure 13 Static Bonded Joint Failure Modes



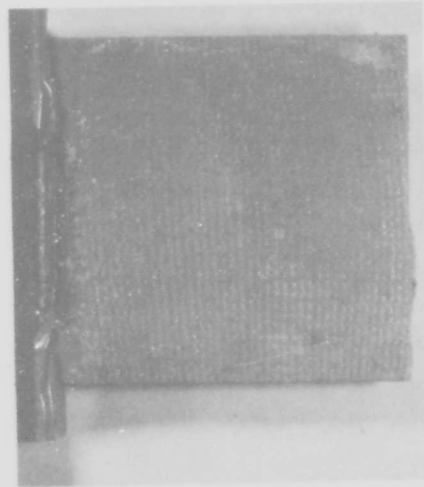
2½X



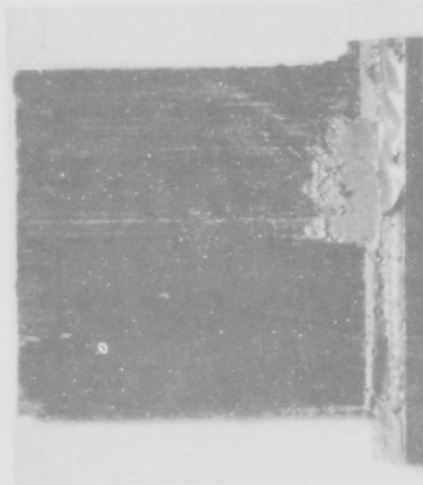
BOTTOM SPECIMEN NO. 4-6



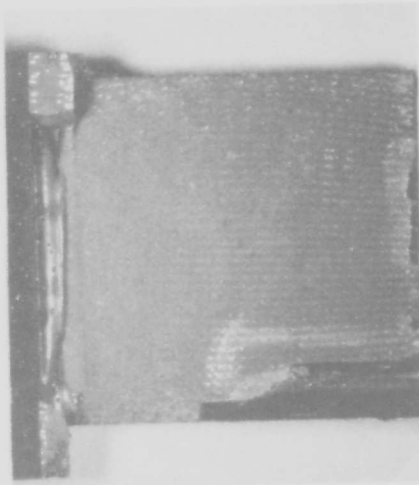
2½X



CENTER SPECIMEN NO. 4-22



2½X



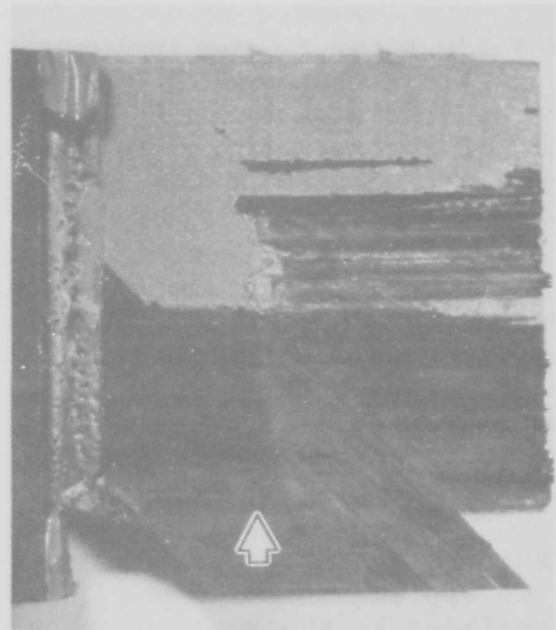
TOP SPECIMEN NO. 5-14

NOTE: THE LEFT-HAND SIDE OF EACH PAIR OF PHOTOGRAPHS IS THE OPPOSITE SIDE OF THE BONDED JOINT TEST AREA SHOWN ON THE RIGHT-HAND SIDE.

Figure 14 Bonded Joint Residual Strength Failures



OPPOSITE SIDE OF R.H. SURFACE



BROKEN GRAPHITE TOW

Figure 15 Bonded Joint Residual Strength Specimen No. 3-7

### 3.5 BOLTED JOINT TESTING

Bolted joints were tested to develop data to examine the fatigue model's applicability. Therefore, the same type of data generated for bonded joints was obtained for bolted joints. The test conditions are summarized in Table III.

The laminate orientation used for bolted joint testing was identical to the laminate adherends of the bonded joint. No attempt was made to incorporate a laminate designed to reduce the stress concentration effects of the bolt hole through use of "buffer strips" (Reference 9). The laminate had 60 percent 0-degree lamina in the load direction, and the bolt hole was drilled directly through the laminate. Another aspect of the bolted joint specimen and test method to be noted is the loss of bolt torque during the spectrum loading. The 3/8-inch-diameter bolts were initially torqued to 200 inch-pounds under 20 percent of the peak spectrum tensile load (truncation). Specimens were then observed to lose some torque during the fatigue loading. Subsequently, the bolts were retorqued at 45-minute intervals, to 200 inch-pounds for the duration of the fatigue test. Three factors combine to loosen the fasteners: "frequency" of the spectrum (approximately 10 loads per second), the simple single fastener joint design, and the unusually large negative GAG load applied in 0.1 second. Fatigue tests conducted on bolted specimens in the Reference 8 program using a random spectrum with a broad-band PSD and a realistically applied (in terms of both rate and magnitude) GAG load have retained significant torque through multiple lifetimes without being retorqued. Although most of the joint data developed was for the case where retorquing of the bolts was a part of the test method, some of the data was developed in tests (Table III) in which the bolts were not retorqued during fatigue loading.

Two laminates were required to obtain the total number of details required for bolted joints. This was not originally a part of the test plan, but a large number of specimens were used in attempting to load via double shear, pinned or bolted. The test conditions of Table III are identified as having specimens from "Set 1" or "Set 2" to designate the use of two laminates for sampling.

Table III BOLTED JOINT TEST CONDITIONS AND PARAMETER ESTIMATES

Condition	Spectrum Truncation (lb.)	Number of Tests	Run-out Limit (lifetimes)	Weibull Residual (1)		Weibull Lifetime (1)		Static P(s)
				Scale (lb.)	Shape	Scale (lifetime)	Shape	
Static Set 1 (3) Set 2 (3)	----	20	----	4790	24.2			
	----	23	----	4390	28.2			
Fatigue (lifetime) Retorqued Retorqued Retorqued Retorqued	4175	16	10-15% wear (4)			.162	.69	95%
	4040	15	10-15% wear (4)			.259	1.25	97.5%
	3875	19	10-15% wear (4)			.952	1.51	99%
	3500	6	10-15% wear (4)			2.03	2.32	>99%
Torqued only at time = 0	3500	19	10-15% wear (4)			.99	.92	
	2500	16	10-15% wear (4)			16.0	1.12	
Residual Strength (5) Retorqued	3550	20	0.025	4640	29.7			
	3550	14	0.25					
	3550	15	1.0			1.64	1.41	
Torqued only at time = 0	3000	15	0.50					
	3000	15	0.75			1.28	.98	

NOTES:

- (1) Maximum Likelihood Estimates
- (2) Probability of survival for truncation load shown.
- (3) Specimens from two different laminates. Fatigue specimens were from Set No. 1. Residual Strength specimens from Set No. 2.
- (4) Wear at bearing hole in terms of initial hole diameter.
- (5) Includes fatigue failures prior to specified run-out limit.

### 3.5.1 Test Results - Specimens Retorqued During Fatigue Loading

The listing of individual test results is given in Appendix II, and the results are discussed in this section. The reliability analyses are given in Section IV, and failure modes are discussed in subsection 3.5.3.

The average static strength was 4600 pounds for Set 1 and 4300 pounds for Set 2. Estimates of the Weibull shape parameter were similar, i.e. 24.2 and 28.2, respectively. The resin content of each set is given in Table IV.

Table IV LAMINATE RESIN CONTENT

Set 1 % of Laminate Weight	Set 2 % of Laminate Weight
28.18	29.43
27.30	27.59
26.03	29.94
28.56	29.93
Average	Average
27.51	29.22

Based on the MLE estimates of Table III, the static probability of survival,  $P(s)$  was calculated to aid in setting truncation load levels. Values of  $P(s)$  are included in Table III.

The results of the truncation load-lifetime experiment are given in Figure 16. The MLE Weibull scale parameter and the first specimen failure for each truncation load level are shown. Both sets of data may be fit closely with a straight line, but the fit is not as good as that for the bonded joint data (Figure 9). In the case of the 2500-pound truncation load, only five results were available, and none of these were fatigue failures. Therefore, this condition is not shown in Figure 16.

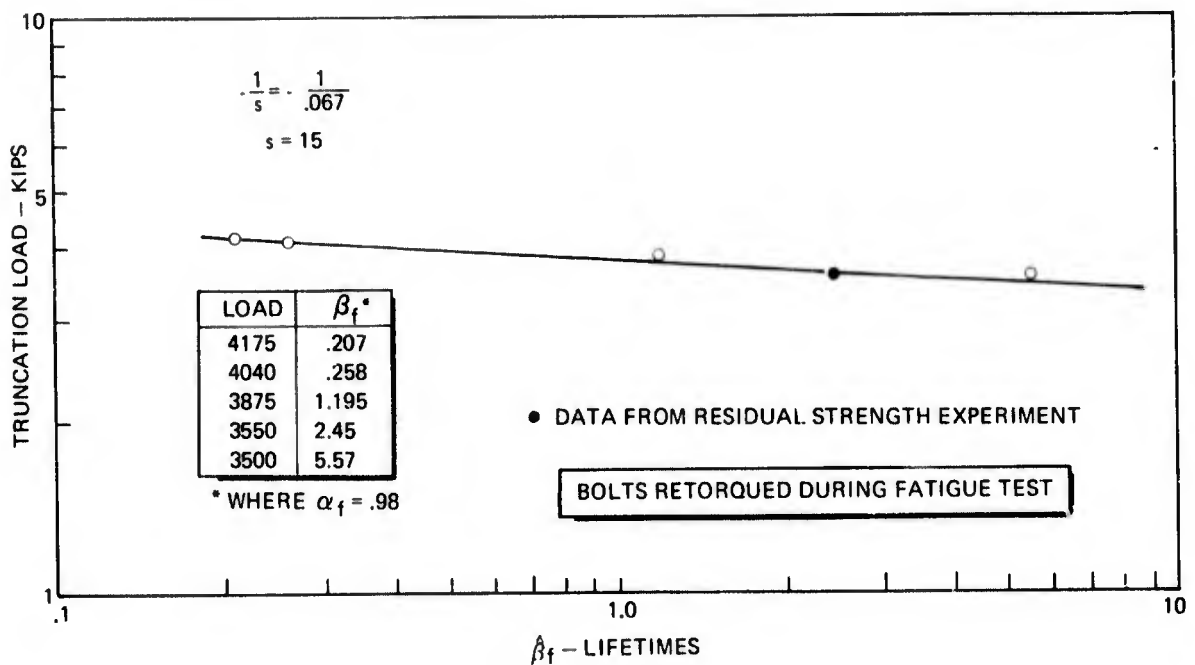
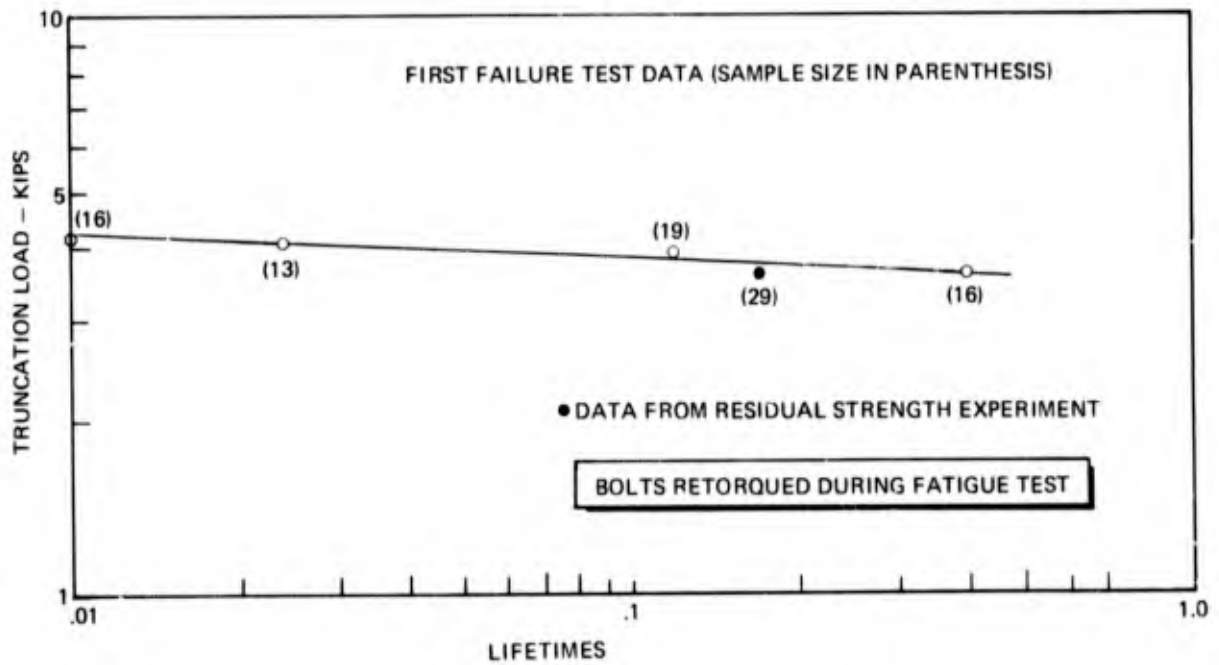


Figure 16 Bolted Joints - Truncation Load Vs Lifetime

Selecting the truncation load level for the residual strength-lifetime experiment became an investigation in itself. A load level that would give an average fatigue life of 3 lifetimes was originally planned. A cursory examination of the truncation-lifetime data led to the selection of a truncation load of 2900 pounds. Four specimens were loaded through 3 lifetimes without failure. These were failed statically at high strength levels.

Fatigue/residual tests were then conducted at truncation loads of 3100, 3300, 3875, 3750, and 3570 in chronological sequence to provide additional data to allow selection of a proper load level. The results are given in Table V and Figure 17. The final load selected was 3550 pounds with a maximum "run-out" of 1 lifetime and two "cutoff" lifetimes of 0.025 and 0.25 to permit developing residual strength data.

The results of the residual strength-lifetime experiment at a 3550-pound truncation load are presented in Figure 18. There were no fatigue failures at 0.025 lifetime; however, 2 of 14 specimens failed at 0.25 and 4 of 15 failed at the 1 lifetime condition. A fatigue "failure" here refers to a specimen whose residual strength following fatigue loading is less than the truncation load or a shear-out failure. Failure modes are discussed in detail in subsection 3.5.3. The specimens that survived were failed statically when they reached the required life. Note that the mean strength of the survivors is high in comparison to the static strength range. Five new specimens were tested statically after the residual strength tests to confirm the original static strength results. The cross-check test average was 4298 pounds; the original static tests averaged 4306 pounds.

An open hole in a fiber-dominated laminate (large percentage of 0-degree fibers in load direction) may exhibit increasing mean residual strength as fatigue life increases. The results of loaded holes in fiber-dominated laminates herein indicate that mean residual strength of joints that survive fatigue loading may also increase as life increases. The implication would be that proof-loading to eliminate the weaker members of a population would extend time-to-first fatigue failure significantly.

### 3.5.2 Test Results - Specimens Torqued Only at Time = 0

Four sets of bolted joint specimens were tested using the procedures described earlier except that these specimens were

Table V BOLT BEARING RESULTS-SELECTION OF TRUNCATION LOAD

Truncation Load (lb.)	Specimen Number	Fixture Number	Lifetimes	Residual Strength (lb.)	Failure Location (Hole)	Failure	Comment
3875	5-19	3	.053	---	Upper	Shear Out	Excessive Compression Damage Both Holes
	4-23	2	.053	---	Upper	Shear Out	
	3-24	1	.053	---	Lower	Shear Out	
	6-23	4	.17	---	Both	Bearing	
3750	1-20	1	.66	4500	Upper	Net Section	Compressor Damage Upper Hole
	3-23	2	.40	4600	Lower	Net Section	
3570	2-11	3	.54	4700	Lower	Net Section	
	4-7	4	.54	4600	Lower	Net Section	
3300	1-21	1	1.51	4500	Upper	Net Section	Considerable wear Lower Hole Tens. & Comp Sides
	3-29	2	1.51	4700	Upper	Net Section	
	5-17	3	1.51	4250	Upper	Net Section	
	6-21	4	1.51	4300	Lower	Net Section	
3100	1-18	1	2.00	4250	Upper	Net Section	
	2-2	2	2.00	4400	Lower	Net Section	
	4-28	3	2.00	3900	Lower	Shear Out	
	5-11	4	2.00	4100	Lower	Net Section	
2900	1-15	1	3.00	4700	Upper	Net Section	
	4-19	4	3.00	4500	Lower	Shear Out	
	2-13	3	3.00	4550	Upper	Net Section	
	6-27	2	3.00	4500	Upper	Net Section	

NOTE: Specimens are from "Set 2"



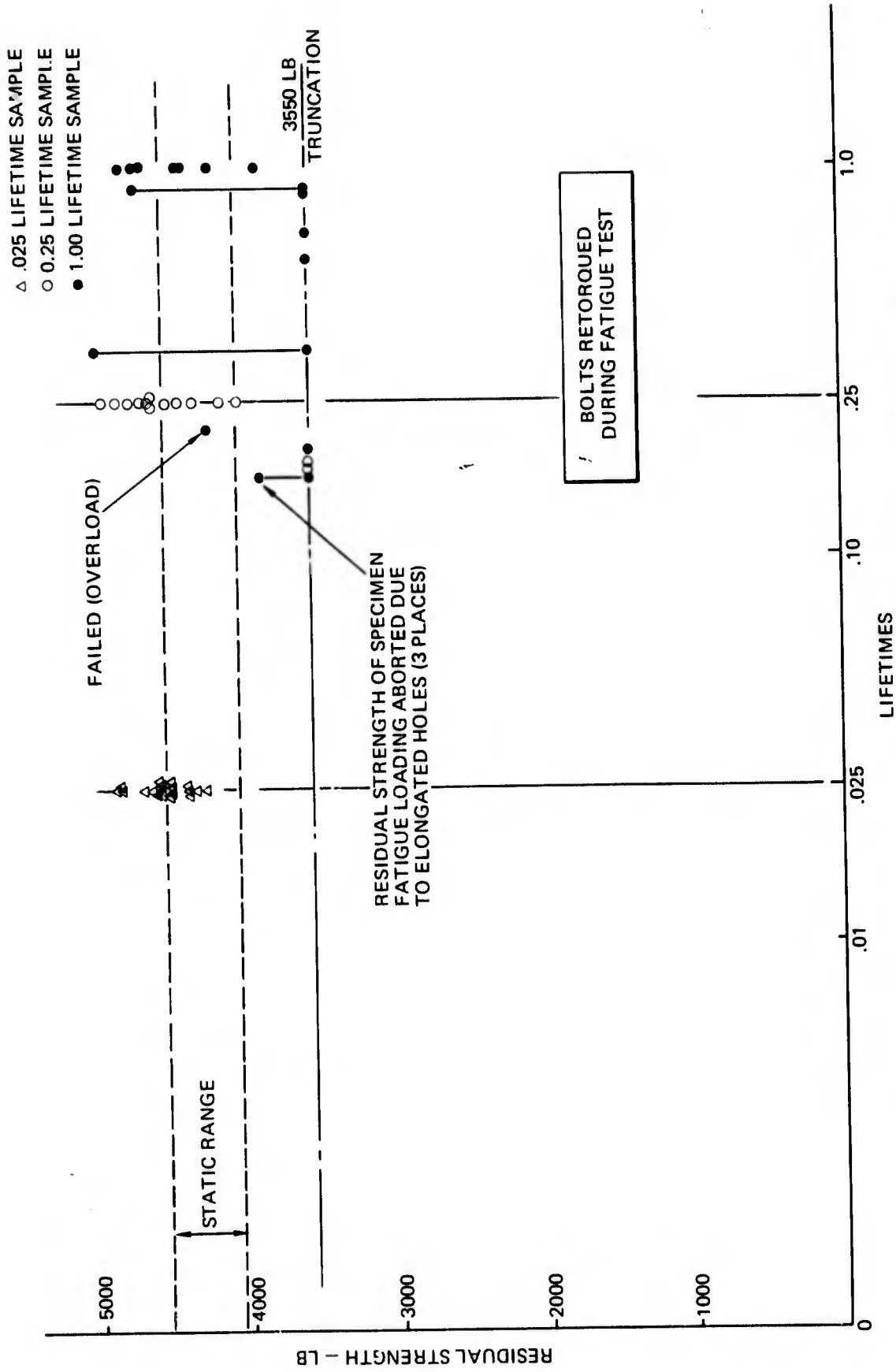


Figure 18 Residual Strength Experiment - Bolted Joints

not retorqued after the fatigue loading began. Specimens were loaded to failure ("failure" same as described above) at truncation load levels of 3500 and 2500 pounds. Then, additional specimens were loaded to a 3000-pound truncation load for two lifetime cutoff points to develop residual strength data.

The data generated without retorquing, Figure 19, is compared to the data developed where the fasteners were retorqued in Table VI. The interval used for retorquing specimens was 45 minutes, which is 0.037 lifetime (27,333 loads). At the truncation load level of 3500 pounds, the observed time-to-first-failure result of specimens that were retorqued was 7 times that of the specimens that were not. The sample Weibull scale parameter estimates differ by a factor of 2. The difference between pooled (for all load levels) shape parameter estimates is not significant. The large differential between the sample shape parameter estimates is reasonable because the estimate of the "retorqued" sample was based on fewer fatigue failures, i.e. only 2 failures in 16 specimens as opposed to 10 failures in 19 specimens for the "no retorquing" sample.

Table VI COMPARISON OF TORQUE EFFECTS IN FATIGUE LOADING

Truncation load, lb.	Retorqued <sup>(1)</sup>		Not Retorqued <sup>(2)</sup>	
	3500	2500 <sup>(4)</sup>	3500	2500
First failure (lifetimes)	0.68	----	0.097 <sup>(3)</sup>	0.65
Weibull Scale	2.03	----	0.99	16.0
Weibull Shape (sample)	2.32	----	0.92	1.12
Weibull Shape (pooled)	0.98		0.96	

NOTES:

- (1) Fasteners were retorqued during fatigue loading.
- (2) Fasteners were not retorqued during fatigue loading.
- (3) Specimen No. 1-10 failed at 0.027 lifetime; however, the retorquing interval was 0.037 lifetime.
- (4) No fatigue failures occurred at this condition.

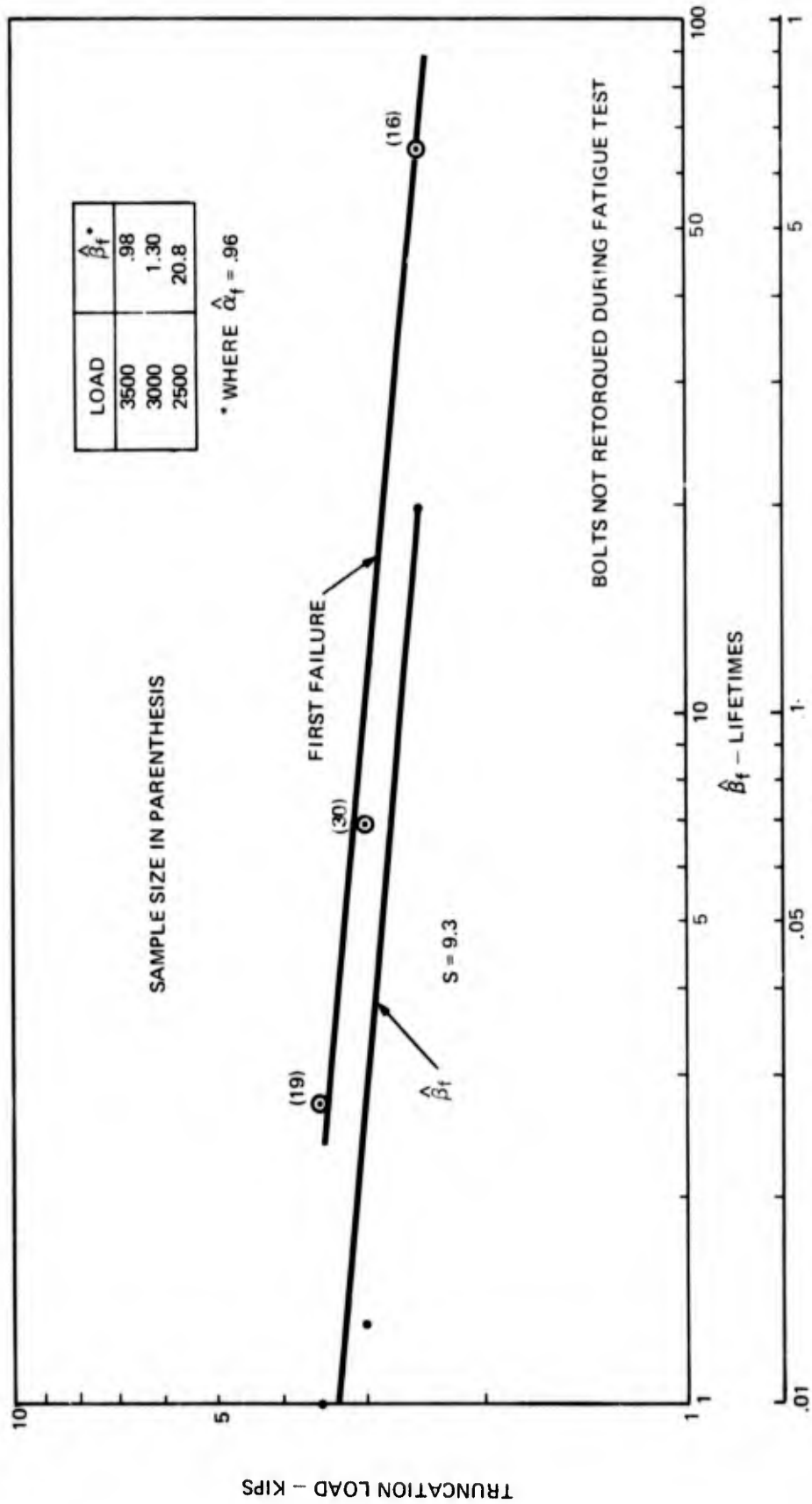


Figure 19 Bolted Joints - Truncation Load Vs Lifetime (Not Retorqued)

No fatigue failures occurred at the 2500-pound truncation load for specimens that were retorqued during loading; therefore, no comparisons can be made.

### 3.5.3 Failure Modes

The failure modes are correlated to individual specimen results in Appendix II. Static failure modes of bolted joint specimens are illustrated in Figure 20.

In the case of fatigue failures, failure modes are identified in Appendix II as follows:

1. Shear Out - This included failures in which the specimen broke on one or both sides of the bolt. (Figure 21).
2. Elongated hole (E.H.) - Bearing failure in laminate occurred primarily on tension side of bolt unless otherwise noted. The comment "excessive compression damage" indicates bearing failure due to delamination of the laminate primarily on the compression side of the bolt (Figure 22).
3. Compression - Failure occurred in the laminate on compression side of loaded bolt.

The number of specimens for each failure mode are shown in Table VII for each truncation load level.

Specimens that failed due to compression buckling were observed at the 4175- and 4040-pound truncation levels. The results of these specimens are shown in Appendix II, but they were not included in the analysis of Section IV. Specimens that failed due to elongated holes where "compression damage" was observed did not become unstable. In these cases, the compression damage was local crushing and delamination (crippling) of the laminate under the concentrated bolt load.

A failure criteria had to be defined for fatigue specimens that had elongated holes. The criteria established was 10 to 15 percent wear of the bearing hole diameter, i.e. 0.038 to 0.055 inch, at either end of the specimen. An attempt was made to use an electronic latch circuit to monitor the wear. However, this was not successful since significant wear occurred on both sides

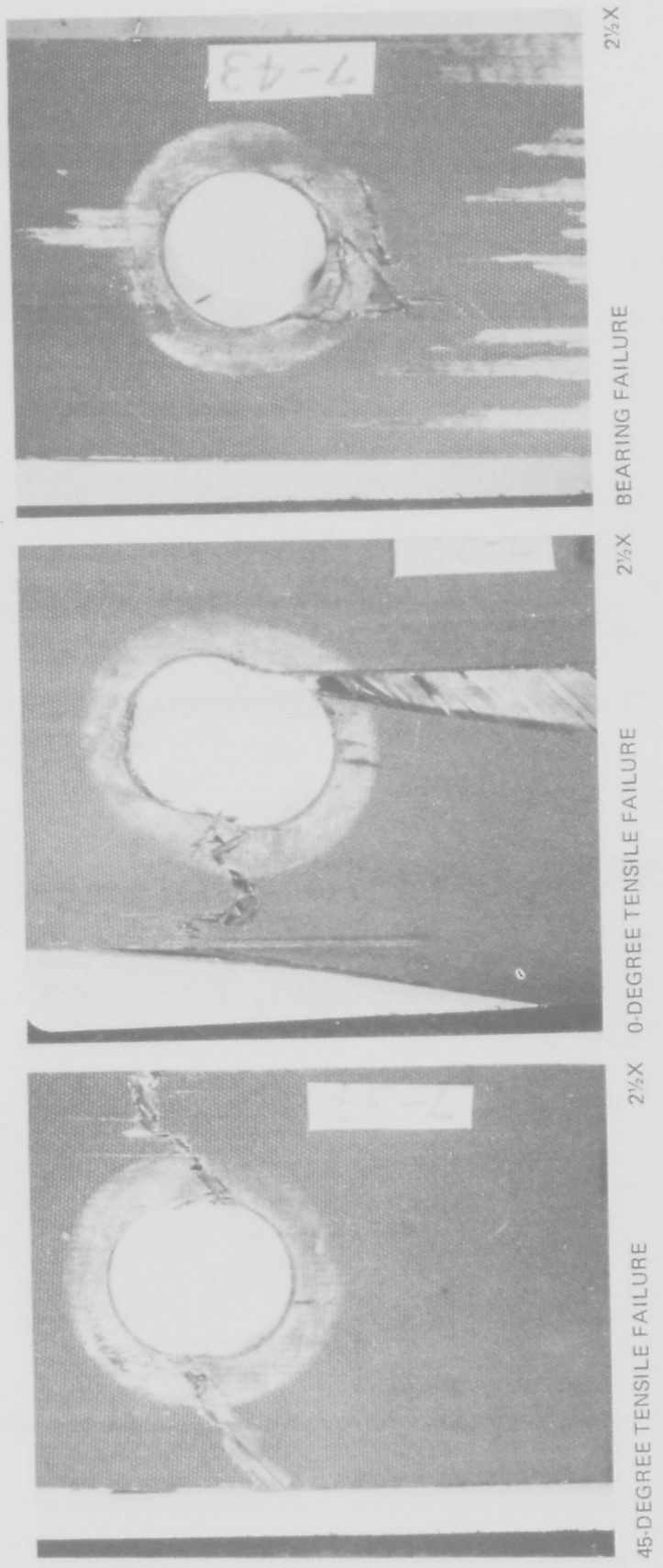
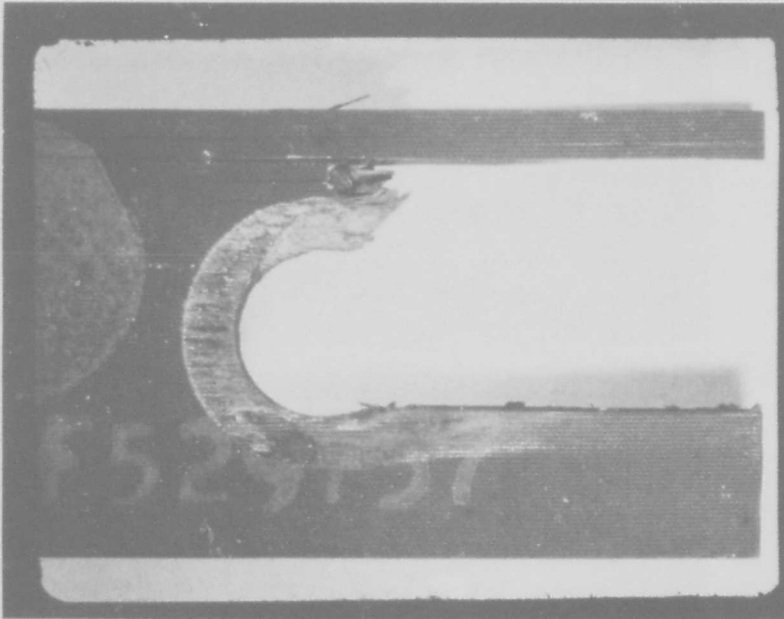


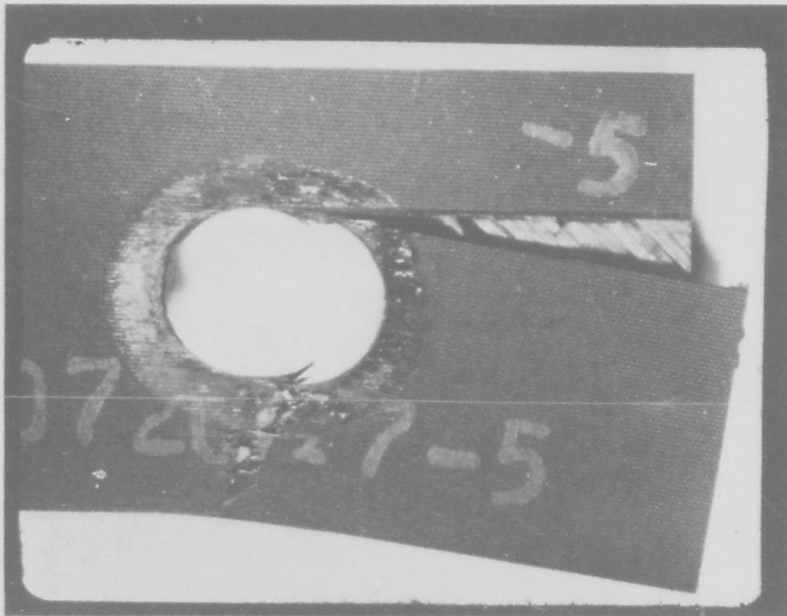
Figure 20 Static Bolted Joint Laminate Failures

CSE 1134



2½X

CSE 1136

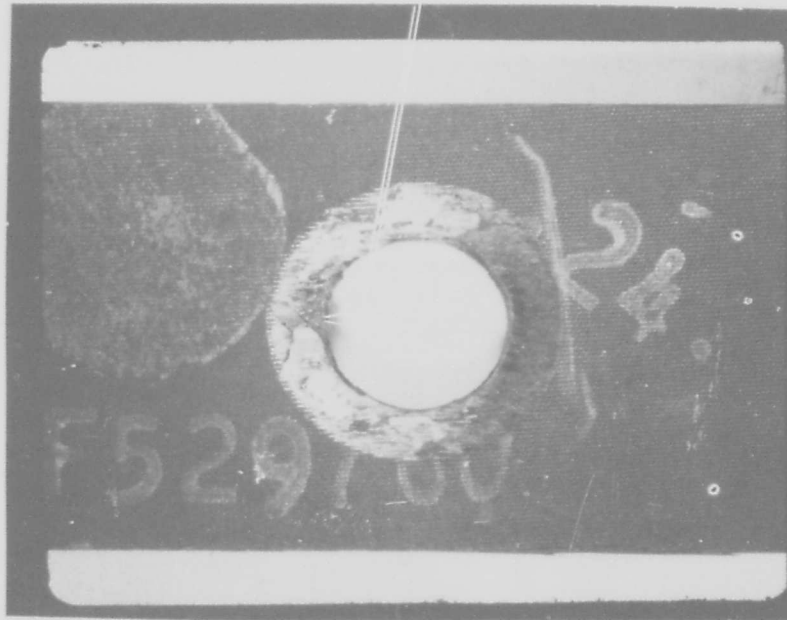


2½X

Figure 21 Shear-Out Fatigue Failures

APPLIED TENSILE LOAD DIRECTION

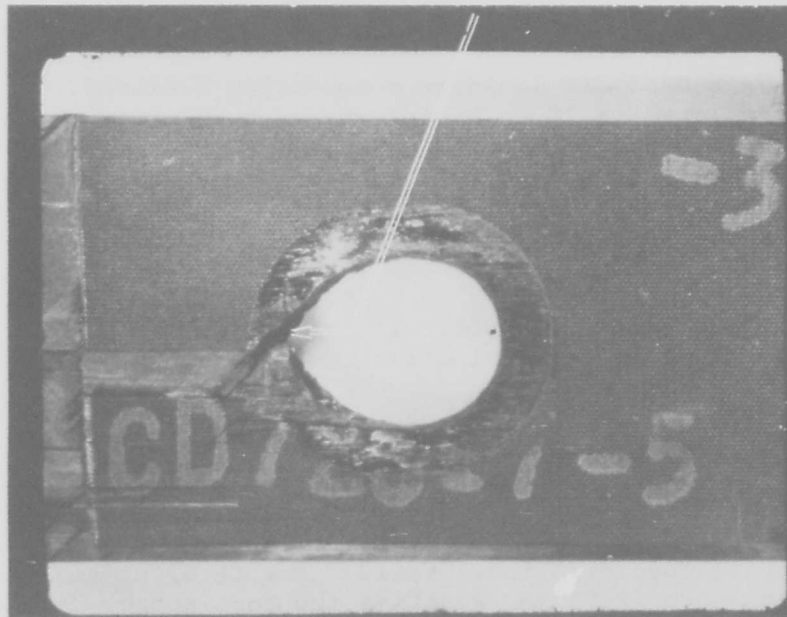
CSE 1133



2½X

APPLIED COMPRESSION LOAD DIRECTION

CSE 1137



2½X

SPECIMENS WHICH HAD COMPRESSION DAMAGE SIMILAR TO THIS ILLUSTRATION ARE DENOTED IN APPENDIX II.

Figure 22 Elongated Hole Fatigue "Failures"

Table VII BOLTED JOINT FAILURE MODE SUMMARY

Truncation Load (lb.)	Number of Tests (1)	Shear Out Failures	Elongated Hole "Failures" (2)	Elongated Hole Failures (7)
<u>Retorqued</u>				
4175	16	15	1	1
4040	13	10	3	1
3875	19	8	11	2
3550	29(3)	7	3	0
3500	16	3	13	1
2500	5(4)	0	2	0
<u>No Retorque</u>				
3500	19	9	10	1
3000	30(5)	11	2	0
2500	16(6)	2	12	0

NOTES:

- (1) This excludes laminate compression failures.
- (2) Failure is 10 to 15 percent wear of original bolt hole diameter.
- (3) At this load level, 19 specimens were stopped at either 0.25 or 1.0 lifetime "run-out".
- (4) Three specimens aborted without failure.
- (5) 17 specimens were stopped at either 0.50 or 0.75 lifetime "run-out".
- (6) Two specimens aborted without failure.
- (7) Failure is residual strength less than truncation load.

of the bolt and the monitoring arrangement included only the wear due to tension loads. Monitoring then became a "go-no-go" responsibility of the test engineers. The percent wear recorded for individual specimens that "failed" due to elongated holes is included in Appendix II and verifies the consistency developed in recognizing "failure." When wear was found to be less than 10 percent (determined by caliper measurement) specimens were retested until wear was sufficient to meet the failure definition. Only about a dozen specimens required retesting, and only about one-half of these required more than 0.015 lifetime additional loading to reach "failure." Since this failure definition was arbitrary, all specimens that were aborted due to

wear criteria were subsequently failed statically to provide residual strength data. Therefore, failure in the case of elongated bolt holes was redefined for analysis purposes as a specimen that had residual strength less than the spectrum truncation load. The number of specimens that failed due to this latter criteria are summarized by load level in Table VII.

SECTION IV  
DATA EVALUATION

The data of Section II was evaluated using the model developed in References 3 and 4. The four significant points that were to be examined with respect to the model through this program were

1. Applicability to bolted joints
2. Applicability to bonded joints over several decades of lifetime
3. Verification of the assumption that the fatigue shape parameter is independent of peak spectrum load level
4. Verification that the residual strength-lifetime relationship for any peak load level can be predicted using parameters estimated from a reference load level.

4.1 WEAR-OUT MODEL

The fatigue model is based on four assumptions (three physical and one of mathematical form).

1. Materials fail because of the presence of preexisting flaws.
2. Flaws grow in a deterministic manner. The manner is determined by material properties, state, and magnitude of the stresses at the flaw perimeter; history of applied stress; and the thermal and mechanical history.
3. The critical load for a structure is a function of instantaneous flaw state, and the distribution of residual strengths defines the flaw field statistics.
4. Damage rate accumulation is of the functional form:

$$\frac{\partial C}{\partial t} = M \cdot C^r, \quad (1)$$

where C is the flaw length and r is the flaw growth rate exponent.

The residual strength function  $F_R(t)$  can be shown to have the form

$$F_R(t) = \left[ F_R(t_0)^{2(r-1)} - A_4(r-1) A_1^S (t-t_0) \right]^{\frac{1}{2(r-1)}} \quad (2)$$

where:

1.  $A_1 = F_{\max}/F_{\text{ref}}$  with  $F_{\max}$  being the truncation load a measure of RMS stress and  $F_{\text{ref}}$  being a reference RMS stress level. (See Appendix III for additional discussion).
2. The term  $A_4$  is related to the history-dependent constant (M) in Equation (1).
3. The term  $r$  is the exponent of the flaw state (C) in Equation (1).
4. The term  $-1/s$  is the slope of the  $(\ln F_{\max})$  vs.  $(\ln t)$  curve and is related to  $r$ .
5. The term  $t$  refers to time and  $t_0$  is a reference time condition.

If the initial assumptions are correct, the results of varying stress history, environmental conditions, and geometry are contained in  $A_4$ .

Note that Equation (2) is a strictly monotonic decreasing function of time. Therefore, time  $t$  must be measured after the initial stress relaxation, discussed in subsection 3.4.2 and 6.1, occurs. If this point in time is considered to be the time origin,  $t = 0$ , Equation (2) may be considered applicable for all positive values of  $t$ .  $F(t=0)$  is the initial static strength of the component possessing a Weibull (extreme value) distribution

$$P(F(t=0) > F) = \exp \left\{ - \left( \frac{F}{\beta_0} \right)^{\alpha_0} \right\}, \quad (3)$$

where  $\alpha_0$  and  $\beta_0$  are the shape and scale parameters, respectively, for the Weibull distribution. Introducing the Weibull flaw distribution (3) into Equation (2), gives the time-varying residual strength distribution of the form

$$P(F_R(t) > F_R) = \exp \left\{ - \frac{\left[ F_R^{2(r-1)} + (r-1) A_4 A_1^S t \right]^{\frac{\alpha_0}{2(r-1)}}}{\beta_0^{2(r-1)}} \right\} \quad (4)$$

for  $F_R > F_{\max}$ ;

$$P(0 < F_R(t) < F_{\max}) = 0 ;$$

and

$$P(F_R(t) = 0) = 1 - P(F_R(t) > F_{\max}).$$

The probabilistic Equation (4) does not involve the reference time  $t_0$ , which appears in Equation (2), and agrees with Equation (3) when  $t = 0$ . For fixed time  $t$ , it follows from Equation (4) that the transformed variable  $F_R(t)^{2(r-1)}$  has a truncated three-parameter Weibull distribution.

The distribution depicted in Equation (4) has a limiting form for  $(F_{\max} / \beta_0)^{2(r-1)} \ll 1$ , which gives the lifetime distribution as

$$P(T > t) = P \left[ F_R(t) > F_{\max} \right] = \exp - (t/\beta_f)^{\alpha_f} \quad (5)$$

where

$$\alpha_f = \frac{\alpha_0}{2(r-1)} \quad (6)$$

$$\beta_f = \frac{\beta_0^{2(r-1)}}{(r-1) A_4 A_1^s} \quad (7)$$

If specimen behavior is found to be consistent with the model, the following responses would be expected.

1. The lifetime shape parameter would be independent of RMS stress, temperature, and humidity.
2. Both the truncation load-endurance data and initial shape parameter to fatigue shape parameter relationship will yield consistent values of  $r$ .
3. Characteristic strengths and endurance will shift log-linearly.

## 4.2 APPLICATION TO BONDED JOINTS

Bonded joint life as a function of truncation load is illustrated in Figure 9. The data range is approximately 0.2 to 7.0 lifetimes. In the previous program (Reference 6), the corresponding experiment had a data range of 1.3 to 6.9 lifetimes; hence, the subject data has broadened the lifetime range a full decade. The shortest life corresponds to a truncation load level (5000 pounds) that has a high risk of static failure; hence, it becomes improbable to increase the time range further by decreasing fatigue life into the neighboring decade. The alternative approach, i.e. to extend testing into the 10-lifetimes and greater decade, was not attempted due to budget constraints.

Under the assumption that the fatigue shape parameter ( $\alpha_f$ ) is known and constant, a value of the flaw growth exponent ( $r$ ) can be determined from Equation (6). Since the relationship between truncation load ( $F_{\max}$ ) and life ( $\beta_f$ ) has been determined empirically (Figure 9), the parameter  $A_4$  can be calculated from Equation (7). Calculation of the product  $A_4 A_1^s$  can be made for any truncation level for which  $F_{\max} - \beta_f$  is applicable; hence, Equations (4) and (5) may be used at any of these same truncation levels. The utility of the model in permitting stress level shifts is therefore dependent upon the initial assumption of  $\alpha_f = \text{constant}$ . This assumption was examined by testing 20 or more specimens at four truncation loads to provide estimates of  $\alpha_f$ , while two other load levels included tests on 9 specimens each. The estimates are shown in Table II. The range of estimates (for sample sizes greater than 5) for  $\alpha_f$  is 1.4 to 2.2 with an average of 1.84. This range of estimated values for the parameter is well within a 90% confidence band centered at the average value. Therefore, this data set tends to confirm previous experience that while the estimated values of  $\alpha$  vary from data set to data set this variation is within statistical expectation. For this analysis,  $\alpha_f$  may be considered to be constant.

#### 4.2.1 Evaluation of Bonded Joint Data

Equation (4) has been programmed on the Hewlett-Packard 9830 calculator to determine certain model parameters through iteration by minimizing the error (variance) between the prediction and sample data (residual strength-lifetime). The data shown in Figure 10 was input along with the parameter values

$$\alpha_0 = 15.0$$

$$\beta_0 = 5.82 \text{ kips}$$

$$A_1 = A_{\text{ref}} = 1.0.$$

In application, the iteration sequence was begun by assuming a value of  $r$ . Then, a value of  $A_4$  was determined through a least-squares fit of the relationship given in Equation (4). This is more easily observed if Equation (4) is rewritten in the form

$$\left\{ \frac{\beta_0^{2(r-1)} \left[ \ln \frac{1}{P} \right]^{\frac{1}{\alpha_f}} - F_R^{2(r-1)}}{A_1^S (r-1)} \right\} = A_4 t \quad (8)$$

where  $P = P(F_R(t) > F_R)$ .

This equation is represented functionally as

$$f(P, F_R) = A_4 t. \quad (9)$$

Therefore, the constant  $A_4$  is the slope of the linear regression equation fitted to the empirical data. The sequence (selection of  $r$ ) is repeated until the error term, i.e. the probabilistic squared difference between the model and the observed data, becomes a minimum.

The error converged to a minimum for the following values

$$A_4 = 6.53 \times 10^5 \frac{(\text{KIPS})^{2(r-1)}}{\text{life}}$$

$$r = 5.6$$

The model probability of survival curves and the data are shown in Figure 23. The fatigue parameters calculated from Equations (6) and (7) are

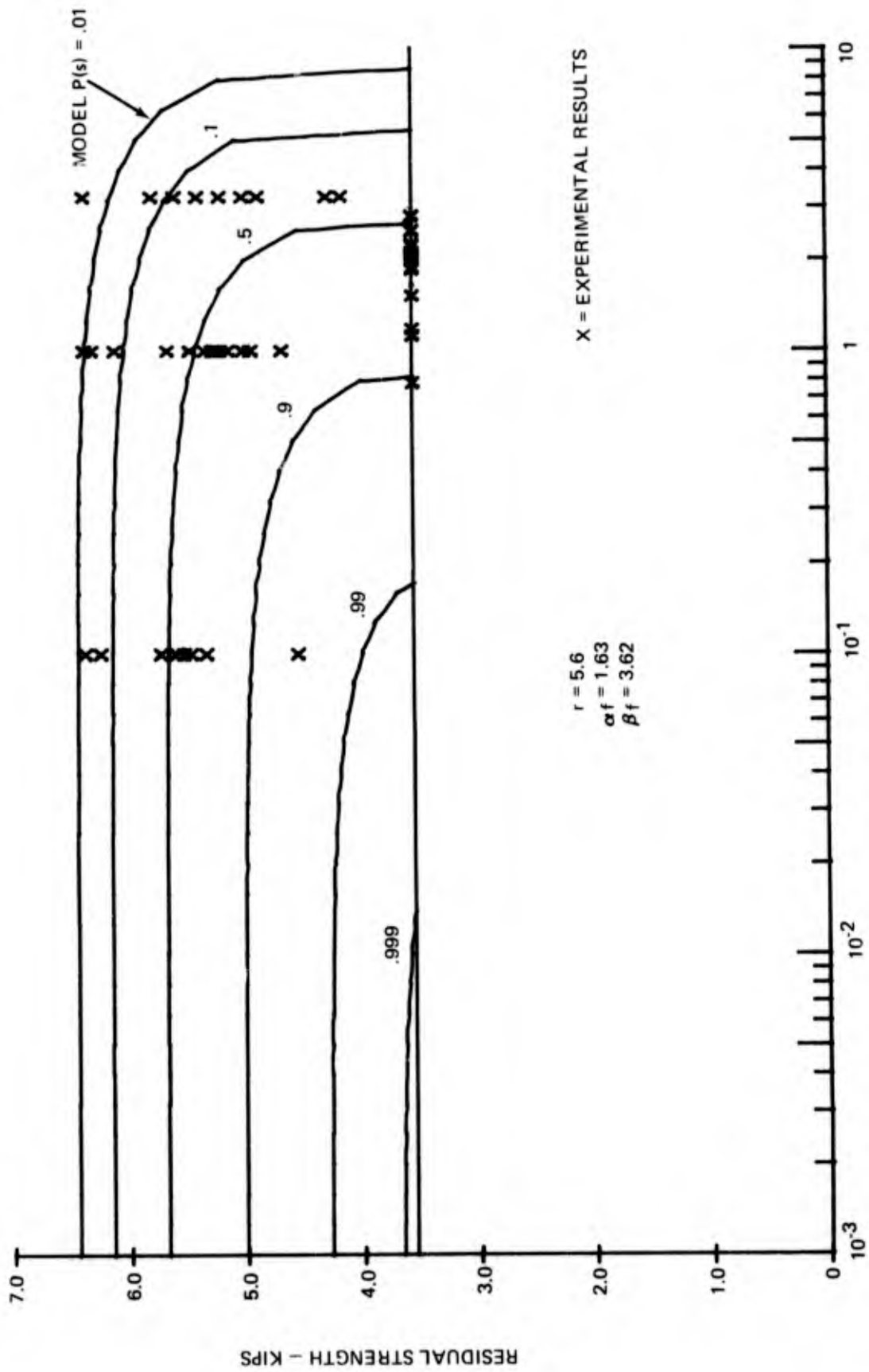


Figure 23 Residual Strength - Lifetime Model for Bonded Joints

$$\hat{\alpha}_f = 1.63$$

$$\hat{\beta}_f = 3.62 \text{ lifetimes.}$$

The overall fit of the model is moderately good. Test results (life and residual strength) plot 37 below and 20 above the median probability of survival,  $P(s)$ , curve. This indicates that the predicted value of life for this joint is somewhat high. (The MLE Weibull estimate, Table II, for the 3.25 lifetime condition predicted  $\beta_f = 3.11$  lifetimes as opposed to 3.62 for the model estimate). Two test results plot below  $P(s) = 90\%$  and seven plot above  $P(s) = 10\%$ . This is 3.5% and 12% respectively, of the sample of 57 specimens and illustrates again the model  $P(s)$  curves to be predicting slightly high.

The estimate of the shape parameter is in close agreement with the pooled MLE estimate (see Section V) determined from the truncation load-lifetime experiment (84 specimens), viz.

$$\hat{\alpha}_f = 1.68.$$

An independent investigation using a bonded specimen of similar design, i.e. double overlap, and identical adhesive material (Reliabond 398), laminate material (Thornel 300/5208) and laminate orientation, but tested in constant amplitude fatigue (Reference 12) reported a pooled (using the normalization method, Section V)  $\hat{\alpha}_f$  of 1.26 for the truncation load range of 2000 to 3100 pounds and 77 fatigue specimens. The referenced program also reported specimen static characteristics similar to the subject program, i.e.  $\hat{\beta}_0 = 5050$  pounds and  $\hat{\alpha}_0 = 11.0$ .

#### 4.2.2 Recalculation of Parameters from Previous Program

The Reference 6 program included a wear-out experiment on bonded joints of similar design to the subject program but with very different static characteristics. The differences were discussed in detail in Section III. The data of the earlier program has been reanalyzed using the methodology discussed above. The results of the new analysis are presented in Figure 24. A comparison of the parameter estimates obtained in each analysis is given below.

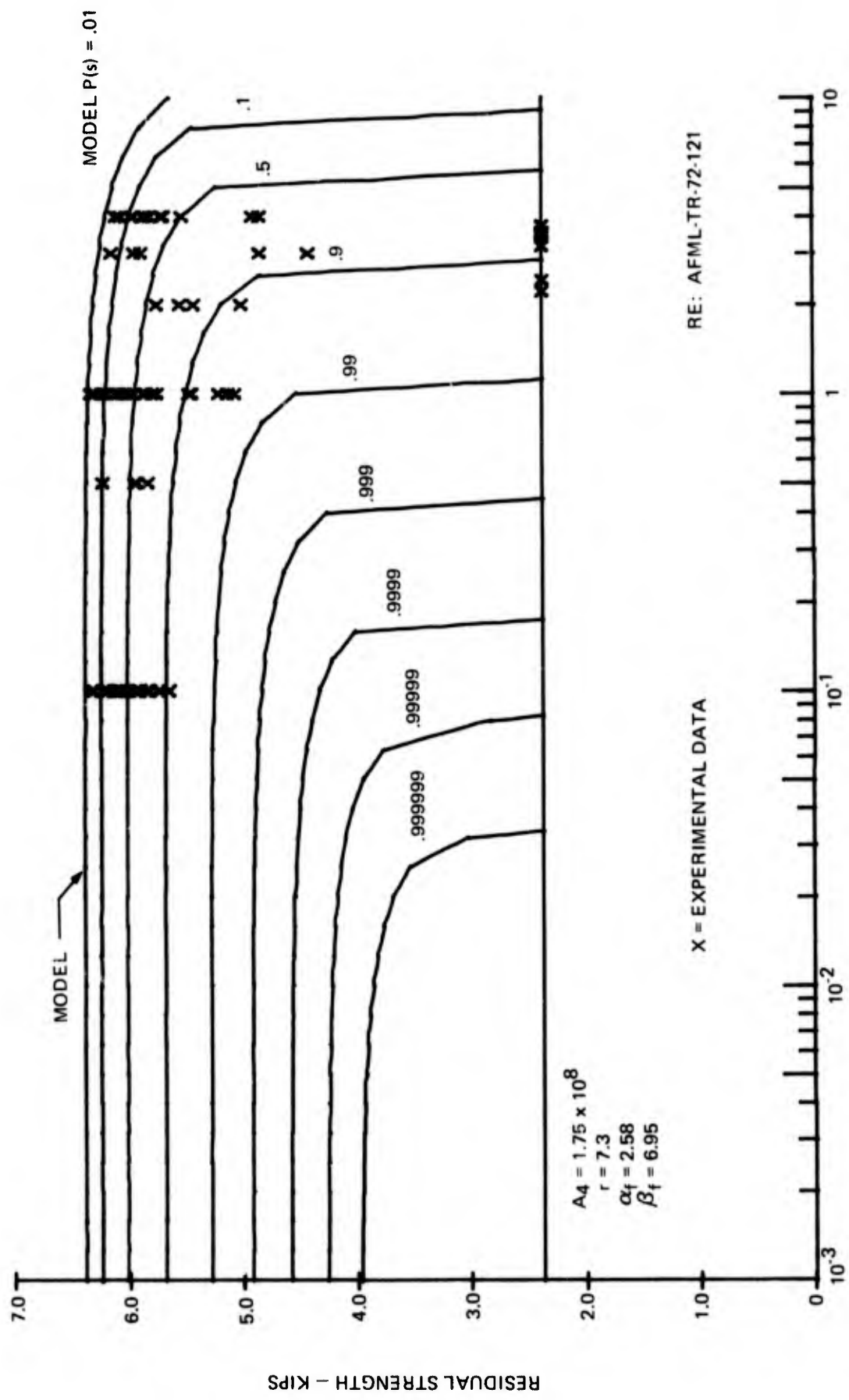


Figure 24 Residual Strength - Lifetime Model for Data of Prior Program

Estimated	AFML-TR-72-121 Data		Subject Program Data
	Previous Value	Recalculated Value	
$\alpha_f$	4.35	2.58	1.63
$\beta_f$	4.90	6.95	3.62
r	4.73	7.3	5.6

The differences in the parameter estimates for the earlier data set are due to the methods used in calculating the parameters. In the analysis reported in Reference 6, values of  $\hat{\alpha}_f$  and  $\hat{\beta}_f$  were determined using MLE equations from the 4-lifetime condition of the residual strength-lifetime experiment. These estimates permitted calculations of r and  $\Lambda_4$  directly from Equations (6) and (7), subsection 4.1. The method used in recalculating the parameters was to determine  $\hat{\alpha}_f$  by pooling the  $F_{\max} - \hat{\beta}_f$  data and the 4-lifetime data (using the MLE method of Section V). The expanded data base of 31 results, including 17 fatigue failures compared to the 21 results with 7 fatigue failures used in the original estimate, permitted calculating  $\hat{\alpha}_f$  with a higher degree of statistical confidence. Then, a new value of r was calculated from Equation (6) and the iteration method described in subsection 4.2.1 was used to minimize the variance between the model and the data in this case by adjusting  $\Lambda_4$ . Then, the new value of  $\hat{\beta}_f$  was calculated from Equation (7).

The "recalculated" values give a much improved fit to the empirical data at 4-lifetimes than the original values, Figure 25; therefore, they are preferred over the original. (Note that the model curves shown in Figure 25 would be shifted to the left for design purposes by applying statistical confidence factors to provide reliable tolerance limits, Reference 6). The overall fit of the model to the data is good; it is certainly better than the model fit to the subject program data. However, the sample size was larger for the earlier program, 80 specimens versus 57, and the maximum lifetime cut-off point was 4 versus 3.25. Thirty-six of the fatigue/residual strength test results (45% of the sample) plot below the median probability of survival curve, 12.5 percent plot below  $P(s) = 90\%$ , and 11 percent plot above  $P(s) = 10\%$ . These calculations indicate the model  $P(s)$  predictions of residual strength/lifetime are well within statistical expectation.

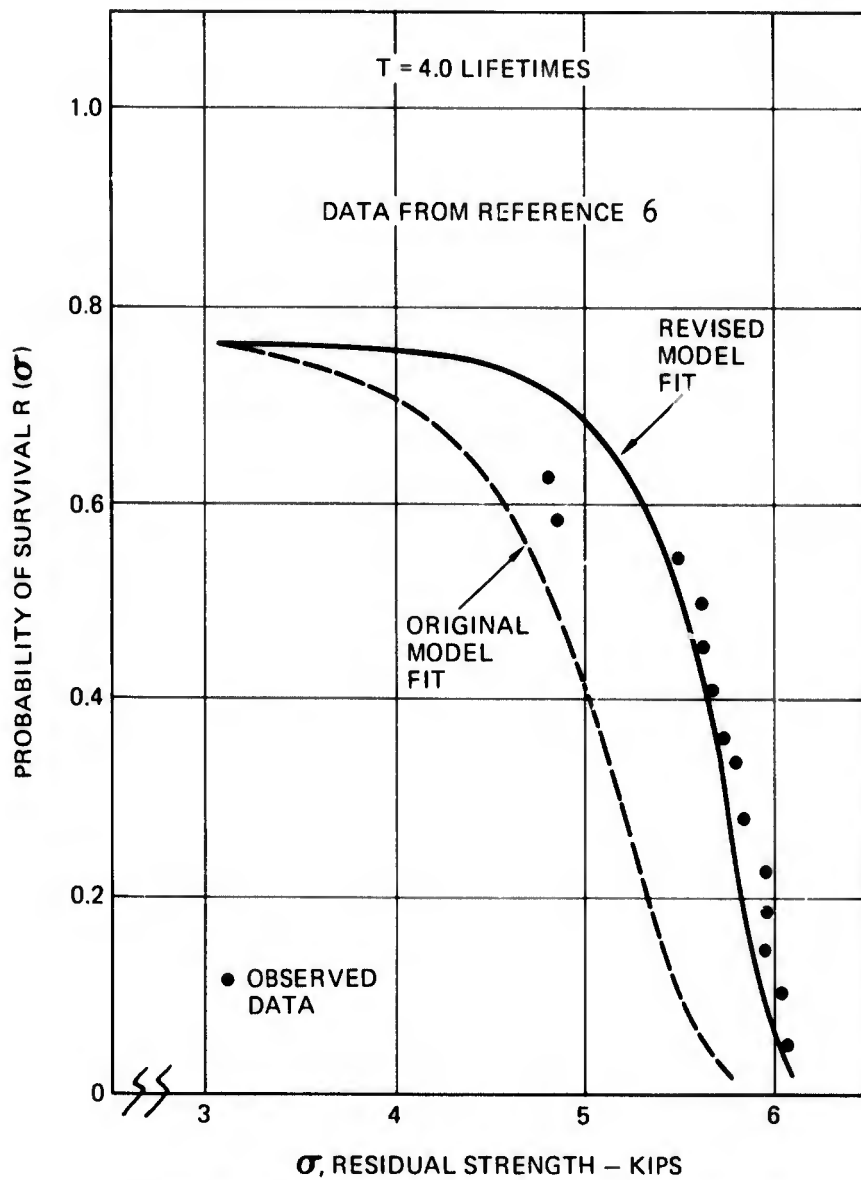


Figure 25 Comparison of Original and Revised Model Fits to 4 Lifetime Data of Reference 6

### 4.2.3 Comparison of Wear-Out Models

Each wear-out model given in Figures 23 and 24 may be "shifted" to the stress (truncation load) level that allows a comparison with the other. The model is shifted by recalculation of the parameter  $A_1$  for the truncation load of interest from the relationship.

$$A_1 = \frac{F_{\max}}{F_{\text{ref}}} \quad (\text{see subsection 4.1}).$$

Since "s" is known from the  $F_{\max}$  versus  $\hat{\beta}_f$  relationship and the values of  $A_4$ ,  $r$ ,  $\hat{\alpha}_0$ , and  $\hat{\beta}_0$  have been determined previously, the model  $P(s)$  percentiles can be recalculated for the load level desired. The subject program model (Figure 23) was shifted to a load level of 3000 pounds (Figure 26) to correspond to the same titanium adherend stress level as Figure 24. Likewise, the earlier model (Figure 24) was shifted to 2850 pounds (Figure 27) for direct comparison to the model in Figure 23. The comparison is summarized in Table VIII. This table illustrates the importance of reliability analysis in the certification of a joint concept and the influence of the parameter  $\hat{\alpha}_0$ . The comparison at both levels has  $\hat{\beta}_f$  of this program greater than the  $\hat{\beta}_f$  of the prior program; however, for reliability (probability of survival) levels of 0.99 and 0.999, the joint of the prior program is superior. This is due to less scatter (greater  $\hat{\alpha}_0$ ) in static strength of specimens used in the prior program.

Table VIII COMPARISON OF WEAR-OUT MODELS-BONDED JOINTS

	Prior Program (Reference 6) Lifetimes	Subject Program Lifetimes
Titanium Stress=71 ksi	(Figure 27)	(Figure 23)
$\hat{\beta}_f$	2.52	3.62
$P(s) = .99$	0.43	0.18
$P(s) = .999$	0.18	0.015
Titanium Stress=60 ksi	(Figure 24)	(Figure 26)
$\hat{\beta}_f$	6.95	10.63
$P(s) = .99$	1.2	0.58
$P(s) = .999$	0.46	0.13
$\hat{\alpha}_0$	32.48	15.0
$\hat{\alpha}_f$	2.58	1.63

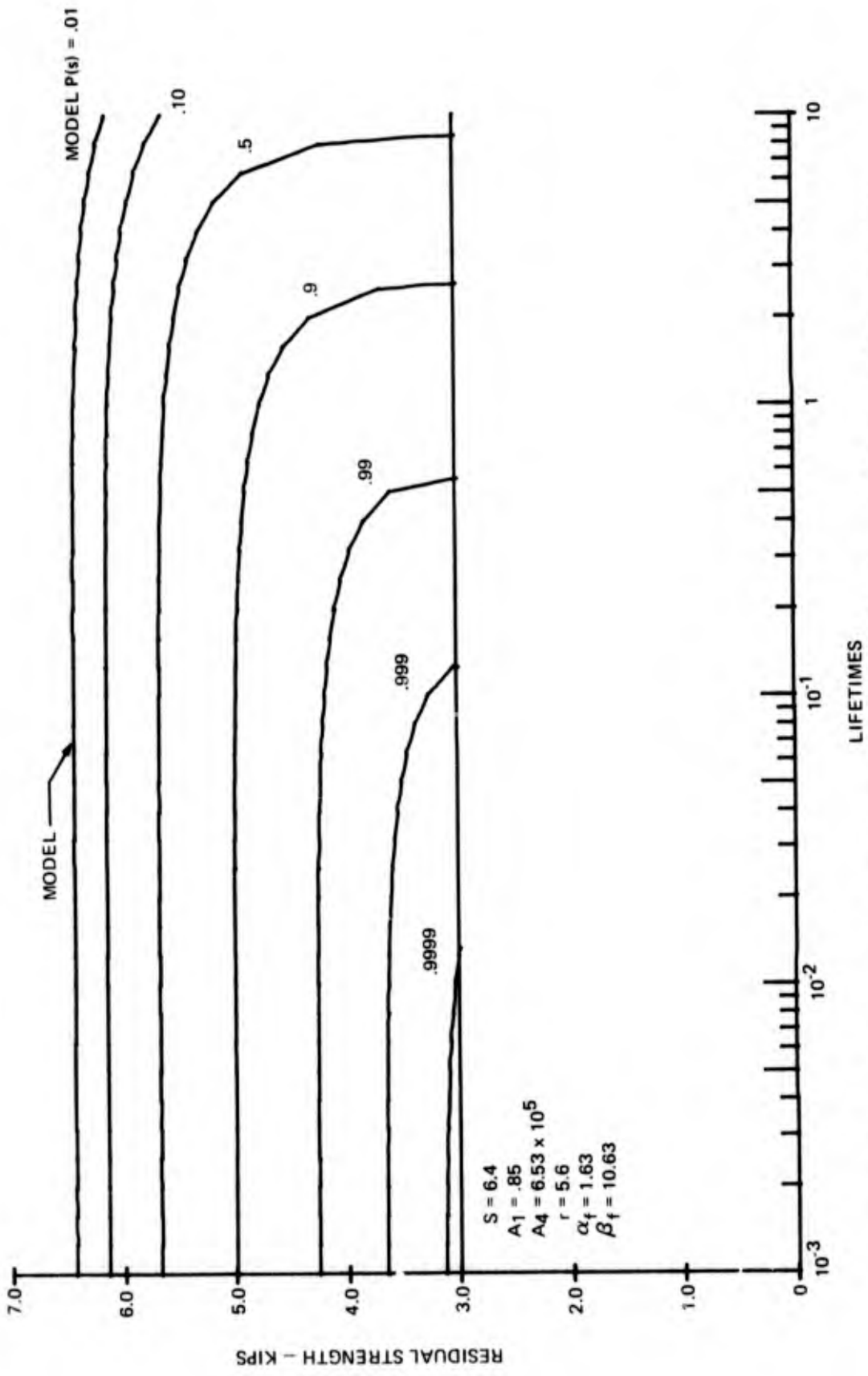


Figure 26 Wear-Out Model of Figure 23 Shifted to 3000 Pounds Truncation

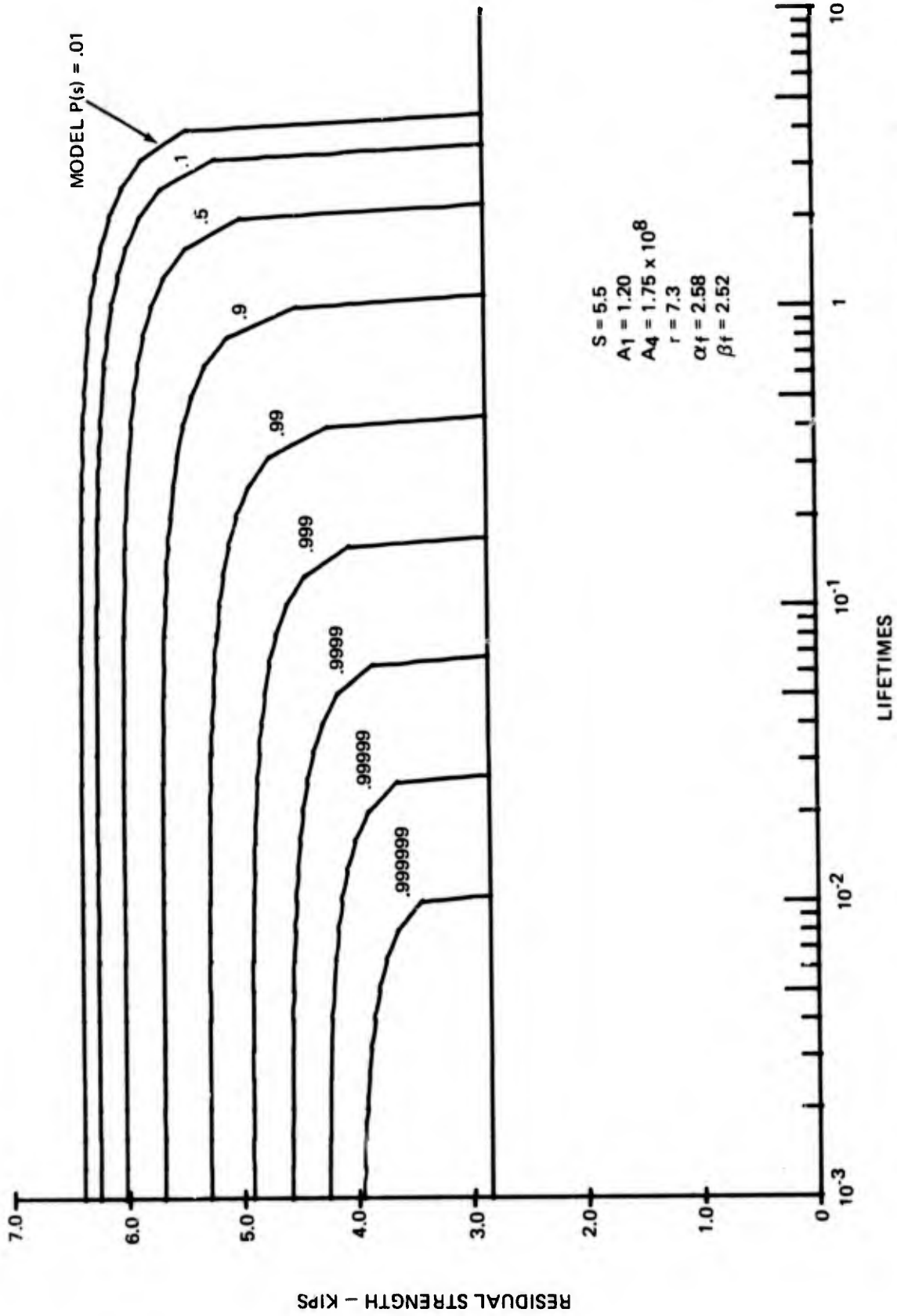


Figure 27 Wear-Out Model of Figure 24 Shifted to 2850 Pounds Truncation

### 4.3 APPLICATION TO BOLTED JOINTS

The models fit to the bolted joint data are given in Figures 28 and 29 for retorqued and non-retorqued joints, respectively. The starting input parameters were

$$\hat{\alpha}_0 = 29.7$$

$$\hat{\beta}_0 = 4.64 \text{ kips}$$

$$A_1 = A_{\text{ref}} = 1.0$$

for both data sets. The "error" was minimized for the following values:

$$\text{retorqued: } A_4 = 4.91 \times 10^{18}$$

$$r = 16.2$$

$$\text{non-retorqued: } A_4 = 5.20 \times 10^{19}$$

$$r = 16.5.$$

The resultant fatigue parameters for each condition are

$$\text{retorqued: } \hat{\alpha}_f = 0.98 \\ (3.55 \text{ kips})$$

$$\hat{\beta}_f = 2.47$$

$$\text{non-retorqued: } \hat{\alpha}_f = 0.96 \\ (3.0 \text{ kips})$$

$$\hat{\beta}_f = 0.60.$$

Both of these models were obtained by iteration of the parameter  $A_4$ . A value of  $r$  was calculated from Equation (6) using a value of  $\hat{\alpha}_f$  obtained from pooling the fatigue data (MLE method of Section V) available at all load levels for each torque condition. For the retorqued sample, pooling at all load levels permitted expansion of the data base from 10 fatigue failures in 29 tests (3550 pound level) to 50 failures in 93

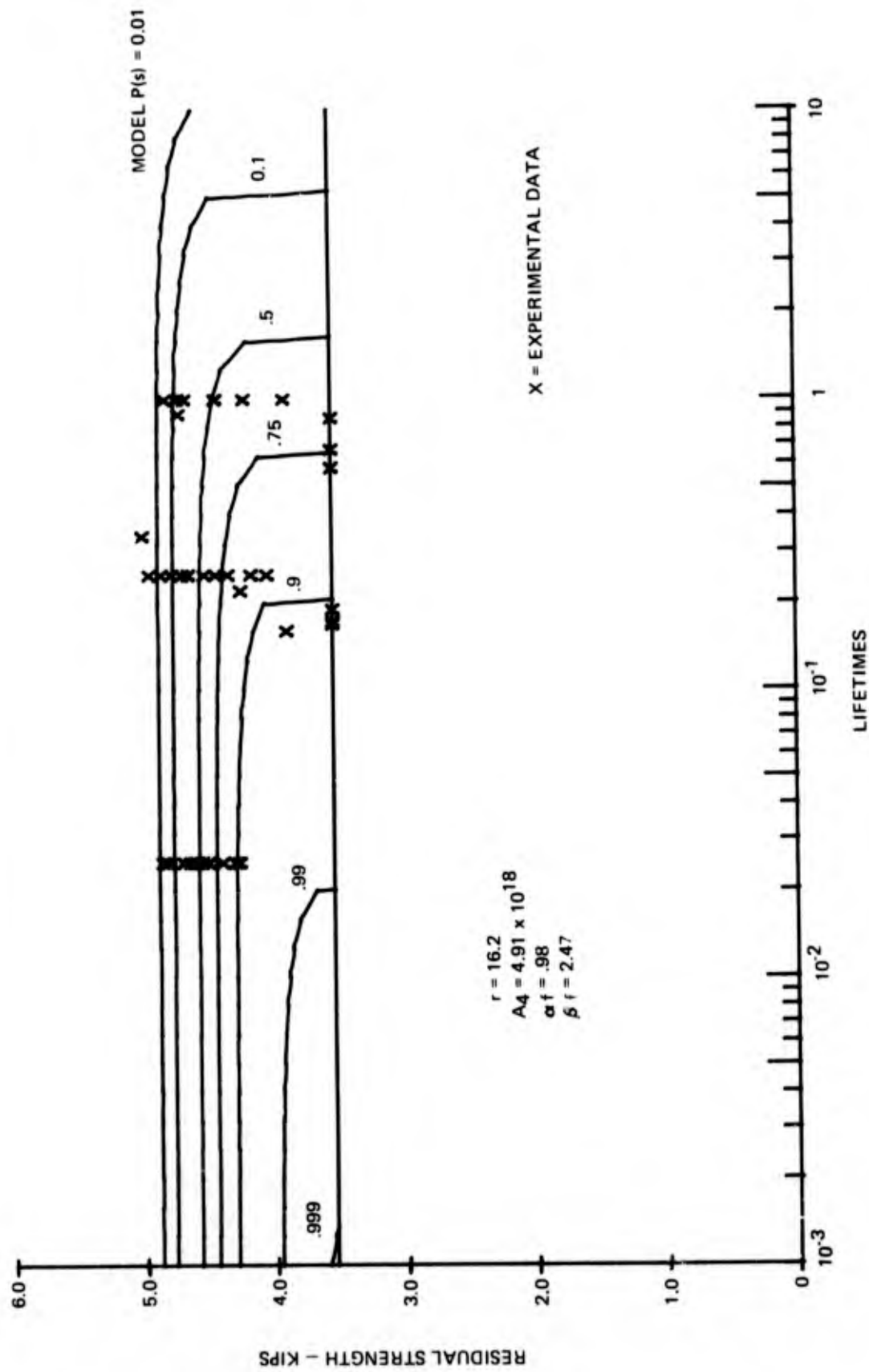


Figure 28 Residual Strength - Lifetime Model Bolted Joints (Retorqued)

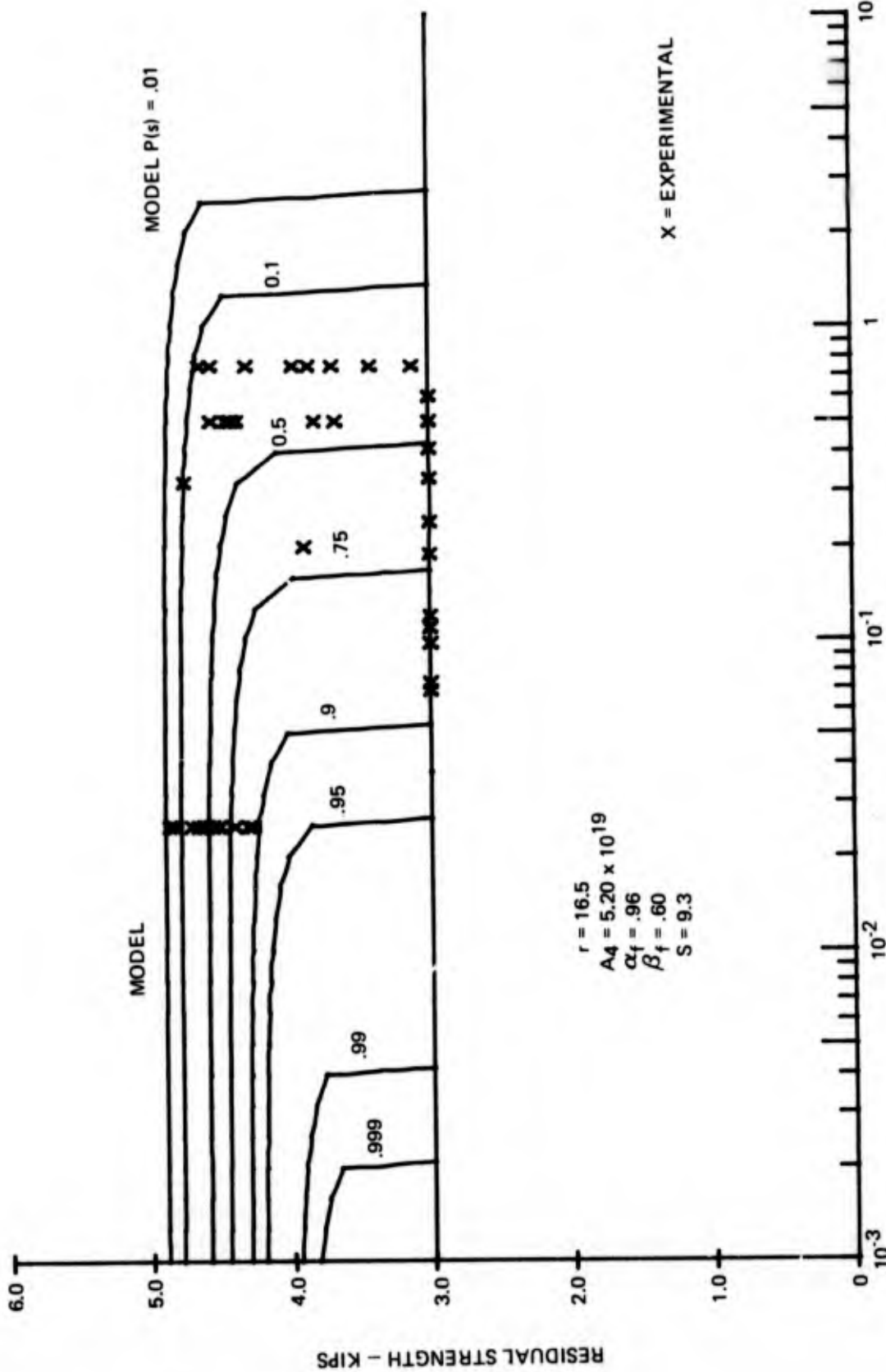


Figure 29 Residual Strength - Lifetime Model Bolted Joints (Non-Retorqued)

tests (all levels). The model "fit" is good. Of the 29 specimens tested in fatigue/residual strength, 14 results plot above and 15 results below the median probability of survival curve. Nine results are below the 75-percentile curve, i.e. 31 percent of the sample and 4 results or 14 percent of the sample are below the 90-percentile curve.

For the "non-retorqued" sample, pooling expanded the data base from 11 fatigue failures in 30 tests (3000 pound level) to 23 failures in 65 tests (all levels). The model determined by iteration of the parameter  $A_4$  did not fit the sample data as well in this case as a model determined by iteration of the parameter  $r$ . The former model is reported (Figure 29), however, to keep the analysis methodology consistent. The model of Figure 29 gives conservative predictions of fatigue life compared to the model determined by iteration of  $r$ , and from a statistical viewpoint, the sample size is not sufficient to disqualify either model on a "best-fit" basis. The model prediction of  $\beta_f = 0.60$  lifetime is significantly less than the value of 1.30 lifetimes predicted by the Weibull MLE estimator (Figure 19). However, the MLE calculation cannot "recognize" the low residual strength values at 0.75 lifetime (Figure 29) as being near the truncation load, i.e. "failure", whereas the model has this capability.

The "retorqued" model was shifted, using  $s=15$  determined from the  $F_{max} - \beta_f$  data (Figure 16), to  $F_{max} = 3875$  pounds ( $A_1 = 1.09$ ) and  $F_{max} = 3500$  pounds ( $A_1 = 0.99$ ). The shifted models are presented in Figures 30 and 31, respectively. Test data was available to compare to the shifted models. The data is superimposed on the applicable figure. Six test results at the 3875 pound load level plot below the median probability of survival,  $P(s)$ , and 13 plot above, which indicates that the model  $P(s)$  curves are conservative. The results at the 3500 pound load level plot 6 above, 7 below, and 4 upon the median  $P(s)$  curve and this indicates that the model fit is good.

#### 4.4 COMPARISON OF JOINT TYPES

The model was used to determine residual strength-fatigue characteristics at percentages of joint strength to permit comparisons between the joint types.

The predicted probability of survival at three levels for bonded and bolted joints tested in this program are compared in Table IX for truncation load levels of 69 and 80 percent of ultimate joint strength.

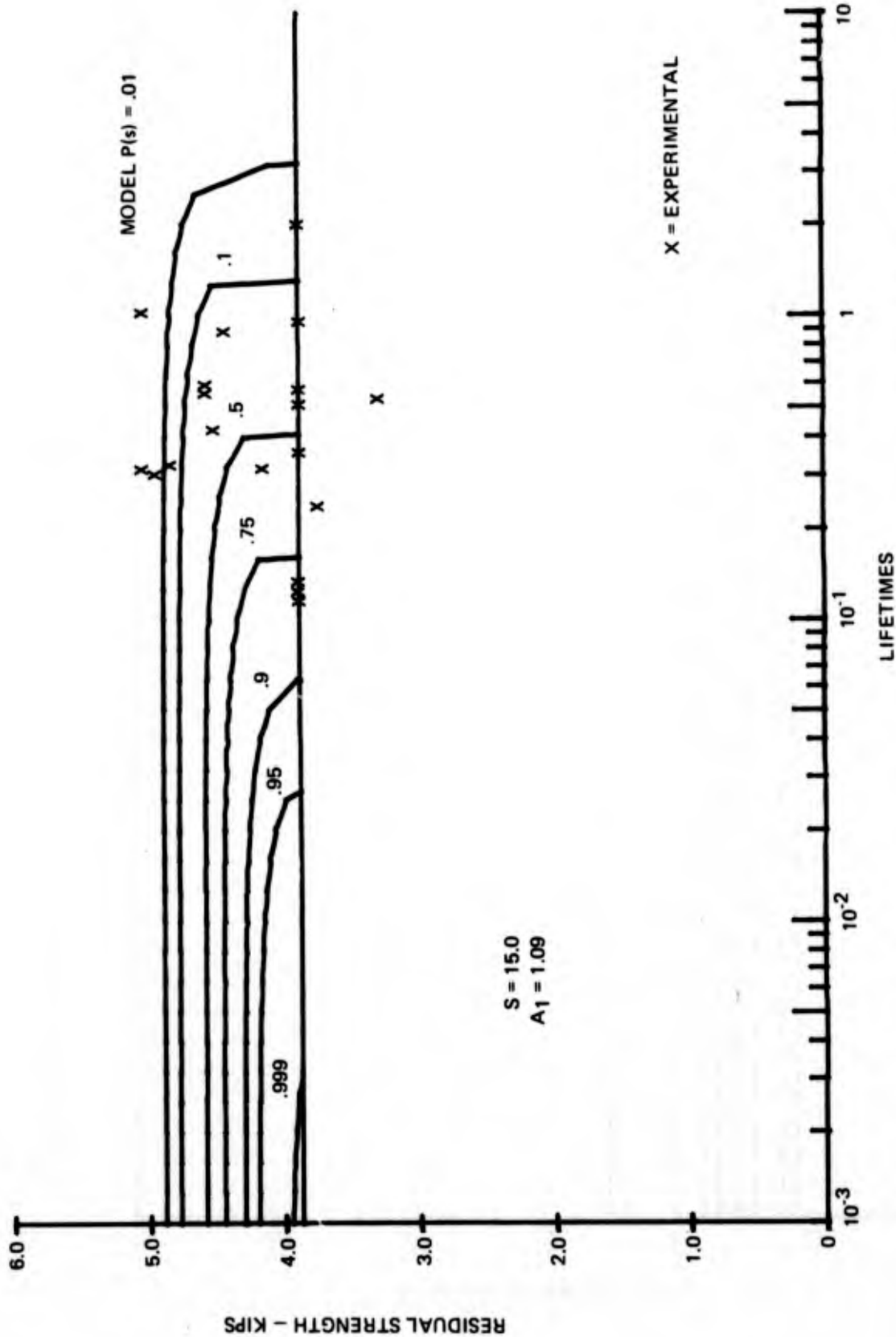


Figure 30 Wear-Out Model of Figure 28 Shifted to 3875 Pounds Truncation



For joints fatigue loaded at a truncation load level of 80 percent of ultimate joint strength, the bolted joint has a value of  $\beta_f$  nearly twice that of the bonded joint. However, at  $P(s) = 0.99$ , the joints are essentially equal.

Table IX COMPARISON OF BONDED AND BOLTED JOINTS

P(s)	Bolted Joint (Retorqued)		Bonded Joint	
	(1)	(3)	(2), (3)	(1)
	3550 lb=82%ULT (life)	3000 lb=69%ULT (life)	4100 lb=80%ULT (life)	3550 lb=69%ULT (life)
$\beta_f$	2.47	30.9	1.44	3.62
0.99	0.02	0.28	0.028	0.18
0.999	0.0015	0.028	(4)	0.015
$\alpha_o$	29.7		15.0	
$\alpha_f$	0.98		1.63	

NOTES:

- (1) Fatigue/Residual Strength data presented in report.
- (2) Fatigue data presented in report.
- (3) P(s) data based on shift of 3550-pound load level model.
- (4) Static failure.

At the truncation load level of 69 percent of ultimate, the bolted joint has a value of  $\beta_f$  nearly 10 times that of the bonded joint. At  $P(s)$  of 0.99 and 0.999, the bolted joint is still superior to the bonded but only by factors of 1.5 and 1.8.

An additional advantage of the bolted joint is that the mechanically fastened joint can be inspected visually for fatigue damage or wear at any point in its lifetime. The bonded joint requires use of NDI (nondestructive inspection) techniques and special equipment to attempt to ascertain fatigue damage (flaw growth).

No attempt is made to compare the structural efficiency of the joint types in terms of strength-to-weight ratios since the laminates of the bonded joint have been designed overly thick to constrain failure to the adhesive bond line.

SECTION V  
STATISTICAL POOLING  
STUDY

The analysis of failure data is an attempt to express observed data in a simple form so that reliable conclusions can be reached. In general, the larger the "effective" sample size the more reliable inferences and conclusions will be. The possibility of pooling data from several sources to estimate the Weibull distribution shape parameter has obvious advantages in application of the fatigue model. A study was conducted to explore techniques for pooling dispersion data from several sources to estimate the Weibull shape parameter. References 13 through 16 are included as background information for this study.

5.1 NORMALIZATION OF DATA BASE

The shape parameter  $\alpha$  of the Weibull distribution is invariant under scale transformations of the Weibull random variable. Therefore, it is heuristically inviting to analyze data from several different Weibull populations having the same shape parameter by scaling (normalizing) the variables to a common base and then treating the scaled data as a single population. Since the Weibull distribution scale parameter  $\beta$  generally will not be known, it is theoretically impossible to scale each variable to a common base. In practice, this can be accomplished (although not theoretically justifiable) by dividing each data point by its estimated scale parameter  $\hat{\beta}$ . This procedure normalizes all the data to a common data base with a Weibull scale parameter  $\beta=1$ . At this point, the shape parameter  $\alpha$  is estimated using the pooled scaled data.

Suppose two samples ( $t_{11}, t_{12}, \dots, t_{1n}$  and  $t_{21}, t_{22}, \dots, t_{2m}$ ) are available from two Weibull distributions with the same shape parameter but different scale parameters  $\beta_1$  and  $\beta_2$  respectively. Then, to apply the pooling procedure, one must obtain the estimates  $\hat{\beta}_1$  and  $\hat{\beta}_2$  from the two original samples respectively and a single pooled normalized sample  $t_{11}/\hat{\beta}_1, t_{12}/\hat{\beta}_1, \dots, t_{1n}/\hat{\beta}_1, t_{21}/\hat{\beta}_2, t_{22}/\hat{\beta}_2, \dots, t_{2m}/\hat{\beta}_2$ . Then this pooled normalized sample of size  $n+m$  is used to estimate the Weibull shape parameter  $\alpha$ .

## 5.2 PARAMETER AVERAGING

Parameter averaging is a statistical technique that is based on the central limit theorem. This theorem states in essence that the sample average of a statistic converges to its mean value. Therefore, if  $k$  estimated shape parameters  $\hat{\alpha}_1, \hat{\alpha}_2, \dots, \hat{\alpha}_k$ , were statistically distributed with a mean of  $\alpha$ , the average value

$$\frac{1}{k} \sum_{i=1}^k \hat{\alpha}_i = \hat{\alpha} \quad (1)$$

would be a "good" estimate of the unknown value  $\alpha$ .

The small sample properties of the statistic given by Equation (1) are of interest. For small sample sizes, the estimated shape parameter  $\hat{\alpha}$  is biased, i.e. its true mean is not the unknown parameter of interest. Therefore, the statistic given by Equation (1) will not have the desired properties of a good statistical estimator unless this bias is corrected. The "averaging" estimating method is inferior to the normalization procedure discussed above; this is illustrated in the numerical example presented later.

## 5.3 MAXIMUM LIKELIHOOD POOLED ESTIMATION OF THE WEIBULL SHAPE PARAMETER

In this section maximum likelihood techniques are used to develop an estimator for the shape parameter  $\alpha$  of the Weibull distribution defined by

$$F(t; \alpha, \beta) = 1 - \exp\left(-\frac{t}{\beta}\right)^\alpha, \quad t, \alpha, \beta > 0. \quad (1)$$

In a typical life test,  $n$  specimens are placed under observation and the accumulated life is recorded as each failure occurs. This is referred to as a "complete sample" test. Various deviations from a "complete sample" test are also considered in this section.

### 5.3.1 Single Censoring From the Right

At some predetermined fixed time or after some predetermined fixed number of sample specimens fail, the test is terminated. When censoring is based on a fixed time, it is said to be Type I. This is consistent with current terminology. When censoring is based on a fixed number of failures, it is said to be Type II.

### 5.3.2 Progressive Censoring From the Right

In many life testing situations progressive censoring of both Type I and Type II are possible. This can be thought of as multiple stage censoring that withdraws only a portion of the survivors; some remain on test and are observed until failure or until withdrawn at a subsequent stage of censoring.

Let  $m$  sets of  $n_i, i=1,2,\dots,m$  items whose failure times have a two-parameter Weibull distribution with common shape parameter  $\alpha$  be placed on test. Associate with each item a right censoring time that can be any positive real number. Let the

$\sum_{i=1}^m n_i$  items under consideration be numbered so that items 1 through  $k_i$  for each set are the only items that have their failure times exactly observed as  $t_{i1}, t_{i2}, \dots, t_{ik_i}$ . Also, assume that items  $k_i + 1$  through  $n_i$  are items that are taken respectively from test before failure at the previously fixed times  $t_{k_i+1}, t_{k_i+2}, \dots, t_{n_i}$  (Type I progressive censoring from the right). The integers  $k_i$  ( $0 < k_i \leq n_i$ ) are random variables. Note that this numbering of the items does not imply an ordering of times associated with each item.

The logarithm of the likelihood function,  $L$ , for the above data situation is given by

$$\ln L = \ln \left\{ C \prod_{i=1}^m \left[ \prod_{j=1}^{k_i} f(t_{ij}) \prod_{j=k_i+1}^{n_i} (1-F(t_{ij})) \right] \right\}, (2)$$

where  $F(t_{ij}) = F(t_{ij}; \alpha, \beta_i)$  is defined by Equation (1);  $f(t_{ij}) = f(t_{ij}; \alpha, \beta_i) = F'(t_{ij})$ ; and  $C$  is a normalizing

constant. Equation (2) can be rewritten as

$$\ln L = \ln C + \sum_{i=1}^m \left\{ k_i \ln \alpha - k_i \alpha \ln \beta_i + (\alpha - 1) \sum_{j=1}^{k_i} \ln t_{ij} - \sum_{i=1}^{n_i} \left( \frac{t_{ij}}{\beta_i} \right)^\alpha \right\}. \quad (3)$$

Differentiating Equation (3) with respect to  $\alpha$  and  $\beta_i$  and setting the result to zero, the following  $m+1$  maximum-likelihood estimation equations are obtained.

$$\frac{\partial \ln L}{\partial \alpha} = \sum_{i=1}^m \left\{ \frac{k_i}{\alpha} - k_i \ln \beta_i + \sum_{j=1}^{k_i} \ln t_{ij} - \sum_{j=1}^{n_i} \left( \frac{t_{ij}}{\beta_i} \right)^\alpha \ln \left( \frac{t_{ij}}{\beta_i} \right) \right\} = 0 \quad (4)$$

$$\frac{\partial \ln L}{\partial \beta_i} = -k_i + \sum_{j=1}^{n_i} \left( \frac{t_{ij}}{\beta_i} \right)^\alpha = 0 \quad i=1, 2, \dots, m \quad (5)$$

Equation (5) can be solved for  $\beta_i$  in terms of  $\alpha$  and  $t_{ij}$  as

$$\beta_i = \left( \sum_{j=1}^{n_i} \frac{t_{ij}^\alpha}{k_i} \right)^{1/\alpha} \quad i=1, \dots, m \quad (6)$$

Substituting Equation (6) into Equation (4) and simplifying, the following nonlinear equation is obtained for  $\alpha$

$$\alpha = \frac{\sum_{i=1}^m k_i}{\sum_{i=1}^m \left\{ \frac{k_i \sum_{j=1}^{n_i} t_{ij}^\alpha \ln t_{ij} - \sum_{j=1}^{n_i} t_{ij}^\alpha \sum_{i=1}^{k_i} \ln t_{ij}}{\sum_{j=1}^{n_i} t_{ij}^\alpha} \right\}} \quad (7)$$

Equation (7) expresses the maximum likelihood estimate of the shape parameter  $\alpha$  as an iterative solution involving the  $t_{ij}$ . In no way does it depend upon the scale parameter  $\beta$ . The estimator given in Equation (7) has been programmed for a HP-9820 desk calculator.

#### 5.4 NUMERICAL EXAMPLE

A numerical example illustrates the pooling techniques. The data in Table X represents ten data sets of ten samples each generated from Weibull distributions having the same shape parameter  $\alpha=10$  and scale parameter  $\beta$  ranging from 10 to 100 in intervals of ten. Each data set was used to evaluate the corresponding shape and scale parameter estimates based on the first two, first three, first five, and finally all ten data values. These estimates illustrate the effect of sample size and are given in Table XI. The data in Table X were normalized based on the corresponding  $\beta$  estimate from Table XI; then, the pooled data from all ten data sets were used to estimate the Weibull shape parameter as a function of sample size. The data of Table X were also analyzed using the MLE. All three pooling methods are summarized in Table XII and Figure 32.

Either the normalization or the MLE method of pooling is superior to the averaging method. There does not appear to be a significant difference between either normalization or MLE in application, although the MLE is desired from a statistical standpoint and would also be easier to compute.

Application of the three methods for a sample size of 2 may be clarified by the following computations.

Table X WEIBULL DISTRIBUTION DATA WITH COMMON  
SHAPE PARAMETER  $\alpha = 10$

Sample Number	Scale Parameter - $\beta$									
	10	20	30	40	50	60	70	80	90	100
1	9.73	26.99	23.51	39.23	52.25	60.26	65.04	70.88	82.43	97.26
2	10.16	20.47	28.76	28.49	42.31	66.57	74.22	90.17	81.11	101.64
3	9.26	19.19	31.40	38.99	51.19	49.20	54.77	78.03	69.39	92.61
4	10.16	19.74	28.39	37.65	48.31	38.35	72.66	60.60	89.05	101.56
5	9.83	18.39	33.60	40.01	47.23	51.60	74.37	87.52	76.50	98.34
6	9.03	17.09	26.05	35.42	44.64	55.70	50.67	75.92	90.10	90.29
7	8.94	21.88	27.83	35.61	49.87	53.99	59.95	80.24	77.70	89.36
8	9.53	17.70	21.76	37.17	44.91	60.07	60.44	77.92	88.57	95.27
9	9.78	14.80	25.47	42.24	45.84	58.07	71.19	80.53	91.27	97.78
10	9.28	21.92	31.65	39.08	54.97	51.67	77.74	83.53	86.61	108.48

Table XI ESTIMATE MLE WEIBULL PARAMETERS FOR TABLE X DATA

Scale Parameter	Sample Size							
	2		3		5		10	
	$\alpha$	$\beta$	$\alpha$	$\beta$	$\alpha$	$\beta$	$\alpha$	$\beta$
10	55.48	10.05	30.68	9.89	38.70	9.98	28.72	9.81
20	8.68	25.17	6.85	23.74	6.41	22.37	6.20	21.20
30	11.90	27.33	10.76	29.32	10.43	30.60	8.94	29.41
40	7.50	36.18	10.07	37.64	14.66	38.51	14.52	38.83
50	11.37	49.54	15.56	50.50	17.79	49.80	13.68	49.91
60	24.09	64.92	10.16	61.80	6.40	57.22	8.96	57.61
70	18.17	71.79	9.54	68.20	13.07	71.34	9.29	69.89
80	9.97	84.85	10.92	83.40	8.73	82.11	12.26	81.94
90	148.62	82.09	19.07	80.19	14.11	82.67	16.03	86.24
100	54.47	100.52	30.46	98.94	38.71	98.37	17.68	99.93

NOTES: (1) Known  $\alpha = 10$

Table XII POOLED ESTIMATED RESULTS FOR WEIBULL SHAPE PARAMETER

Sample Size	Normalized		Averaged		Maximum Likelihood	
	Observed	Bias Corrected(1)	Observed	Bias Corrected	Observed	Bias Corrected(2)
2	13.8	12.8	35.0	Not Available	14.6	11.0
3	11.5	11.0	15.4	Not Available	11.9	10.0
5	10.2	9.9	16.9	11.3	11.1	10.1
10	10.2	10.1	13.6	11.7	10.8	10.3

The "true" value of  $\alpha$  is 10.

(1) The observed estimator tends to systematically over estimate the true value of the shape parameter (see Reference 16)

(2) Based on three equivalent sample sizes

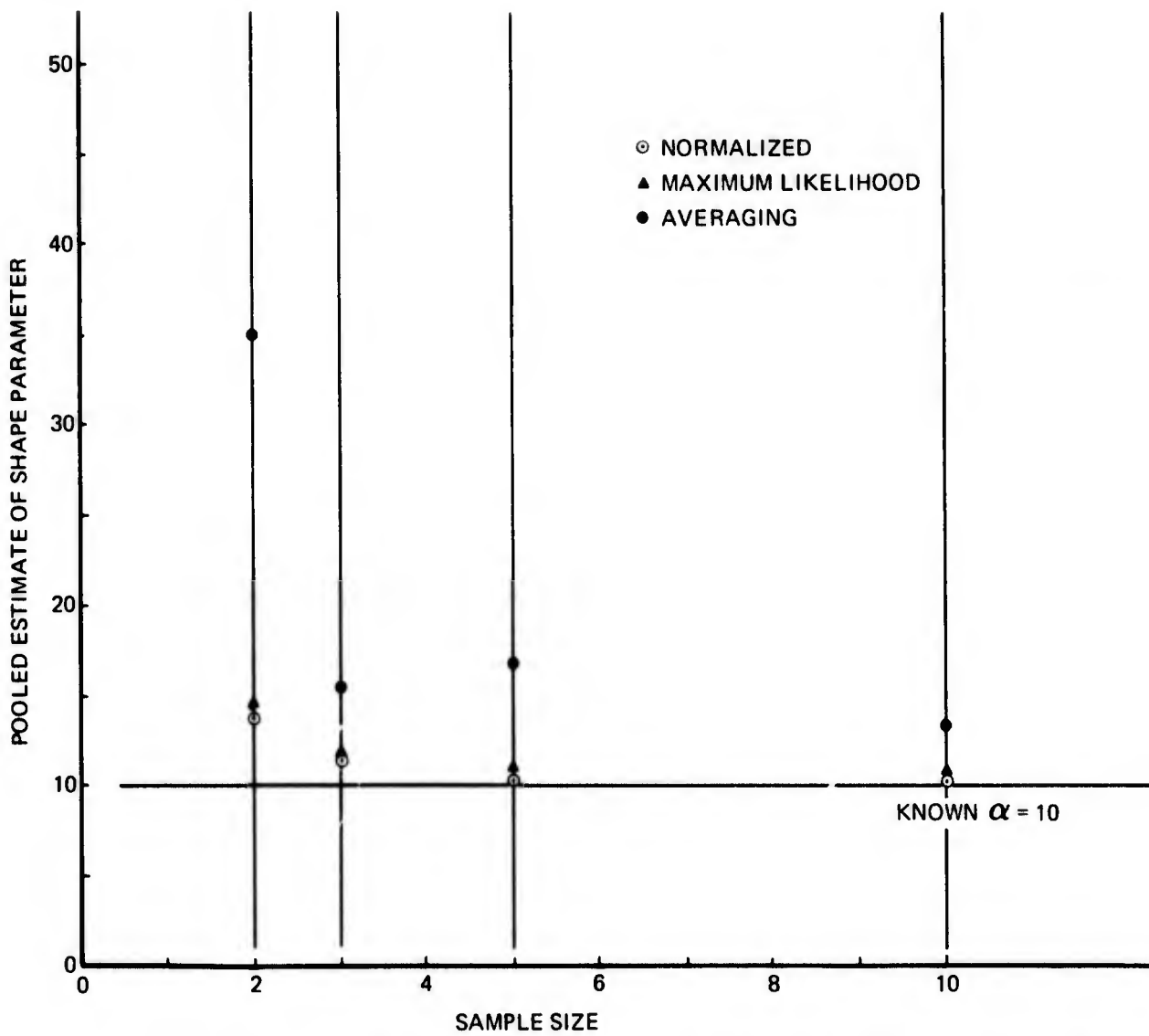


Figure 32 Comparison of Pooling Methods for Estimating Weibull Shape Parameters

(1) Parameter averaging method:

values of  $\hat{\alpha}_i$  are taken directly from Table XI for a sample size of 2 to calculate the pooled estimate  $\hat{\alpha}$ .

$$\hat{\alpha} = \frac{1}{k} \sum \hat{\alpha}_i = \frac{1}{10} (55.48 + 8.68 + \dots + 54.47) = 35.0$$

(2) Normalization method:

The sample is normalized based on  $\hat{\beta}$  for sample size of 2 from Table XI and the entries of Table X, i.e.

$$X_1 = \frac{9.73}{10.05} ; X_2 = \frac{10.16}{10.05} ; X_3 = \frac{26.99}{25.17} ; X_4 = \frac{20.47}{25.17} ;$$
$$\dots ; X_{20} = \frac{101.64}{100.52}$$

Then, the  $X_i$  values are used to determine  $\hat{\alpha}$  from the MLE Weibull equation,

$$\hat{\alpha} = \frac{n \sum X_i^\alpha}{n \sum X_i^\alpha \ln X_i - \sum X_i^\alpha \sum \ln X_i}$$

$$\hat{\alpha} = 13.8.$$

(3) Maximum likelihood method:

The data in the first two rows of Table X are substituted directly into Equation (7) with  $m = 10$ ,  $k_1 = k_2 = 2$ , and  $n_1 = n_2 = 2$ . The iterative solution of equation (7) then gives  $\hat{\alpha} = 14.6$ .

SECTION VI  
CONCLUSIONS AND  
RECOMMENDATIONS

The conclusions and recommendations of the subject program are summarized in this section.

6.1 CONCLUSIONS

The following conclusions are based on the results of this investigation.

1. The probabilistic fatigue model was found to represent the wear-out behavior of bonded joints over a range of 0.2 to 7.0 lifetimes and for spectrum truncation loads as high as 95 percent of average ultimate joint strength.
2. The model fatigue shape parameter for bonded joints was found to be constant (within the limits of statistical expectation) over the truncation load range of 63 to 95-percent of ultimate static strength.
3. The general characteristics of the bonded joint observed under fatigue loading as reported in AFML-TR-72-121 were also observed in this investigation, i.e., mean residual strength degrades gradually and variability broadens rapidly with increasing life.
4. The model assumption that the truncation load-lifetime relationship may be represented by a power law was verified for both bonded and bolted joint specimens.
5. The fatigue model was shown to represent the experimental "retorqued" bolted joint data very well and to yield conservative predictions of probability of survival for the bolted joints that were not retorqued during testing.
6. This initial program on bolted joints under random flight-by-flight spectrum loading, which included negative loads and high GAG cycles, identified prob-

lems associated with testing techniques and failure definitions not previously documented.

7. Composite bolted joints appear to have fatigue characteristics that will give improved reliability over adhesively bonded joints for structural connections. The bolted joint has the added attribute of increased reliability in terms of being available for visual inspection of fatigue wear or damage.
8. The average residual strength of bolted joints improves over average static strength for short durations of fatigue loading.
9. Three methods of pooling test data to improve the estimate of the Weibull shape parameter have been documented and compared by a numerical example. The maximum likelihood method of pooling was exercised in this program for both bonded and bolted joint test data to give improved estimates of  $\alpha_f$  for use in calculating the model parameter  $r$ .

## 6.2 RECOMMENDATIONS

The following recommendations are based on the results of this investigation.

1. The evaluation of composite bolted joints under random fatigue loading should be continued using a fighter spectrum that has a more realistic PSD and GAG load than the spectrum that was used in this investigation.
2. A definition of a bearing fatigue failure should be established for use in developing bolted joint data on laminated composite materials. In addition, a suitable test method for recognizing a bearing failure should be established.
3. As an alternate to Item (2) above, bolted joint fatigue characteristics can be evaluated in terms of residual strength and application of the fatigue model developed in References 3 and 4.
4. The initial shape and scale parameters  $\alpha_0$  and  $\beta_0$ , should be evaluated on specimens that have been fatigue

loaded for a brief duration so that stress relaxation effects may be compensated for in model application.

5. The use of proof-loading to censor weak specimens of a population to extend time-to-first failure should be examined for both bonded and bolted joint elements.
6. The fatigue model and reliability methodology of Reference 3 should be used for evaluation and certification of structural adhesively bonded joints.

A P P E N D I X I  
R E S U L T S O F  
B O N D E D J O I N T T E S T S

The individual test results on bonded joint specimens are given in the Tables of this Appendix.

Table XIII STATIC ULTIMATE STRENGTH OF GRAPHITE-  
TO-Ti BONDED JOINT SPECIMENS

Specimen Number	Ultimate Load (lb.)
6-9	5300
6-2	4150
5-2	5050
5-15	5200
4-1	5900
4-10	5350
3-25	4950
3-10	5600
2-26	5150
2-5	5100
1-18	5500
1-4	<u>4600</u>
Average Strength	5154

Notes:

(1) Load rate 0.1 in/min. head deflection



Table XV BONDED JOINT RESIDUAL STRENGTH/FATIGUE TEST RESULTS  
TRUNCATION LOAD 3550 POUNDS

	0.1 Lifetime		1.0 Lifetime		3.25 Lifetimes			Residual Strength (lb.)
	Specimen Number	Residual Strength (lb.)	Specimen Number	Residual Strength (lb.)	Specimen Number	Date Failed	Fixture No. & Location	
1	1-15	5525	5-14	5460	2-23	31 Jan 74	(1)	2.11
2	3-21	5590	4-22	5330	4-19	1 Feb 74	7-T	2.50
3	4-8	5460	5-26	6305	4-2	1 Feb 74	6-C	1.52
4	5-25	6240	3-11	6110	5-23	4 Feb 74	6-T	1.12
5	3-14	4550	4-14	5200	4-23	5 Feb 74	8-C	2.49
6	2-22	5590	6-15	6370	5-8	5 Feb 74	5-B	2.00
7	3-9	5330	4-21	4940	2-15	6 Feb 74	7-T	2.03
8	4-18	5720	3-18	5135	1-3	6 Feb 74	5-C	2.25
9	4-15	5720	4-5	5655	2-16	7 Feb 74	5-B	1.18
10	3-6	5590	3-1	4940	1-21	7 Feb 74	6-C	2.08
11	6-24	6370	3-5	6370	1-2	7 Feb 74	6-B	1.88
12	3-4	5590	6-19	4680	6-10	7 Feb 74	6-T	2.79
13	1-7	5720	3-7	3055	6-11	8 Feb 74	8-C	0.78
14			1-13	4940	3-15	11 Feb 74	5-C	1.85
15			4-7	5135	3-12	12 Feb 74	5-T	2.22
16			6-16	5265	5-20	13 Feb 74	7-	2.80
17			2-18	5005	2-24	Run-out	7-B	3.25
18			6-4	5460	3-23	Run-out	7-C	3.25
19			4-6	5265	4-11	Run-out	8-B	3.25
20					6-14	Run-out	8-T	3.25
21					3-20	Run-out	6-B	3.25
22					3-22	Run-out	7-C	3.25
23					6-21	Run-out	7-B	3.25
24					2-21	Run-out	7-	3.25
25					1-16	Run-out	7-	3.25

NOTES: (1) T = Top, C = Center, B = Bottom location within stated fixture.

A P P E N D I X   I I  
R E S U L T S   O F  
B O L T E D   J O I N T   T E S T S

The individual test results on bolted joint specimens are given in the Tables of this Appendix. It was observed from the data of Table XVII that there was no correlation between specimen thickness and lifetime for the thicknesses studied; hence, subsequent tables do not include thickness measurements.

Table XVI STATIC BOLTED JOINT TEST RESULTS-SINGLE SHEAR<sup>(1)</sup>

Specimen Set No. 1		Specimen Set No. 2		Set No. 2 Cross-Check		
Number	Ultimate Load (lb.)	Failure Mode	Number	Ultimate Load(2) (lb.)	Number	Ultimate Load(2) (lb.)
8-57	4650	Tension	1	4560	1	4390
8-37	4350	Tension	2	4200	2	4320
8-18	4310	Tension	3	4200	3	4020
8-42	4700	Tension	4	4080	4	4440
7-50	5000	Tension	5	4080	5	4320
8-2	5000	Tension	6	4560		
7-22	4500	Tension	7	4440		
7-15	4200	Tension	8	4320		
8-7	4825	Tension	9	4320		
8-25	4925	Tension	10	4560		
8-26	4900	Tension	11	4560		
7-57	4550	Tension	12	4200		
7-58	4500	Bearing	13	4080		
7-42	4800	Bearing	14	4140		
7-34	4800	Tension	15	4440		
8-34	4900	Tension	16	4380		
7-41	4640	Bearing	17	4200		
8-36	4975	Tension	18	4200		
7-43	4400	Bearing				
8-27	4775	Bearing				

NOTES:

- (1) Deflection rate 0.1 in/min used in testing.
- (2) Failure Mode of Set No. 2 was net section tension.

Table XVII BOLTED JOINT SINGLE SHEAR TEST RESULTS (4)

SPEC. NO.	TEST DATE	THICKNESS (IN.)	FIXTURE NO.	LIFE-TIMES	FAILURE MODE	FAILURE LOCATION (HOLE)	COMMENTS	MEASUREMENTS				WEAR FAILED HOLE
								UPPER HOLE INITIAL (IN.)	UPPER HOLE FINAL (IN.)	LOWER HOLE INITIAL (IN.)	LOWER HOLE FINAL (IN.)	
7-46	Dec 12	.115	3	.033	Shear-out	Lower		.377	.408	--	--	
7-11	12	.112	1	.53	↓	Upper	Excessive wear lower hole also	--	--	.375	.483	
7-32	12	.115	4	.99	↓	Lower	(2)	.374	.396	--	--	
7-18	13	.108	3	.04	E.H.	Lower	(1)	.372	.377	.375	.403	7%
7-17	13	.105	1	.14	Compression	Upper	Comp. side of hole initial failure	--	--	.376	.390	
7-35	13	.106	2	.07	Compression	↓	(2)	--	--	.375	.384	
7-52	18	.106	4	.43	Shear-out	Lower	(2)	.375	.402	--	--	
7-9	18	.106	1	.25	↓	Lower	(2)	.375	.393	--	--	
7-7	18	.117	3	.38	↓	Lower		--	--	.380	.383	
3-8	19	.122	2	.49	↓	Upper		--	--	.380	.380	
5-29	Jan 31	.111	3	.02	↓	Upper	(3)	.380	.525	--	--	
1-15	31	.105	3	.05	↓	Lower		--	--	.376	.380	
1-13	31	.107	3	.054	↓	Upper		.375	.381	--	--	
8-49	Feb 6	.116	2	.0073	↓	Lower		.375	.382	--	--	
8-54	6	.114	4	.051	↓	Lower		--	--	.379	.380	
8-52	6	.116	3	.017	↓	Upper		--	--	.375	.375	
8-6	6	.104	1	.017	↓	↓		--	--	.375	.375	
8-47	6	.110	2	.010	↓	↓		--	--	.375	.380	

NOTES:

- (1) Outer ply delamination on lower hole.
- (2) Excessive wear on compression side of failed hole also.
- (3) Excessive compressive damage on upper hole.
- (4) 4175 Lb. Truncation Level

Table XVII (2) (Continued)

SPEC. NO.	TEST DATE	THICKNESS (IN.)	FIXTURE NO.	LIFE-TIMES (1)	FAILURE MODES	FAILURE LOCATION (HOLE)	COMMENTS	MEASUREMENTS				WEAR FAILED HOLE	RETEST - ADDITIONAL LIFETIMES	FAILURE MODE & LOCATION
								UPPER HOLE INITIAL (IN.)	UPPER HOLE FINAL (IN.)	LOWER HOLE INITIAL (IN.)	LOWER HOLE FINAL (IN.)			
7-10	Dec 18	.116	1	.42	EH	Upper	Excessive compression damage	.374	.433	.375	.382	16%		
7-14	18	.116	1	.11	Shear-out	Lower		.375	.375	--	--			
7-5	18	.109	3	.37		Lower		.376	.384	--	--			
7-5	18	.120	3	.05		Upper		--	--	.375	.376			
7-37	19	.114	4	.24		Lower		.376	.376	--	--			
7-39	19	.111	3	.11		Upper		--	--	.374	.384			
7-4	20	.110	4	.18	E.H.	Both	See retest results	.376	.398	.376	.394	6%	.02	Lower Hole - Compression
7-16	20	.114	1	.15	E.H.	Lower	Tension damage	.374	.376	.376	.425	13%		
7-2	21	.118	3	.38	Shear-out			.376	.378	--	--			
7-19	21	.118	4	.33		Upper	Excessive compression damage	.375	.393	--	--			
8-6	Feb 6	.110	1	.024		Upper		--	--	.375	.375			
8-55	6	.118	3	.024		Lower	Excessive compression damage	.375	.380	--	--			
8-14	6	.115	2	.018	Compression			.375	.375	--	--			
8-20	7	.115	2	.034	Compression	Upper	Compression damage upper hole	.375	.400	--	--			
8-7	7		1	.17	E.H.	Upper	Tension damage	.375	.415	.375	.390	11%		

NOTES: (1) Does not include retest results.  
(2) 40,000 Lb. Truncation Level

Table XVII (3) (Continued)

SPEC. NO.	TEST DATE	THICKNESS (IN.)	FIXTURE NO.	LIFE-TIMES (2)	FAILURE MODE	FAILURE LOCATION (HOLE)	COMMENTS	MEASUREMENTS				RETEST - ADDITIONAL LIFETIMES	FAILURE MODE & LOCATION
								UPPER HOLE INITIAL (IN.)	UPPER HOLE FINAL (IN.)	LOWER HOLE INITIAL (IN.)	LOWER HOLE FINAL (IN.)		
7-31	Dec 6	.108	4	.24	EH	Upper	Delamination-tension side	.374	.430	.376	.378	15%	
7-24	6	.115	1	.41	EH	Lower		.376	.377	.377	.420	11%	
7-6	6	.115	3	1.06	EH		See retest results	.376	.383	.376	.393	4%	.042
7-31	7	.116	1	.96	Shear-out			.376	.377	--	--		
7-55	7	.104	3	.13	Shear-out			.376	.378	--	--		
7-51	7	.113	4	1.00	EH		Tension damage	.374	.378	.375	.427	14%	
7-49	7	.117	3	.35	Shear-out	Upper	Excessive compress. damage	--	--	.376	.350		
4-28	7	.118	2	.36	EH	Upper	Tension damage	.381	.435	.378	.381	14%	
7-53	10	.115	3	.53	EH	Both	(1)	.376	.436	.376	.464	16%	
7-54	10	.108	4	.89	EH	Lower	Excessive compress damage	.376	.394	.376	.433	15%	
7-45	10	.116	1	.50	Shear out			.375	.386	--	--		
7-62	10	.113	2	.33	EH		Tension damage	.376	.388	.376	.434	15%	
3-2	11	.120	2	.58	EH		Tension damage	.376	.382	.372	.430	16%	
7-47	11	.108	2	.13	Shear-out			.375	.380	--	--		
7-52	11	.115	1	.12	Shear-out			.376	.378	--	--		
7-38	12	.111	3	.56	EH		See retest results	.376	.388	.374	.403	8%	.0017
7-48	12	.110	4	.59	EH		Tension damage	.375	.382	.374	.422	13%	
5-23	12	.125	2	.30	EH		Excessive compress. damage	.376	.378	.381	.436	14%	
7-12	12	.110	1	.32	EH		Excessive compress. damage	.376	.382	.376	.430	14%	

NOTES: (1) Excessive compression damage upper hole; delamination tension side lower hole.  
 (2) Does not include retest results.  
 (3) 3875 Lb. Truncation Level

Table XVII (4) (Continued)

Specimen No.	Test Date	Thickness (in.)	Fixture No.	Lifetimes (3)	Failure Mode	Failure Location (Hole)	Comments	Measurements				Wear Failed Hole	Retest Additional Lifetimes	Failure Mode & Location
								Upper Initial (in.)	Hole Final (in.)	Lower Initial (in.)	Hole Final (in.)			
8-35	Jan 7	.114	3	.68	E.H.	Upper		.375	.409	.375	.396	8%	.014	E.H. Upper hole .440
8-15	8	.120	3	.28	E.H.	Lower		.375	.376	.376	.406	8%	.017	E.H. Lower hole .418
8-10	8	.118	4	.55				.375	.376		.408	8%	.014	E.H. Lower hole .418
8-11	8	.111	1	.55			Compressive damage & delam	.376	.379		.446	19%		
8-8	8	.106	2	.28			Compressive damage	.375	.379		.415	10%		
8-17	9	.116	2	.68	Shear-out			.376	.405		-			
8-28	9	.116	3	.27	E.H.	Upper		.388	.388	.375	.407	8%	.40(2)	Shear-out upper hole
8-50	9	.118	4	.17		Upper	Compressive damage	.420	.420	.376	.394	12%		
8-23	10	.118	1	.82		Both	Compressive damage upper hole	.376	.413	.376	.394	10%		
8-41	16	.116	1	.68		Upper		.374	.444	.374	.402	18%	.13	E.H. & Delam. upper hole
8-31	16	.116	4	.68	Shear-out			-	-	.376	.396		.16	Shear-out lower hole
8-40	17	.118	2	.68	E.H.	Both		.376	.545(1)	.376	.384	45%	.84	E.H. upper hole .545
1-9	Feb 1	.121	2	.58		Both	Compressive damage lower hole	.380	.594	.375	.444	56%		
1-15	1	.26	2	.40		Lower	Delam. Tension side	.375	.380	.375	.460	22%		
4-13	1	.108	4	.11		Upper	Compressive damage	.380	.437	.380	.400	15%		
1-10	1	.111	1	.59		Lower		.380	.390	.380	.429	13%		
1-11	6	.119	1	1.75		Lower		.376	.384	.375	.400	7%		

NOTES:

- (1) This measurement made following retest.
- (2) Excessive hole elongation on lower hole in retest - CENSOR.
- (3) Does not include retest results.
- (4) 3500 Lb. Truncarion Level

Table XVII (2) (Continued)

SPEC. NO.	TEST DATE	THICKNESS (IN.)	FIXTURE NO.	LIFE-TIMES	FAILURE MODE	FAILURE LOCATION (HOLE)	COMMENTS	MEASUREMENTS				WEAR FAILED HOLE
								UPPER HOLE INITIAL (IN.)	UPPER HOLE FINAL (IN.)	LOWER HOLE INITIAL (IN.)	LOWER HOLE FINAL (IN.)	
8-24	Jan 18	.115	2	.14	E.H.	Upper	(1)	--	--	--	--	--
8-30	Jan 23	.110	4	.82	↓	Lower		.376	.330	.379	.429	13"
8-21	Jan 25	.115	3	2.83	↓	Both	Comp. Damage Upper Hole	.375	.408	.376	.404	9%
8-12	Jan 31	.118	1	3.43	--	--	Test Discontinued	.376	.376	.375	.378	--
5-1	↓	.120	2	3.10	--	--	↓	.376	.380	.378	.382	--
8-53	↓	.120	4	4.10	--	--		.376	.379	.376	.386	--

NOTES:

(1) Excess hole damage in both tension and compression. Specimen damaged during drilling - CENSOR

(2) 2500 Lb. Truncation Level



Table XIX BOLTED JOINT RESIDUAL STRENGTH/FATIGUE TEST RESULTS  
TRUNCATION LOAD 3550 POUNDS

Specimen Number	0.025 LIFETIME			0.25 LIFETIME			Specimen Number	Residual Strength (psi)	Failure Mode	Residual Strength (lb.)
	Test Fixture	Lifetime	Residual Strength (lb.)	Specimen Number	Test Fixture	Lifetime				
3-12	2	0.025	4510	2-9	1	0.25	4780	3-1	0.16 (1)	3900
6-20	4	0.025	4560	3-21	2	0.25	4650	4-27	0.19 (1)	5000
1-13	1	0.025	4270	5-5	3	0.25	4860	5-3	0.34	
2-24	2	0.025	4700	6-7	4	0.25	4950	6-14	0.58	
5-6	3	0.025	4510					6-18	1.00	4435
6-6	4	0.025	4650							
2-15	1	0.025	4510	1-12	1	0.25	4170	4-18	.22 (2)	4250
3-14	2	0.025	4560	1-5	1	0.169				
5-30	3	0.025	4400	3-28	3	0.173				
3-25	4	0.025	4510	2-8	2	0.25	4700	5-16	.86	3910
1-27	1	0.025	4560	4-1	4	0.25	4440	1-23	1.00	4430
2-26	2	0.025	4600	5-2	1	0.25	4050	2-25	1.00 (1)	4715
5-22	3	0.025	4340	2-6	2	0.25	4650	1-14	1.00	4670
6-5	4	0.025	4600	3-6	3	0.25	4650	3-7	1.00	4725
1-25	1	0.025	4825	4-12	4	0.25	4530	4-22	1.00	4820
3-4	2	0.025	4825							
4-21	3	0.025	4860							
6-13	4	0.025	4600							
2-12	1	0.025	4400	1-26	1	0.25	4345	2-20	.67	
5-4	2	0.025	4400					6-8	1.00	4215

NOTES:  
(1) Loading discontinued due to elongated bearing holes  
(2) Failed due to overload

Table IX BOLTED JOINT FATIGUE TEST RESULTS-SPECIMENS NOT RETORQUED

Truncation	Specimen Number	1974 Date Failed	Test Fixture	Life	Failure Mode	Residual Strength Fixture	Residual Strength Load
3500 lb.	1-2	4-15	1	.35	Shear Out		
	1-3	4-15	2	.097	Shear Out		
	1-7	4-15	3	.46	Elongated Hole	4	3620
	1-8	4-15	4	.20	Shear Out		
	1-9	4-15	2	.14	Net Section		
	1-10	4-16	4	.027	Elongated Hole and ply delamination	1	3300 bad delam on comp side before residual
	1-16	4-16	2	.14	Elongated Hole	1	4280
	1-20	4-17	1	.83	Elongated Hole and ply delamination	4	4140
	2-27	4-19	4	1.73	Elongated Hole and compression damage	3	4230
	2-28	4-17	3	.66	Elongated hole and slight ply delamination	3	3860
	1-22	4-16	2	.53	Shear Out		
	2-19	4-17	2	.27	Elongated hole and ply delamination	2	3600 bad delam on comp side before residual
	2-3	4-17	2	.11	Elongated hole and compressive damage	4	3960
	2-13	4-17	1	1.17	Shear Out		
	2-1	4-17	2	.19	Elongated hole and compressive damage	3	4330
	2-18	4-19	3	1.83	Net Section		
	2-23	4-17	1	.54	Elongated Hole		
	2-22	4-17	2	.33	Shear Out	2	4200
	2-5	4-17	2	.098	Shear Out		
	2500 lb.	2-17	5-15	4	7.00	Aborted	4
4-11		4-18	3	4.52	Elongated hole and compressive damage	1	3950
4-8		4-19	3	0.26	Elongated hole and compressive damage	1	4100
4-2		4-22	3	0.45	Elongated hole and compressive damage	2	3970
4-3		4-22	3	4.25	Elongated hole and compressive damage	3	4210
4-5		4-25	1	3.00	Elongated hole and compressive damage	3	4450
4-24		4-26	2	3.11	Shear Out		
4-9		4-24	4	2.89	Elongated hole and compressive damage	2	3660
4-20		5-3	1	4.67	Elongated hole and compressive damage	4	4270
3-20		5-1	2	1.62	Elongated hole and compressive damage	4	3830
4-30		5-2	2	1.41	Elongated hole and compressive damage	3	3310
3-11		5-2	2	0.78	Elongated hole and compressive damage	1	4430
3-16		5-2	3	0.65	Shear Out		
3-19		5-3	3	0.31	Elongated hole and compressive damage	4	3780
3-18		5-15	1	2.70	Aborted	1	4590
3-22		5-3	2	0.67	Elongated hole and ply delamination	2	3370 bad elong on tensile side before residual

Table XXI BOLTED JOINT RESIDUAL STRENGTH/FATIGUE TEST RESULTS  
SPECIMENS NOT RETORQUED

Truncation	Specimen Number	1974 Date Failed	Test Fixture	Life	Residual Strength (lb.)
3000 lb. (Run-out = 0.5 life)	3-2	5-9	3	0.5	4370
	3-26	5-9	2	0.20	3900
	3-27	5-10	3	0.5	3820
	3-17	5-10	2	0.5	4440
	5-9	5-10	3	0.5	4410
	5-8	5-10	2	0.32	4740
	5-27	5-10	2	0.41	
	5-7	5-13	2	0.5	3670
	5-24	5-13	3	0.073	
	5-23	5-13	3	0.11	
	5-21	5-14	3	0.5	4550
	5-25	5-14	2	0.5	4550
	5-26	5-14	4	0.5	4410
	5-13	5-14	3	0.12	
	6-10	5-14	1	0.5	4410
3000 lb. (Run-out = 0.75 life)	6-26	5-14	3	0.24	
	6-15	5-14	1	0.75	3970
	6-19	5-14	2	0.19	
	6-23	5-14	3	0.098	
	6-30	5-14	4	0.75	4300
	6-1	5-14	3	0.33	
	6-22	5-14	2	0.75	3860
	6-3	5-16	1	0.75	3690
	6-4	5-17	3	0.50	
	6-11	5-17	4	0.75	3420
	X-5	5-17	2	0.75	3120
	X-1	5-17	1	0.75	4550
	X-2	5-17	2	0.069	
	X-3	5-17	3	0.60	
	X-4	5-17	4	0.75	4630

APPENDIX III  
 TRUNCATION LEVEL AND  
 RMS LEVEL IN RANDOM  
 FATIGUE TESTING

As discussed in References 5 and 7, the spectrum simulation is based on mission profile timing and mission segment exceedance curves. For the purposes of this discussion, suppose that the spectrum to be generated is governed by one segment whose exceedance is Gaussian. This type of segment is illustrated in Figure 33. The parameter  $N_0$  is the number of crossings of the mean load per thousand hours, and can be converted to an average loading frequency in Hertz. The irregularity factor,  $R$ , is the ratio of mean crossings,  $N_0$ , to peak load occurrences,  $N_p$ . For this discussion, assume  $R = 1$ . The parameter  $\sigma$  is inversely proportional to the slope of the exceedance curve, and is the measure of intensity for the exceedance curve. The "rms level" of the curve is  $\sigma$ . These relationships are embodied in the equation of the line on the exceedance or cumulative frequency diagram,

$$N_x = N_0 e^{-\frac{x^2}{2\sigma^2}}$$

where  $x$  is the load, stress, or load factor parameter, measured from the mean. Also shown in Figure 33 is the truncation load,  $X_T$ . The dispersion of the loads is measured by the clipping ratio,  $\gamma$ , defined as

$$\gamma = X_T/\sigma$$

To simulate such a spectrum in the simulation procedure SHAM, the values of  $R$ ,  $N_0$ , and  $\sigma$  are input. Also, a value of  $X_T$  and the ground-air-ground load, say  $X_G$ , are input. As mentioned above, all the load quantities can be input in any type of consistent units of load, stress, or acceleration.

To allow the computer to nondimensionalize the spectrum, a scaling quantity is used. It is called PLOAD, and is divided into all the load values before they are written on magnetic tape. Normally, PLOAD is equal to  $X_T$ , and they are both usually equal to limit load or the once-per-airplane lifetime load.

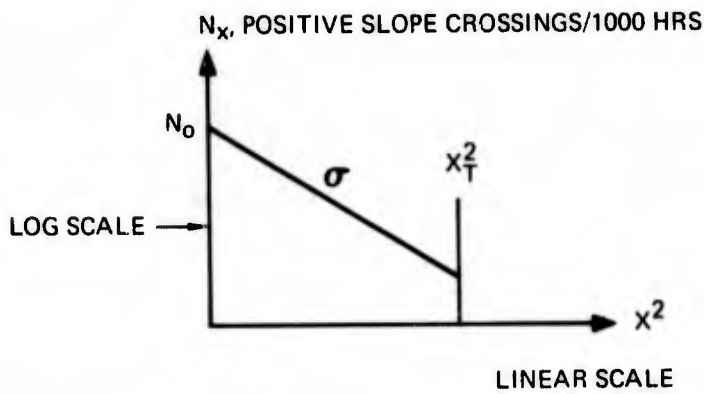


Figure 33 Cumulative Frequency Diagram

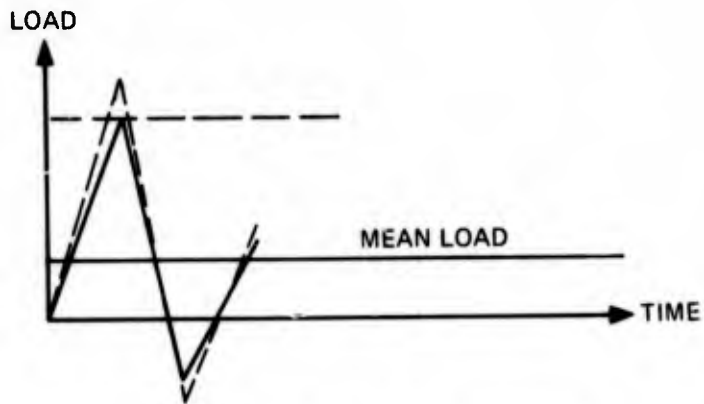


Figure 34 Effect of Changing  $P_T$  and  $P_H$

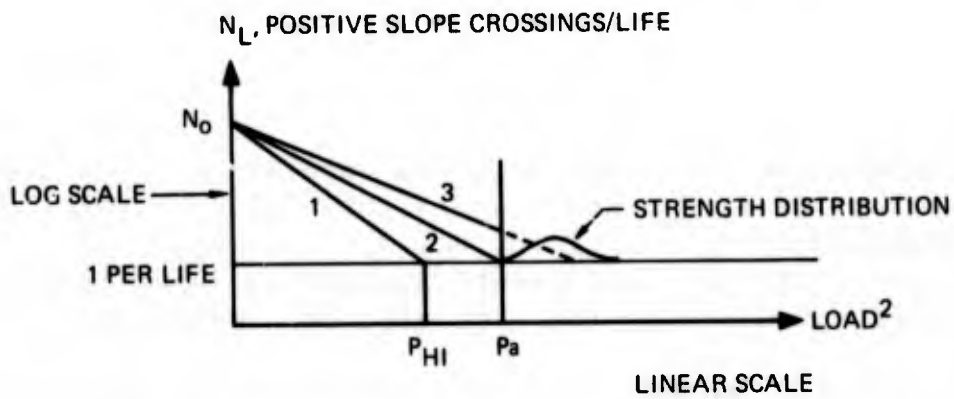


Figure 35 Relationship of  $P_H$  to Strength Distribution

This is not necessarily always true, however. The spectrum may be purposely truncated at an  $X_T$  below PLOAD to vary the clipping ratio. Another distinct possibility is that over the desired simulation time, the load statistics may reach neither  $X_T$  or PLOAD. In this case, the maximum load reached is  $X_m$ . Nevertheless, as far as the magnetic tape is concerned, PLOAD is the maximum permissible load value and is defined as 511 integer "load counts". All other loads are scaled down from PLOAD, and converted to integers ranging from -511 to +511. To relate this to the spectrum used in this program the truncation level is +81.7% and -66.7% of PLOAD. On the magnetic tape, then, the value of R is fixed, the maximum  $N_o$  is fixed (explained below), the maximum value of  $X_T/PLOAD$  or  $X_o/PLOAD$  is fixed, and the maximum value of  $X_G/PLOAD$  is fixed<sup>m</sup>. All other values are set by the test engineer as described below.

The test engineer must relate the integers on the magnetic tape to a number of pounds applied at a hydraulic ram. To do this, a "truncation percentage" and a "hundred percent load" are required. Call these  $P_T$  and  $P_H$ , respectively.  $P_H$  and  $P_T$  specified for each D-A servo (see Figure 5).

The effect of changing  $P_T$  and  $P_H$  can be seen in Figure 34. Here the first spike is the highest load in the spectrum, corresponding to  $X_m$ , the negative spike corresponds to  $X_G$ , and the next spike is any other small load. The dotted line shows the effect of increasing  $P_H$ . The dashed line shows that by lowering  $P_T$  while raising  $P_H$ , the intensity of the spectrum is increased, while maintaining the peak load on the specimen.

These effects can also be seen in Figure 35, which is like Figure 33 except that the abscissa is now in load coordinates that relate to the specimen being tested. As mentioned above,  $N_o$  can be slightly changed in the lab. This is because the computer will not recognize any periods below 50 milliseconds.

Referring to Figure 35, suppose that specimens are tested at a load of  $P_H$ , with  $P_T$  at 100%, and no fatigue failures occur. For the case where  $P_H$  is increased to  $P_a$ , the allowable static load for the specimen, and still no fatigue failures occur, it becomes necessary to intensify or magnify the spectrum, without causing a static failure. This is done by raising  $P_H$  to a value above  $P_a$ , and then specifying  $P_T$  so that the specimen is not loaded over  $P_a$ . The specimen will "see" many more occurrences of  $P_a$ , but will still not be expected to fail statically. It should be noted that this use of  $P_T$  effectively decreases  $\gamma$ , the clipping ratio. (Note the clipping ratio is not increased, by lowering  $P_H$ .

The process of increasing  $P_H$  serves to increase  $\sigma$ . Once  $P_H$  is increased above  $P_a$ , and  $P_T$  is used to truncate,  $P_a$  occurs more than once per lifetime. Since the ordinate is a logarithmic scale, substantial increases in  $\sigma$  may be obtained while truncating a relatively small number of loads in the spectrum.

## REFERENCES

1. Whitaker, I.C. and Besuner, P. M., A Reliability Analysis Approach to Fatigue Life Variability of Aircraft Structures, AFML-TR-69-65 AD853263, April 1969.
2. Halpin, J. C.; Kopf, J. R.; and Goldberg, W., "Time Dependent Static Strength and Reliability for Composites," Journal of Composite Materials, Vol. 4, October 1970.
3. Halpin, J. C.; Jerina, K. L.; and Johnson, T. A., Characterization of Composites for the Purpose of Reliability Evaluation, AFML-TR-72-289 AD 764356, 1972. Also ASTM STP 521, 1973, pp. 5-64.
4. Halpin, J. C.; Johnson, T. A.; and Waddoups, M. E., International Journal of Fracture Mechanics, 8, (1972).
5. Manning, S. D.; Lemon, G. H.; and Waddoups, M. E., Composite Wing for Transonic Improvement, Volume III, "Structural Reliability Studies," AFFDL-TR-71-24 AD 756893, March 1971.
6. Wolff, R. V. and Lemon, G. H., Reliability Prediction for Adhesive Bonds, AFML-TR-72-121 AD 763707, March 1972.
7. Waddoups, M. E.; Wolff, R. V.; and Wilkins, D. J., Reliability of Complex Large Scale Composite Structure - Proof of Concept, AFML-TR-73-160 AD 913266L, July 1973.
8. "Life Assurance of Composite Structures", AFML Contract F33615-73-C-5104, 1973.
9. Fant, J. A., Conceptual Design of Advanced Composite Airframes, AFML-TR-73-4, February 1973.
10. Elkin, R. A., Manufacturing Methods for Establishing Polymeric Adhesive Bonding Processes, AFML-TR-73-299, December 1973.
11. F-15 Composite Wing Flight Test Report, MDC A2157, 17 February 1973, Seventh Quarterly Technical Report, F33615-71-C-1536.
12. Berens, A. P. and West, B. S., "The Evaluation of an Accelerated Characterization Technique for Reliability Assessment of Adhesive Joints," Air Force Materials Laboratory Contract No. F33615-72-C-2161.

13. Chiao, J. J.; Lepper, J. K.; Hetherington, N. W.; and Moore, R. L.; "Stress-Rupture of Simple S-Glass/Epoxy Composites," Journal of Composite Materials, Vol. 6 (July 1972) pp. 358-370.
14. Jaech, J. L., "Estimation of Weibull Distribution Shape Parameter When no More Than Two Failures Occur per Lot," Technometric, Vol. 6, No. 4, Nov. 1964 pp. 415-422.
15. Bain, L. J., "Results for One or More Independent Censored Samples from the Weibull or Extreme-Value Distribution" Technometrics, Vol. 15, No. 2, May 1973, pp. 279-288.
16. Cohen, A. C. and Helm, F. R., "Estimation in The Exponential Distribution," Technometrics, Vol. 15, No. 2, May 1973, pp. 415-418.
17. Thoman, D. R.; Bain, L. J.; and Antle, C. E., Technometrics, Vol. II, No. 1, August 1969, pp. 445-460.